STUDY OF LIQUID TURBULENCE SPECTRA
BEHIND GRIDS
USING ELECTROMAGNETIC INDUCTION

By

PRAMOD KUMAR PANDE

A Thesis

*Submitted in fulfilment of the requirements for
the award of the degree of Doctor of Philosophy in*
CIVIL ENGINEERING
of the
UNIVERSITY OF ROORKEE

DEPARTMENT OF CIVIL ENGINEERING
UNIVERSITY OF ROORKEE
ROORKEE

1967

CERTIFICATE

Certified that the thesis entitled "STUDY OF LIQUID TURBULENCE SPECTRA BEHIND GRIDS USING ELECTRO-MAGNETIC INDUCTION" which is being submitted by Mr. P.K. Pande in fulfilment of the requirements for the award of the degree of Doctor of Philosophy in Civil Engineering of the University of Roorkee is a record of the student's own work carried out by him under my supervision and guidance. The matter embodied in this thesis has not been submitted for the award of any other degree.

This is to further certify that he has worked for a period of 2 years and 9 months from July 1964 to April 1967 for preparing this thesis.

Roorkee

Dated May 10, 1967.

R.J.Garde

(R.J.GARDE)
Professor of Civil Engineering
University of Roorkee
Roorkee, U.P.

*****

ABSTRACT

The work reported in this thesis includes the development of a device, based on the method of electromagnetic induction, for measuring turbulent velocity fluctuations in water. This method for turbulence measurements in water was first used by Grossman (26) and later studied by Day (14) and Gratz (25) at the University of Wisconsin, where the experimental work reported here was carried out. In the present work, the r.m.s. value of u_1' fluctuations as well as their spectra were measured. These measurements were made in a 2'' dia. lucite pipe along a diameter for proving of the equipment. Studies were then conducted of the decay and energy spectra downstream of various grids - singly as well as in combination.

The linear decay law, based on Kolmogoroff's hypothesis has not been found to be adequate to describe the decay behind a grid. Also it was found that a change in initial conditions brought about a change in the decay law as well. This can be attributed to the fact that the similarity of spectrum of energy does not hold good over a very wide range of wavenumbers. This deviation from similarity was also experimentally verified.

A generalised theory of similarity of spectra
and decay law was proposed by Goldstein, wherein account
was taken of the effect of Reynold's numbers and the
initial conditions on the law of decay as well as on
similarity of spectra. The postulates of this theory
have been confirmed with the experimental data obtained,
in as much as the results can be explained on the basis
of the above theory.

-:o:-

ACKNOWLEDGEMENTS

-:o:-

TABLE OF CONTENTS

CHAPTER   PAGE

-:o:-

LIST OF FIGURES

Fig.	Description	Page

Fig.	Description	Page

-:o:-

CHAPTER - I

INTRODUCTION

1.1 Preliminary Remarks :

Turbulence is a phenomenon encountered in nearly every field where fluid motion is involved. Though a familiar notion, turbulence cannot be defined easily, so as to describe its detailed characteristics. Various definitions have been suggested from time to time, to include the essential characteristics of turbulence. Hinze (28, pp. 1) sums up the definition as 'turbulent fluid motion is an irregular condition of flow in which the various quantities show a random variation with time and space coordinates, so that statistically distinct average values can be discerned'. Thus randomness must be associated with the flow for it to be turbulent. Any motion described in terms of periodic functions is not turbulent.

1.2 Classification of Turbulence :

Turbulent flows may be classified according to the manner in which they occur or according to their characteristics. Turbulence can be generated by friction forces at fixed walls or by the flow of adjacent layers of fluids with different velocities. There is, however, a distinct difference between the types of turbulence generated in the two cases. The turbulence generated and continuously influenced by fixed walls is generally known as 'wall turbulence' while the turbulence in the absence of walls is designated as

'free turbulence'.

Depending on its characteristics, the turbulence may be either 'homogeneous' or 'non-homogeneous'. Homogeneous turbulence has the same quantitative structure at all points in the flow field i.e. its characteristics are independent of the coordinate position. Homogeneous turbulence is further defined as being 'isotropic' when the characteristics are independent of coordinate direction also, otherwise it is 'anisotropic'. If the turbulence structure is dependent on coordinate position, we have a non-homogeneous turbulence, which by definition is anisotropic also.

1.3 Equations Governing Turbulent Flows :

The earliest worker to have noticed the existence of two modes (laminar and turbulent) of flow appears to be Hagen (52), who found that a change in flow characteristics invalidated his equation for resistance to pipe flow. It was, however, Osborne Reynolds (52) who first gave the specific formulation of a similarity parameter to define the mode of flow . The parameter, known as Reynolds number, was first described by him in a paper in 1883 and comprised of a length, velocity and kinematic viscosity - $uL/_{\nu}$. He found that the onset of turbulence is associated with a definite value of $uL/_{\nu}$. It is interesting to note that the word turbulence was first introduced to define the flow beyond the laminar range by Lord Kelvin in 1887 (52). Besides the formulation of this similarity parameter, Reynolds also introduced the idea of time averaged (mean)

velocity and fluctuations in turbulent flow. He assumed that the instantaneous velocity u may be separated into a mean velocity $\bar{u}$. and a turbulent fluctuating velocity u' (see Figure below) and that the instantaneous fluid velocity
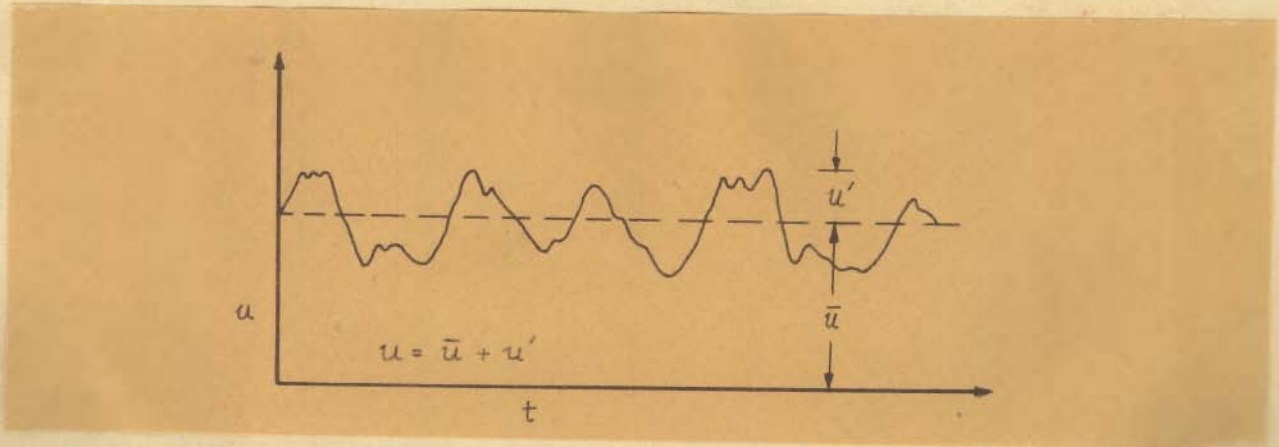
satisfies the Navier-Stokes equations for a viscous fluid. On the above concept, and using special averaging rules - known as Reynolds rules of averages - he extended the Navier-Stokes equations and formulated a set of equations called Reynolds equations, applicable to turbulent flows. These differ from the Navier-Stokes equations only in the presence of additional terms added to the mean values of stresses due to viscosity. These additional terms are called the 'Reynolds stresses', 'Eddy Stresses', or 'turbulent stresses'. The Reynolds equations for an incompressible fluid take the form;

$$\rho \left(\frac{\partial \bar{u}_i}{\partial t} + \bar{u}_j \frac{\partial \bar{u}_i}{\partial x_j} \right) = - \frac{\partial \bar{p}}{\partial x_i} + \frac{\partial}{\partial x_j} \left(\mu \frac{\partial \bar{u}_i}{\partial x_j} - \rho \overline{u_i' u_j'} \right) + \bar{F}_i$$

$$\dots\dots(1.1)$$

where ρ - mass density of the fluid

$\bar{u}_i$ - mean velocity of flow in x_i direction

$\bar{p}$ - mean pressure

μ - coefficient of viscosity of the fluid

u_i' and u_j' - turbulent velocity fluctuations in x_i and x_j directions respectively.

$\overline{F}_i$ - body force in x_i - direction.

The terms $\rho \overline{u_i' u_j'}$ represent the turbulent stresses.

The Reynolds equations are very valuable to explain the existence of eddy stresses in turbulent flow, but at the present time it has not been possible to solve these equations for more than a very limited number of problems. Further hypotheses about Reynolds stresses have to be made in order to obtain some definite results from these equations.

1.4 Phenomenological Theories of Turbulence :

One set of theories, known as the 'phenomenological' or 'semi-empirical' theories of turbulence is based on making further assumptions regarding Reynolds' stresses and thereby studying the mean velocity distribution in turbulent flows.

Boussinesq (48), a contemporary of Reynolds, was the first to work on the problem of making further assumptions about Reynolds stresses as stated above. He introduced the concept of an 'apparent' or 'turbulent' or 'eddy' viscosity ϵ_m , such that

$$ - \overline{u_i' u_j'} = \epsilon_m \left(\frac{\partial \overline{u}_i}{\partial x_j} + \frac{\partial \overline{u}_j}{\partial x_i} \right) \qquad \ldots \ldots (1.2) $$

According to Boussinesqs' concept, ϵ_m was a constant scalar quantity . Later it was found, however, that ϵ_m varied with flow conditions and could not be looked upon as a fluid property analogous to the kinematic viscosity ν . Even in the case of atmospheric turbulence, where this concept could be applied with some degree of success, ϵ_m was more

correctly described as a tensor of the second order rather than a scalar.

Another important advance towards formulating a semi-empirical theory of turbulence was made by Ludwig Prandtl (48) in 1925. By analogy with the kinetic theory of gases, he postulated that as the masses/of fluid migrated laterally, they carried with them the mean velocity (and hence the momentum) of their point of origin. This momentum was assumed to be preserved through a length ℓ called the 'mixing length'. Working on this premise he gave for turbulent shear stress the expression

$$\tau = \rho \ell^2 \left| \frac{\partial \bar{u}_1}{\partial X_2} \right| \frac{\partial \bar{u}_1}{\partial X_2} \qquad \ldots\ldots\ldots(1.3)$$

for nearly parallel turbulent flow.

Just as in the case of Boussinesq's eddy viscosity, the mixing length has to be specified before proceeding further with the analysis. The main advantage of this approach being that it is generally easier to make a plausible assumption for 'ℓ' which is just a length than for ϵ_m which is the product of a length and a velocity. In fact the mixing -length concept can be considered as an assumption regarding the make-up of ϵ_m

$$\epsilon_m = \ell^2 \left| \frac{d\bar{u}_1}{dX_2} \right| \qquad \ldots\ldots\ldots(1.4)$$

Taylor (59) reasoned that there was no physical justification for assuming conservation of momentum in turbulent mixing process. This is based on the fact that due to pressure fluctuations to which each lump of fluid is subjected during its path over the distance 'ℓ', the momentum of the lump will

not remain constant. Taylor suggested the conservation of vorticity instead of the momentum and derived the expression,

$$\frac{dp}{dx_1} = \frac{d\tau}{dx_2} = \rho \mid u_2' \mid \lambda \frac{d^2\bar{u}_1}{dx_2^2} \qquad \ldots\ldots(1.5)$$

He developed the theory to the three-dimensional case also in his 'generalised vorticity transport theory' and 'modified vorticity transport theory'.

Von Karman (23), in what is known as Karmans' similarity hypothesis, assumed the local flow pattern to be statistically similar in the neighbourhood of every point with only the time and length scales being different. For parallel mean flow he gave

$$\tau = \rho \lambda^2 \left(\frac{d\bar{u}_1}{dx_2} \right)^2 \qquad \ldots\ldots\ldots(1.6)$$

where 'λ' is given by

$$\lambda = k \mid \frac{d\bar{u}_1}{dx_2} \mid \Big/ \mid \frac{d^2\bar{u}_1}{dx_2^2} \mid \qquad \ldots\ldots\ldots(1.7)$$

k being the Karman constant, having a value of 0.4 found experimentally.

Improvements over the mixing length theories given above have been made by Prandtl (48), Goertler (48), Von Karman (68) and Lettau (41). Besides, Reichardt (48) and Baron (48) have proposed theories which are inductive in nature as against the deductive nature of mixing length theories.

The above theories have been subject to considerable criticism, mainly because while these predict the mean velocity distributions in many practical problems

successfully, they do not give any insight into the mechanism of turbulence. Discussions regarding them have been given by Goldstein (23), Lin and Tchen (45) Pai (48), and others (41,28).

1.5 Statistical Theory of Turbulence :

In order to gain an understanding of turbulent flow in general, the fields of turbulent fluctuations must be studied in detail rather than studying the mean velocity distributions alone. Since the turbulent fluctuations are random in nature, the application of the methods of statistical mechanics seems most logical for the study of turbulent flows. The origin of the modern statistical theory of turbulence lies in the poineering work of G.I.Taylor (60,62) who introduced the correlation between the velocities at two points as one of the quantities needed to describe the turbulence. He assumed the turbulence to be statistically homogeneous and isotropic in order to simplify the analysis and described measurements which showed that the turbulence generated downstream from a grid in a wind tunnel was approximately homogeneous and isotropic.

Further important contributions to the subject were made by Taylor (61,63,64) in 1938. He demonstrated the skewness of the probability distribution of the difference between the velocities at two points and also the existence of an interaction between components of the turbulence having different length scales. Another of his contributions was the introduction into turbulence theory of the result that the Fourier transform of the correlation between two veloci-

ties   is an energy spectrum function in the sense that it describes the distribution of kinetic energy over the various Fourier wave-number components of the turbulence. This concept has proved to be of immense value for further work in this field.

Von Karman (69) perceived that correlations between velocities at two (or more) points were tensors, Karman and Howarth (71) were able to show that for isotropic turbulence the two point correlation tensor could be expressed in terms of a single scalar. They also gave the well known Karman-Howarth equation connecting the double and triple correlation functions. Though the idea of using the Navier-Stokes equations to relate mean velocity products of different order had been advanced by Keller and Friedmann (4) in 1924`, they could not proceed f r without the simplification of homogeneity and isotropy.

Robertson's theory of invaria ts (51), wherein he showed how an isotropic tensor of arbitrary order could be expressed in terms of the known invariants of the rotation group, was another big advance in the development of the kinematics of isotropic turbulence. The same methods have been used to analyse the kinematic of axisymmetric turbulence.

As already mentioned, the concept of the energy spectrum function, which is the Fourier transform of the correlation function, was introduced in turbulence by Taylor. The spectral approach has proved to be very useful in studying many problems connected with dynamic aspects of turbulence. The turbulent kinetic energy per unit mass of flow in any

direction $\overline{u_1'^2}$ can be considered as consisting of the sum of contributions from fluctuations of all frequencies . If $E_1'(n)$ dn be the contribution of frequencies between n and n + dn to $\overline{u_1'^2}$, then

$$\int_0^\infty E_1'(n)dn = \overline{u_1'^2}$$

and $$\int_0^\infty F_1(n)dn = 1$$

where $$F_1(n) = E_1'(n) \Big/ \overline{u_1'^2}$$

The function $F_1(n)$ is known as Taylor's normalised spectrum function. It represents the contribution of each frequency n to the total kinetic energy of flow.

While Taylor had introduced the spectrum function for one-dimension only, the concept has been extended to the three-dimensional case as well . Thus for the study of any turbulence field a study can be made either of the correlation tensor or of the spectral tensor.

The dynamic equation giving the change of spectrum with time can be obtained from the Navier-Stokes equations (or the Reynolds equations), it takes the form

$$\frac{\partial E}{\partial t} + W = -2\nu k^2 E .$$

where E is the three-dimensional spectrum function (related to double velocity correlation) and W is a quantity represen- ting the transfer of energy among various frequencies (related to triple velocity correlation), ν is the kinematic viscosity of the fluid and k the wave number given by $k = \dfrac{2\pi n}{\overline{u}}$

where   n is the frequency and $\bar{u}$ the mean velocity of flow.
A similar equation is obtained for the correlations, involv-
ing, a correlation of nth order and another one of $(n+1)^{th}$
order.

One cannot proceed much farther with the above
equation without more specific knowledge of W. One of the
approaches in solving the above equation, therefore, has been
to postulate or assume some appropriate form for W. Such
forms have been suggested by Obukhoff, Kovasznay, Heisenberg,
and others (4,28,44).

Another approach for obtaining information about
the change of spectrum is based on the concept of 'self-
preservation' or 'similarity' introduced by von-Karman
(2,69,72). According to this concept the shape of the
correlation function or the spectrum remains similar in
course of time. Assuming that similarity of spectrum holds,
some conclusions about the functional form of $E(k)$ can be
drawn from more basic physical principles such as dimensional
considerations. However, observations indicated that the
spectrum function does not preserve its shape over the whole
range of wave numbers. The assumption of similarity during
decay of turbulence with time , therefore, needs a sound
physical basis in order to understand its limitations. The
required basis for one kind of similarity of the turbulence
viz., the small scale structure, was suggested by Kolmogoroff
(36,37,38) as well as by Obukhoff, Onsager, and Von
Weizsacker (4,28) in what is known as the 'equilibrium
theory'. The mechanism of large scale structure of turbulence

was similarly discussed by Lin (43) , Batchelor and Proudman (45) and Batchelor (3).

The various proposals for assuming the non-linear transfer of energy across the spectrum alongwith the similarity hypothesis can be used to determine the spectrum function completely and such solutions have been given by Chandrasekhar (12), Proudman (49), Lin (44), Goldstein (22) and others. Various laws for decay of turbulence have been proposed on the basis of the above concepts and a detailed discussion can be found in the books by Batchelor, Hinze, Lin or Pai (4,28,44,43).

The theories of equilibrium and similarity spectra and the decay laws obtained therefrom, however, apply under such conditions where the assumptions underlying the theories are fulfilled. It is, therefore,quite necessary to know under what condition will a particular theory fail to give correct results and to what extent. Goldstein (22) has proposed a generalisation of the theory of similarity and equilibrium spectra and derived a general decay law therefrom. In his opinion the decay law depends on the initial conditions as well as the Reynolds number. The theory has however, to be supported by experimental evidence which as yet is scanty. A more detailed discussion of the statistical theories of turbulence is presented in the next chapter.

1.6 Measurement of Turbulence :

On the experimental side, a large number of measurements of turbulence - both isotropic and anisotropic - have been made. One of the first measurements to be made was

of the decay of kinetic energy of a grid-produced turbulence
which has been repeated many times under different conditions.
Measurements have also been made to test the assumptions under-
lying various theories, to determine the shape of the corre-
lation and spectrum functions and the micro scales and inte-
gral scales. A detailed discussion of the measurements and
their comparison with theories is not possible here and refer-
ence may be made to the works of Dryden and coworkers (15,16,
17,18), Hall (27), Simmons and Salter (54,55) Batchelor and
Townsend (6,7,8), Baines and Peterson (1), Stewart and
Townsend (51), Grant and Nisbet (24), Tsuji (66,67), Sato(53),
Frankiel (20,21), Laufer and coworkers (42), Von Karman (70,73),
or to comprehensive reviews in books on turbulence (4,28,44,48).
The measurements have been made principally with the hot wire
anemometer in a wind tunnel. The hot wire anemometer, first
originated by King (34), has been developed to a great extent
over the period of years and is now more or less a standard
instrument for turbulence measurements in wind tunnels. Along-
with appropriate electronic circuits, the hot wire is capable
of undertaking varied types of measurements, examples of which
can be found in papers by Townsend (65), Corrsin (13),
Hubbard (29) and Dryden and Keuthe (28).

While quite successful for measurements in wind-
tunnel, the hot-wire anemometer is less suitable for use with
liquids because of its delicate construction and the effect
of air bubbles or impurities in water on the calibration of
the hot wire. Various investigators have tried other methods
for turbulence measurements in liquids with varying degrees of

success. None of them can, however, be said to have reached a degree of perfection like that of the hot wire for air. The measuring techniques for water are thus still in the development stage.

1.7 The Problem :

As already mentioned, information regarding the shape of spectrum during decay can be obtained on the basis of similarity hypothesis and equilibrium theory, and laws governing the decay of turbulence derived therefrom. A linear decay law is obtained if one starts with Kolmogoroffs' hypothesis. This type of decay law (linear) has also been found to conform with experimental data obtained by various investigators. Goldstein (22), however, proposed a generalisation of the equilibrium hypothesis and also a generalised decay law. According to this generalisation, the similarity hypothesis is probably only asymptotically correct for a range of large wave numbers, the range depending on initial conditions. A change in initial conditions should therefore bring about changes in the law according to which any grid-produced turbulence decays.

The present work is a continuation of a project started at the University of Winsconsin in 1960, with the purpose of building a device for measuring turbulence in water in duct-flow, using the method of electromagnetic induction. The capability of this method for turbulence measurements in water has already been demonstrated by the work of Grossman (26). In principle, the method consists of

measuring the e.m.f. fluctuations induced in the flow, on account of turbulent velocity fluctuations, when the duct carrying the water is placed in a strong magnetic field. The e.m.f. induced due to any component of velocity fluctuation is in a direction perpendicular to both the fluctuation direction and the direction of the magnetic field. The earlier workers on the Wisconsin Project include Day (14), and Gratz (25).

The phase of the work reported in this thesis comprises of the following :-

i) To develop further the measuring device, in order to improve the frequency response of the system, specially in the low frequency ranges. Certain changes in the system, including the addition of a multiple channel F.M. taperecorder and an operational amplifier impedance-isolation circuit, had to be made to this end.

ii) Study of the distribution and spectra of u_1' - fluctuation in a pipe along any diameter and their comparison with published results to check the performance of the system.

iii) Study of the decay of kinetic energy and u_1' - spectra downstream from various grids and the effect on these changing the initial conditions. The change in initial conditions was effected by inserting one grid upstream of the other at various distances.

Using water as a fluid the above studies were carried out in a 2 inch diameter lucite pipe with three grids. The grids had different mesh sizes but the same solidity ratio.

-:o:-

CHAPTER - II

STATISTICAL THEORIES OF TURBULENCE

2.1 Preliminary Remarks :

As mentioned earlier, due to their complexity and random nature, the details of turbulent flow require statistical description. Intensive studies have been made for isotropic homogeneous turbulence, because of the comparative ease with which it can be treated mathematically. Less is known of anisotropic homogeneous turbulence and very little is known of non homogeneous turbulence. The basic concepts of the isotropic case, however, gradually find their way into the study of other types. It is proposed to deal with some of these basic concepts in a somewhat detailed manner in this chapter.

As in any other case, there are two aspects of turbulent motion to be studied - one the mathematical description needed to represent the turbulent motion at one instant in a statistical manner, taking into account continuity and the symmetry conditions that may exist (kinematics of turbulent motion) and the other the variation of this statistical representation with time (dynamics of decay of turbulence). These two aspects can be studied either in terms of the correlation tensor or the spectral tensor and the results of one transformed to the other because of the Fourier transform relationship between the two.

The discussion in the present chapter will mainly comprise of the theory for homogeneous isotropic turbulence.

2.2 Kinematics of Homogeneous Turbulence :

In order to develop the theoretical concepts used for the description of the homogeneous turbulence we need to define the various types of correlations or the spectral tensor and also show the relationship between the two. The correlations can be Eulerian or Lagrangian depending on the method of description. While Lagrangian correlations are useful for a study of diffusion phenomena, the major developments in the field of statistical theory of turbulence have been in the study of Eulerian correlations. This discussion will be limited to the Eulerian space and time correlations only.

a) Eulerian Correlations:- Some of the commonly encountered Eulerian correlations are defined below. The definitions are general, without any consideration of the type of turbulence. The restrictions of homogenity and isotropy become necessary for further developments.

Double Velocity Correlation:-   The double velocity correlation $(Q_{i,j})_{AB}$ is defined as

$$(Q_{i,j})_{A,B} \;=\; \overline{(u'_i)_A (u'_j)_B} \;=\; ij^{th} \text{ component of a}$$

second order tensor describing the correlation of ith velocity fluctuation at A and j^{th} velocity fluctuation at B .....(2.1)

The related correlation coefficient is given by

$$(R_{i,j})_{A,B} \;=\; \frac{\overline{(u'_i)_A (u'_j)_B}}{\sqrt{\overline{(u'^2_i)}_A \; \overline{(u'^2_j)}_B}} \qquad \ldots\ldots\ldots(2.2)$$

A special case exists when $A = B$, then

$$(Q_{i,j})_{A,B} = \overline{u_i'\ u_j'} \qquad \text{Typifying the Reynolds stress tensor.}$$

Higher velocity correlations can also be defined in a similar manner as also the double correlation involving one velocity component and pressure or any other scalar. In the latter case, it is a first order tensor.

Eulerian Time Correlation :- The Eulerian time correlation is ordinarily written as a coefficient.

$$R_{ij}(t) = \frac{\overline{u_i'\ (\tau)\ u_j'\ (\tau - t)}}{\sqrt{\overline{u_i'^2\ (\tau)}\ \overline{u_j'^2(\tau - t)}}} = ij^{th} \text{ component of a second}$$

order tensor describing the correlation between the ith component of velocity fluctuation at a fixed point at time τ and the jth component of the velocity fluctuation at the same point at time $(\tau - t)$

........(2.3)

The one dimensional coefficient with the added restriction of statistical steadiness becomes ;

$$R_E(t) = \frac{\overline{u_i'\ (\tau)\ u_i'\ (\tau - t)}}{\overline{u_i'^2}} \qquad ....(2.4)$$

b) Micro and Macro Scales of Turbulence : If the restriction of homogeneity is placed on turbulence, the double velocity correlation Q_{ij} is found to have only three non-zero components, out of which two are equal. Hence only two correlation coefficients need to be considered. They are

$$f(x_1) = \frac{\overline{u_1'(\xi_1)u_1'\ (\xi_1 + x_1)}}{\overline{u_1'^2}} = \begin{array}{l}\text{double longitudinal} \\ \text{correlation} \\ \text{coefficient......(2.5)}\end{array}$$

and
$$g(x_2) = \frac{\overline{u_2'(\xi_2)u_2'(\xi_2+x_2)}}{\overline{u_2'^2}}$$
= double lateral correlation coefficient....(2.6)

Where X_1 and X_2 are coordinate axes and the points ξ_1 and $\xi_1 + x_1$ are separated by the distance x_1 as shown in Figure below, and similarly for ξ_2 and $\xi_2 + x_2$.
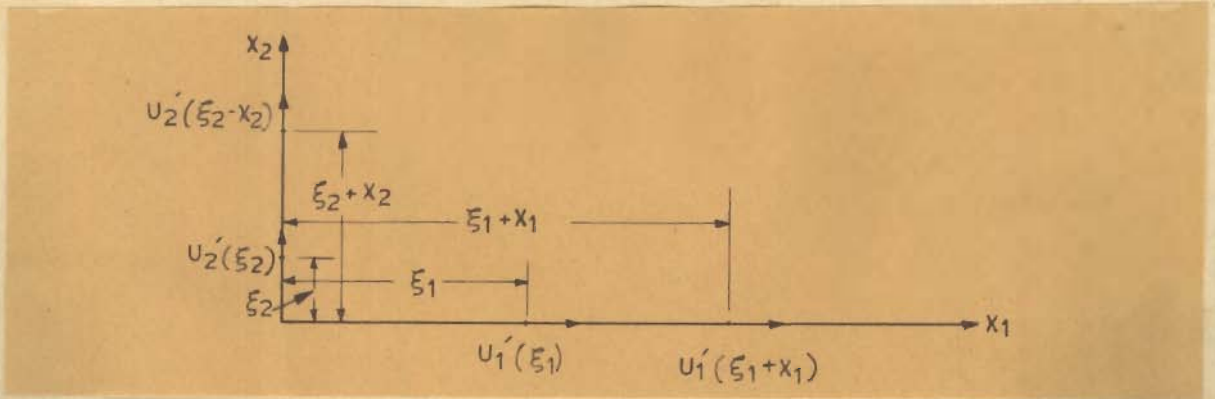
The initial shape of the correlation curves $f(x_1)$ vs x_1 and $g(x_2)$ vs x_2 approaches that of an inverted parabola. Taylor (60) argued that the intersection of this parabola with the X_1 or X_2 -axis gives a measure of the average size of the smallest eddies. The length, λ_f or λ_g so obtained is known as the 'micro' or 'dissipation' scale.
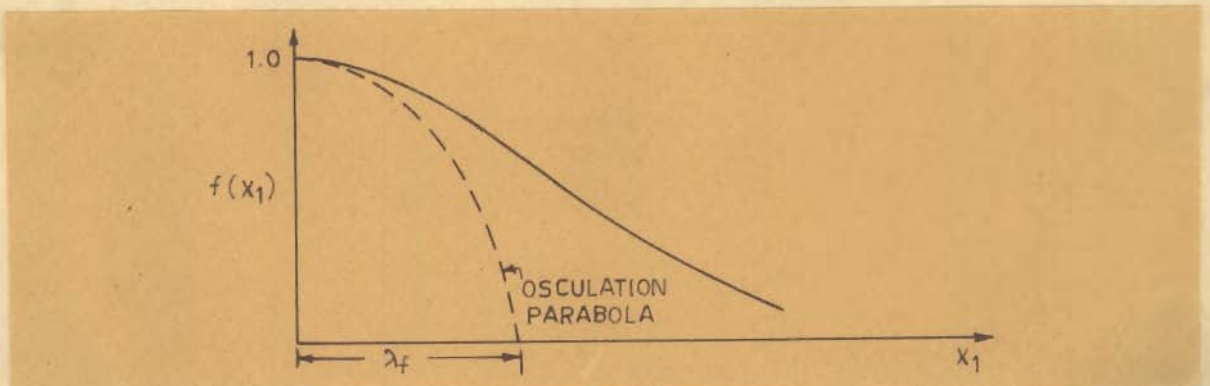
$$f(x_1) \approx 1 - x_1^2/\lambda_f^2 \quad \text{and} \quad g(x_2) \approx 1 - x_2^2/\lambda_g^2$$
........(2.7)

The above, alongwith equations (2.5) and (2.6) after some manipulations give

$$\frac{1}{\lambda_f^2} = -\frac{1}{2}\left(\frac{\partial^2 f}{\partial x_1^2}\right)_{x_1=0} \quad ; \quad \frac{1}{\lambda_g^2} = -\frac{1}{2}\left(\frac{\partial^2 g}{\partial x_2^2}\right)_{x_2=0}$$

$$\dots\dots(2.8)$$

and $\quad \dfrac{1}{\lambda_f^2} = \dfrac{1}{2u_1'^2}\ \overline{\left(\dfrac{\partial u_1'}{\partial x_1}\right)}_{x_1=0} \quad ; \quad \dfrac{1}{\lambda_g^2} = \dfrac{1}{2u_2'^2}\ \overline{\left(\dfrac{\partial u_2'}{\partial x_2}\right)}^2_{x_2=0}$

$$\dots\dots(2.9)$$

The macro or integral scale is a measure of the longest connection between velocities at two points in a flow field: This is defined as

$$\Lambda_f = \int_0^\infty f(x_1)\,dx_1 \quad \text{and} \quad \Lambda_g = \int_0^\infty g(x_2)\,dx_2 \dots\dots(2.10)$$

If $f(x_1) = 0$ at $x_1 = x_1^*$, then $\Lambda_f = x_1^*$ provided the correlation curve is rectangular. Otherwise, which is the actual case, Λ_f and x_1^* are different.
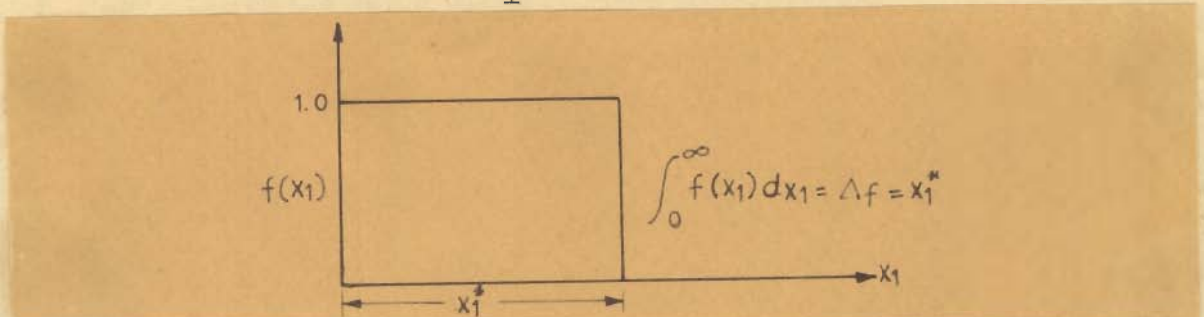
In a manner similar to the above, the micro-and macro-Eulerian time scales can be defined as follows :-

$$R_E(t) \simeq 1 - t^2/\tau_E^2 \dots\dots(2.11)$$

whence $\quad \dfrac{1}{\tau_E^2} = \dfrac{1}{2u_1'^2}\ \overline{\left(\dfrac{\partial u_1'}{\partial t}\right)}^2_{t=0} \qquad \dots\dots(2.12)$

and $\quad \mathcal{T}_E = \int_0^\infty R_E(t)\,dt \qquad\qquad \dots\dots(2.13)$

A general relationship between the Eulerian space and time relationship for any turbulent flow is difficult to predict. However, if the homogeneous field being considered

has a constant mean velocity say $\bar{u}_1$ in the x_1-direction and if $\bar{u}_1 \gg u_1'$, we can make use of Taylor's hypothesis :

$$\partial/\partial t = - \bar{u}_1 \frac{\partial}{\partial x_1} \qquad \ldots\ldots\ldots(2.14)$$

which gives us ;

$$f(x_1) \equiv R_E (t) \qquad \ldots\ldots\ldots(2.15)$$

$$\text{and} \quad \Lambda_f = \bar{u}_1 \, \mathcal{T}_E \qquad \ldots\ldots\ldots(2.16)$$

Such conditions, as are needed for the above approximations to hold fairly well, exist in the case of isotropic homogeneous turbulent flow generated by grids.

c) Correlations in Isotropic Turbulence :- If in addition to homogeneity, the conditions of isotropy are also imposed on the turbulence, the correlations can be studied in more detail. The deduction of correlation tensors in isotropic turbulence is greatly facilitated by the theory of invariants as expounded by Robertson (51). He showed that an isotropic tensor of arbitrary order could be expressed in terms of the known invariants of the rotation group.

In the case of isotropic turbulence, since there is no preferred choice of the coordinate system, the correlations must be basically characterised by the directions of the velocity components relative to the vector joining the two points A and B at which the velocities are considered . We can in this case define certain correlation coefficients as shown in the sketch below.
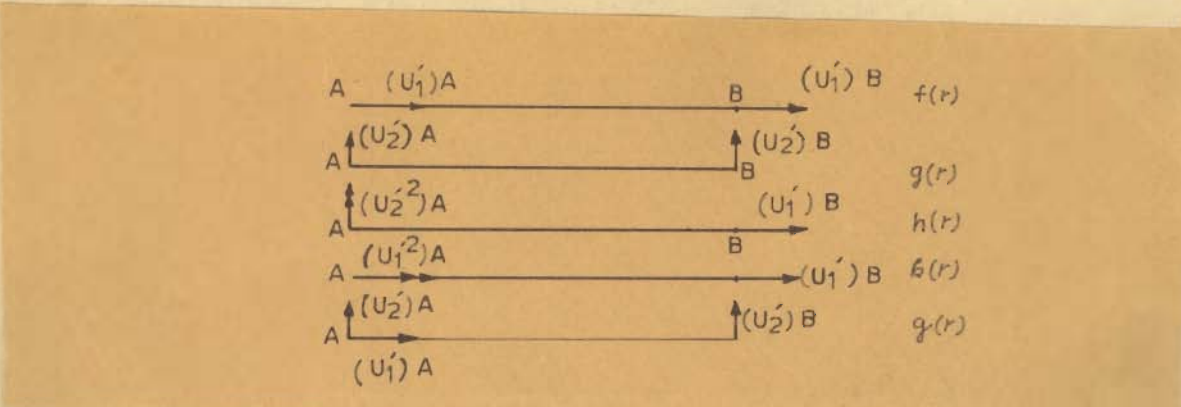
Making use of the Robertson's theory of invariants, the double velocity correlation can be expressed in terms of $f(r)$ and $g(r)$, and the expression turns out to be

$$(Q_{ij})_{A,B} = \overline{u'^2} \left(\frac{f(r)-g(r)}{r^2} \cdot r_i r_j + g(r)\delta_{ij} \right)$$

$$\ldots\ldots\ldots(2.17)$$

where $\overline{u'^2} = \overline{u'^2_1} = \overline{u'^3_2} = \overline{u'^2_3}$ from isotropy

$$r_i = (x_i)_A - (x_i)_B$$

and δ_{ij} is the Kronecker delta.

Relation (2.17) was also derived by Von Karman (71) direct calculation. Karman and Howarth (71) also deduced the relationship ;

$$g = f + \frac{r}{2} \frac{\partial f}{\partial r} \qquad \ldots\ldots\ldots(2.18)$$

which was experimentally verified by MacPhail (47).

Thus from equations (2.17) and (2.18) it can be seen that in homogeneous isotropic turbulence, all the correlation functions of the second order can be expressed in terms of a single correlation function $f(r)$ or $g(r)$.

Also for this case one obtains ;

$$\lambda_f = \lambda_g \sqrt{2} \qquad \ldots\ldots\ldots(2.19)$$

In a manner similar to above one can obtain for the triple velocity correlation ;

$$(S_{i\,k,j})_{A,B} = (\sqrt{\overline{u'^2}})^3 \left(\frac{k-h-2q}{r^3} r_i r_j r_k + \delta_{ij} r_k \frac{h}{r} + \delta_{ik} r_j \cdot \frac{q}{r} \right.$$

$$\left. + \delta_{jk} r_i \frac{q}{r} \right) \qquad \ldots \ldots \ldots (2.20)$$

where h, k and q are related as follows

$$\left. \begin{array}{l} k = -2h \\[1mm] q = -h - \dfrac{r}{2}\dfrac{\partial h}{\partial r} \end{array} \right\} \qquad \ldots \ldots (2.21)$$

Thus the triple correlation can again be expressed in terms of a single scalar function.

The same techniques may be applied for higher order correlations also . Third order correlations were measured by Townsend (65) , Stewart (56), and Kistler, O'Brien and Corrsin (44).

d) Spectrum of Turbulence :- Taylor (61) was the first to introduce the use of spectrum in turbulence theory and obtain the relation between the correlation function and spectrum function in the mathematical form.

The kinetic energy of the turbulence fluctuations can be analysed according to its distribution over the various frequencies occuring in these fluctuations. Considering a quasi-steady field of flow, there exists a constant average value of $\overline{u'^2_1}$ which can be considered to consist of the sum of the contribution of all frequencies n. If $E'_1(n)$ dn be the contribution to $\overline{u'^2_1}$ of the frequencies between n and n+dn, then one has

$$\int_0^\infty E'_1(n)\, dn = \overline{u'^2_1} \qquad \ldots \ldots (2.22)$$

If $F_1(n) = E'_1(n)/\overline{u'^2_1}$

Then, $\int_0^\infty F_1(n)\, dn = 1 \qquad \ldots \ldots \ldots (2.23)$

where $F_1(n)$ is the normalised Taylor's one dimensional spectrum function. As shown by Taylor, this function is related to the Eulerian time correlation as follows :-

$$R_E(t) = \int_0^\infty F_1(n) \cos 2\pi n t \; dn \qquad \ldots\ldots(2.24)$$

and

$$F_1(n) = 4\int_0^\infty R_E(t) \cos 2\pi n t \; dt \qquad \ldots\ldots(2.25)$$

i.e. one is the Fourier transform of the other.

Taylor made spectrum measurements, behind a grid in a wind tunnel, of the velocity fluctuation as registered by a hot wire fixed in the wind tunnel. This gives a fluctuation in time, but his assumption "the sequences of changes in u_1' at the fixed point are simply due to the passage of an un-changing pattern of turbulent motion over the point" made the variation essentially same as that in space. The above assumption has been represented mathematically by eqn. 2.14. When this condition holds, the observed spectrum corresponds to a one-dimensional fourier analysis of the field of turbulence in the direction of the flow. Equations (2.14), (2.15), (2.24) and (2.25) can then be combined to connect the observed time spectrum with the space correlation function, as follows :-

$$f(x_1) = \int_0^\infty F_1(n) \cos \frac{2\pi n x}{\bar{u}_1} \; dn \qquad \ldots\ldots\ldots(2.26)$$

$$F_1(n) = 4\int_0^\infty f(x) \cos \frac{2\pi n x}{\bar{u}_1} \; dx \qquad \ldots\ldots\ldots(2.27)$$

Also,

$$\underset{n\to 0}{\text{Lim}} \; F_1(n) = 4 \mathcal{I}_E = \frac{4}{\bar{u}_1} \Lambda_f \qquad \ldots\ldots\ldots(2.28)$$

and

$$\frac{2\pi^2}{\bar{u}_1^2} \int_0^\infty n^2 F_1(n) dn = \frac{1}{\lambda_f^2} = \frac{1}{\bar{u}^2 \tau_E^2} \qquad \ldots\ldots(2.29)$$

The above relationships are for the one dimensional spectrum only and hold good when the flow is homogeneous with

a constant mean velocity $\overline{u}_1 \gg u_1'$ as mentioned earlier while obtaining eqns.(2.14) and (2.15).

Since turbulence is actually three dimensional, its spectrum should also be three dimensional. The Taylor spectrum is just a one dimensional cut of the spatial spectrum. A harmonic analysis in three dimensions then gives the energy spectrum tensor. Introducing the wave number k_1 instead of frequency n, such that $k_1 = 2\pi n/ \overline{u}_1$, one has the Fourier transform relations between the correlation and spectrum tensors.

$$Q_{ij}(x_1, x_2, x_3, t) = \int_{-\infty}^{+\infty}\!\!\!\int\int dk_1 dk_2 dk_3 E_{ij}(k_1, k_2, k_3, t)\exp$$

$$\left\{ i(k_1 x_1 + k_2 x_2 + k_3 x_3) \right\}$$

and $E_{ij}(k_1, k_2, k_3, t) = \dfrac{1}{8\pi^3} \int_{-\infty}^{+\infty}\!\!\!\int\int dx_1 dx_2 dx_3 Q_{ij}(x_1, x_2, x_3, t) \exp.$

$$\left\{ -i(k_1 x_1 + k_2 x_2 + k_3 x_3) \right\} \quad\ldots\ldots(2.30)$$

In the case of isotropic turbulence, the correlation tensor can be expressed in terms of two scalars f and g. Since f and g are different, the one dimensional spectrum functions $F_1(k_1)$ and $F_2(k_1)$ corresponding to them are also different, though

$$\int_0^\infty dk_1 F_2(k_1) \int_0^\infty dk_1 F_1(k_1) = \overline{u'^2}$$

Also , for isotropic turbulence one can introduce the wave number k and distance r and get from equation (2.30)

$$Q_{ii}(r,t) = 2\int_0^\infty dk \ \frac{\sin kr}{kr} \ E(k,t)$$

and

$$E_{(k,t)} = \frac{1}{\pi} \int_0^\infty dr.kr \sin kr \ Q_{ii}(r,t) \quad\ldots..(2.31)$$

where $E(k,t)$ is the three dimensional energy

spectrum function such that

$$E(k,t) = 2\pi k^2 E_{ii}(k,t)$$

and
$$\int_{0}^{\infty} dk\, E(k,t) = 3/2\ \overline{u'^2} \qquad \ldots\ldots(2.32)$$

The relation between $E(k,t)$, $F_1(k_1,t)$ and $F_2(k_1,t)$ can be shown to be

$$E(k,t) \quad 1/2.\ k_1^2 \frac{\partial^2 F_1(k_1,t)}{\partial k_1^2} - 1/2.\ k_1 \frac{\partial F_1(k_1,t)}{\partial k_1}$$

$$\ldots\ldots(2.33)$$

and
$$F_2(k_1) = 1/2.\ \left(F_1(k_1) - k_1 \frac{\partial F_1(k_1)}{\partial k_1} \right) \ldots\ldots(2.34)$$

Thus the measurement of $F_1(k_1)$ alone can give the three dimensional spectrum function for homogeneous isotropic turbulence . The concept of spectrum of turbulence has been the subject of many theoretical and experimental studies (31,32,33,43).

2.3 Dynamics of Homogeneous Turbulence :

The dynamics of turbulence, that is the variation of the statistical representation of turbulent motion with time, is governed by the Navier-Stokes equations, there being no average motion.

$$\frac{\partial u'_i}{\partial t} + u'_j \frac{\partial u'_i}{\partial x_j} = -\frac{1}{\rho}\frac{\partial p'}{\partial x_i} + \nu \nabla^2 u'_i \qquad \ldots(2.35)$$

The above equation can be used in the investigation of turbulent motion in one of the following two manners.

The first approach is to obtain an explicit solution of eqn. (2.35) . If the initial conditions are given numerically, the equations can be solved for a realised field by a numerical step by step integration with respect to t. Such a procedure is very laborious and unlikely to reveal the

fundamental features of a statistical problem. However, in the absence of a wholly successful alternative method it may be worthwhile to obtain solutions for realised fields in some sample cases. Such an approach has been used by Emmons (4) for the hypothetical case of a two dimensional turbulent flow between two fixed parallel planes.

The second method is to convert equation (2.35) into a set of equations for the variation of statistical quantities with time and then to solve them in terms of the statistical specification of the turbulence at the initial t_0.

To obtain the equation for the change of double-velocity correlation with time, we can write eqn. (2.35) for point A and B, multiply the equation for A by $(u_k')_B$ and that for B by $(u_l')_A$, add the two and take an average. The pressure term vanishes identically from the condition of incompressibility and the equation reduces to

$$\frac{\partial}{\partial t} (Q_{i,j})_{A,B} - \frac{\partial}{\partial r_k} \left\{ (S_{ik,j})_{A,B} + (S_{kj,i})_{A,B} \right\}$$

$$= 2\nu \nabla^2 (Q_{ij})_{A,B} \qquad \ldots\ldots(2.36)$$

Thus the equation for change of double correlation contains the triple-correlation in it. Similarly the equation for triple correlation contains the fourth order correlation and so on.

The equation describing the behaviour of energy spectrum with time and space coordinates can be obtained from eqn. (2.36) and is

$$\frac{\partial}{\partial t} E_{ij}(k_1,k_2,k_3,t) = W_{ij}(k_1,k_2,k_3,t) - 2\nu k^2 E_{ij}(k_1,k_2,k_3,t)$$

$$\ldots\ldots(2.37)$$

where W is connected to the triple correlation and represents the transfer of energy among various frequencies.

In the case of isotropic turbulence, since the double and triple correlations can be expressed in terms of a single scalar, it should be possible to reduce eqn.(2.36) to a single equation. Karman and Howarth (54) foundit to be ;

$$\frac{\partial}{\partial t} \; (\overline{u'^2} \, f) + 2(\overline{u'^2})^{3/2} \; (\frac{\partial h}{\partial r} + \frac{4h}{r}) = 2 \nu \overline{u'^2} (\frac{\partial^2 f}{\partial r^2} + \frac{4}{r} \cdot \frac{\partial f}{\partial r})$$

$$\dots\dots(2.38)$$

A direct experimental verification of the above equation was made by Stewart (56).

Also in the isotropic case, eqn. (2.37) can be written as follows :

$$\frac{\partial}{\partial t} \; E(k,t) \; = W(k,t) - 2 \nu k^2 E(k,t) \;\; \dots\dots(2.39)$$

where $W(k,t) \; = 2\pi k^2 \, W_{ii}(k,t)$

Eqn. (2.39) also shows that

$$\int_{o}^{\infty} W \, (k,t) \; dk \;\; = 0$$

which means that no energy is lost or generated while it is redistributed among various scales. The rate of dissipation is obtained from eqn. (2.39) by integrating it with respect to k from k = 0 to k = ∞ .

$$\varepsilon \;\; = - \; \frac{d\overline{u'^2}}{dt} \;\; = - \int_{o}^{\infty} \frac{\partial E}{\partial t} \; dk = -2 \nu \int_{o}^{\infty} k^2 E \; dk$$

$$\dots\dots(2.40)$$

Here again, without a more specific knowledge of W, it is not possible to proceed much further with eqn. (2.39). However, it has been found possible to obtain some plausible formulas connecting $W(k,t)$ and $E(k,t)$ and make reasonable deductions.

As seen above, each nth-order equation obtained for describing the dynamics of turbulent flow contains moments of order $(n+1)$ as a direct consequence of the non-linearity of the Navier-Stokes equations. The number of variables is thus more than the number of equations by one.

The only case where it is possible to solve eqns. (2.38) or (2.39), directly is the limiting case where the effect of the 'convective' term represented by h or W is neglected i.e. the description holds good for the asymptotic behaviour of the turbulence for dominating viscous effects. The solution in this case is

$$f = \exp(-r^2/8\nu t) \qquad \ldots\ldots\ldots(2.41)$$

or

$$E(k,t) = E(k,t_o) \exp(-2\nu k^2(t-t_o)) \qquad \ldots\ldots(2.42)$$

indicating that f has the shape of a Gaussian error curve, which was found to be approximately true in the final stages of decay by Batchelor and Townsend (8).

A general feature of the dynamic equation, which was shown by Loitsianski (28) by taking the fourth moment from each term of eqn. (2.38) is that

$$\overline{u_1'^2} \int_o^\infty r^4 f(r,t)\,dr = J \qquad \ldots\ldots(2.43)$$

is an invariant under the assumption that

$$\lim_{r\to\infty} \left(r^4 \frac{\partial f}{\partial r} \right) = 0$$

and

$$\lim_{r\to\infty} \left\{ r^4 k(r) \right\} = 0$$

The integral (2.43) is known as 'Loitsianskis' invariant'. The interpretation given by Loitsianski is that the integral gives the total amount of disturbance caused by

the turbulence generating system. Some doubts on the in-
variance of the Loitsianskii's integral have, however,
been cast by Batchelor and Proudman (5).

As already indicated, the non-linearity of the
dynamic equation does not allow a direct solution to be
obtained for eqns. (2.38) or (2.39). The approaches
for solving eqns. (2.38) or (2.39) can be divided into two
broad classes. In the firstclass, models of dynamical pro-
cesses are postulated on physical grounds. Theories of Kolmo-
goroff (36,37,38) Onsager (28), Von Karman and Lin (73)
belong to this class.

In the second class there are two approaches.
One consists of neglecting moments of order n + 1 in equations
for moments of order n. The works of Chou and Deissler (28)
belong to this approach. Another approach is to relate fourth
order moments to second order moments on the basis of a normal
probability distribution and thus close the moment equations.
Proudman and Reid, Tatsumi and Ogura (4,28) have worked on
this approach.

In the case of eqn. (2.39) making some assumption
for W(k) in an explicit functional form renders it amenable
to solution. Such theories (physical transfer theories) have
been proposed by Obukhoff, Kovasznay, Heisenberg, Chandrasekhar
and Von-Karman (4,28,44) and Goldstein (22).

a) Physical Considerations :- A physical model for turbulent
-energy production and dissipation at high Reynolds numbers
was suggested by Kolmogoroff (36,37,38). According to him the
boundary conditions determine the mechanism of turbulence

production from the instability of the mean flow. Eddies
of small wave numbers (large eddies) produced from the in-
stability of the mean flow produce eddies of higher wave
number through inertial interaction and these in turn break
down into eddies of much higher wave number. Turbulence energy
thus cascades from eddies of low wave numbers to eddies of
high wave numbers, the viscosity effects also becoming more
and more important with increasing wave number. This cascad-
ing of turbulent energy continues until wave numbers of eddies
are so high that not all the energy is transferred to the next
higher order, but part is dissipated into heat by viscous
forces.

For the large scale structure of turbulence (eddies
of small wave numbers) Lin (44), making use of the Loitsianski's
invariant, showed that the principal part of the spectrum
function remains unchanged. Thus the large scale motions
are permanent in as far as the time dependence of $E(k)$ dec-
reases with decrease in k becoming zero at k = 0.

Regarding the small scale structure of turbulence,
Kolmogoroff reasoned that at high Reynolds numbers, the
range between wave numbers of large eddies and of those
dissipating all their energy by viscosity is large. In this
case in the energy cascading process the region of eddies of
high wave-numbers should be far enough removed from the pro-
duction region so as to be independent of the external condi-
tions producing forces that generate the initial largest eddies.
Therefore, in any turbulent field at high Reynolds number, a
domain Q can be defined which is small enough that it will
possess local isotropy. The domain Q will contain eddies of

high wave numbers describing a motion that is isotropic and
steady state.

Obviously, the fundamental quantities upon which the
structure of motion in the domain ℓ will depend are the mean
rate of dissipation of energy per unit mass of the fluid ϵ
(which determines the intensity of the energy flow in the
cascading phenomenon) and the kinematic viscosity ν . Based
on these considerations Kolmogoroff made his first hypothesis.

" At sufficiently high Reynolds numbers there is a
range of high wave numbers where the turbulence is statistically
in equilibrium and uniquely determined by the parameters ϵ
and ν . This state of equilibrium is universal " (28).

When this equilibrium range is sufficiently wide,
it is further argued that the lower wave number components
in the equilibrium range will contribute so little to the
total viscous dissipation that a subrange will exist in which
the properties will be determined solely by ϵ. Since in this
subrange the inertial transfer of energy is the dominating
factor, this is called the inertial subrange . This forms the
basis of Kolmogoroff's second hypothesis :

" If the Reynolds number is infinitely large, the
energy spectrum in the inertial subrange is independent of ν,
and solely determined by ϵ " (28).

The concepts introduced by Kolmogoroff in his two
hypotheses can be used to determine the shape of the energy
spectrum function $E(k)$ in locally isotropic turbulence. Since
turbulence in this region is independent of external condi-
tions, any change in the length scale and time (or velocity)

scale of turbulence can only be a result of the effect of parameter ϵ and ν . From dimensional arguments we obtain

for length scale $\qquad \eta = (\nu^3/\epsilon)^{1/4} \qquad \ldots\ldots(2.44)$

for velocity scale $\quad v = (\nu\epsilon)^{1/4} \qquad \ldots\ldots(2.45)$

and dimensional considerations also lead to a spectrum function of the form

$$E(k) = \epsilon^{1/4} \nu^{5/4} \, \emptyset (\eta k) \ldots\ldots\ldots(2.46)$$

where $\emptyset$ is a universal dimensionless function of ηk.

For the inertial subrange, according to Kolmogoroff's second hypothesis, equation (2.46) must reduce to a form independent of ν . Here we get from dimensional reasoning again

$$E(k) = \alpha\epsilon^{2/3} k^{-5/3} \qquad \ldots\ldots(2.47)$$

Equation (2.47) is frequently called the Kolmogoroff's spectrum law. The same result was, however, obtained by Onsager (28) and von-Weizsacker (28) independently of Kolmogoroff and of each other.

The scales η and v defined above also occur in the study of the small scale structure of turbulence even when the Reynolds number is not high. This cannot be interpreted on the basis of Kolmogoroff's theory, but follows from considerations of self-preservation during decay, which has been discussed later.

b) Physical Transfer Theories :- The basis of physical-transfer theories is the assumption of a relation between $W(k,t)$ and $E(k,t)$. The specific form of relationship between $W(k,t)$ and $E(k,t)$ depends on the particular mechanism of energy transfer considered. Heisenberg's (44) eddy-viscosity transfer theory

can be said to be amongst the most successful physical transfer theories.

While considering the rate of dissipation of energy by eddies with wave numbers less than a particular value of k, Heisenberg distinguished between the energy directly dissipated in the form of molecular motion and thermal energy and the energy transferred in the form of kinetic energy to all eddies with wave numbers exceeding the specified k. He argued that the transfer mechanism is essentially similar to viscous dissipation provided the molecular viscosity is replaced by a suitable eddy viscosity. The expression for energy transfer then becomes

$$\int_0^k W(k)\, dk = -2\, \nu_t(k) \int_0^k k^2 E(k)\, dk \quad \dots \dots (2.48)$$

Heisenberg further assumed that $\nu_t(k)$ can be expressed as

$$\nu_t(k) = k_H \int_k^\infty \sqrt{\frac{E(k)}{k^3}}\, dk \quad \dots \dots (2.49)$$

where k_H is a numerical constant of order unity. This gives on substitution in eqn. (2.43) ;

$$\frac{\partial}{\partial t} \int_0^k E(k)\, dk = -2 \left(\nu + k_H \int_k^\infty \sqrt{\frac{E(k)}{k^3}}\, dk \right)$$

$$\int_0^k k^2 E(k)\, dk \quad \dots \dots (2.50)$$

For the equilibrium range,

$$\frac{\partial}{\partial t} \int_0^k E(k)\, dk \approx \frac{\partial}{\partial t} \int_0^\infty E(k)\, dk = -\epsilon = -2\nu \int_0^k k^2 E(k)\, dk$$

$$\dots \dots (2.51)$$

Combination of eqns. (2.50) and (2.51) results in

$$\epsilon = 2 \left(\nu + k_H \int_k^\infty \sqrt{\frac{E(k)}{k^3}}\, dk \right) \int_0^k k^2 E(k)\, dk \quad \dots (2.52)$$

Bass (4) and independently Chandrasekhar (4) obtained an

exact solution of Eqn. (2.52) in the form

$$E(k) = (\frac{\epsilon\epsilon}{9k_H})^{2/3} k^{-5/3} (1 + \frac{8}{3} \frac{\nu^3}{k_H^2 \epsilon} k^4)^{-4/3}$$

$$\ldots\ldots(2.53)$$

In the region where the effect of viscosity is negligible, eqn. (2.53) reduces to

$$E(k) = (8\epsilon/9k_H)^{2/3} k^{-5/3} \qquad\ldots\ldots(2.54)$$

which is identical with Kolmogoroff's spectrum law in the inertial subrange. For large values of k where viscosity plays an important part eqn. (2.53) reduces to ;

$$E(k) = (\epsilon k_H^2/2\nu^2)^2 \cdot k^{-7} \qquad\ldots\ldots(2.55)$$

Kovasznay (4) postulated that the contribution to W(k) comes from a narrow wave number band in the immediate vicinity of k. Since under these circumstances, W(k) can only be a function of μ(k) and k, it follows from dimensional arguments that

$$\int_0^k W(k)dk = -\alpha \left\{ E(k) \right\}^{3/2} k^{5/2} \qquad\ldots\ldots(2.56)$$

where α is an absolute constant.

From eqn. (2.56) and eqn. (2.39) he obtained for E(k)

$$E(k) = (\frac{\epsilon^2}{\alpha 10})^{1/3} k^{-5/3} \left\{1 - \frac{\alpha}{2} (k/k_d)^{2/3} \right\}^{4/3} \Big.^2$$

$$\ldots\ldots(2.57)$$

where $k_d = \left\{\epsilon/\nu^3\right\}^{1/4}$

Obukhoff (28) assumed that the energy transfer across the wave number k is analogous to the energy transfer from the main motion to the turbulent motion through the turbulent shear stresses; and it follows, therefore,

$$\int_0^k W(k)dk = -\alpha \left\{2\int_0^k k^2 E(k)dk \right\}^{1/2} \int_k^\infty E(k)dk \quad\ldots(2.58)$$

where α is an absolute constant. From the above he obtained a solution for E(k) which reduces to constant x $k^{-5/3}$ in the inertial subrange.

Von Karman (28) visualised that the transfer function W(k) may be interpreted as the difference between the energy supplied by the eddies with wave numbers less than k and the energy transferred to the smaller eddies with wave numbers greater than k. On this basis he defined ;

$$W(k) = 2\alpha \left(E^{\beta} k^{r} \int_{0}^{k} E^{\beta'} k^{r'} dk - E^{\beta'} k^{r'} \int_{k}^{\infty} E^{\beta} k^{r} dk \right) \dots (2.59)$$

which includes, as special cases, the assumptions made by Obukhoff, Kovasznay and Heisenberg and obtained

$$E(k) = E(k_e) 2^{17/6} \frac{(k/k_e)^4}{\left(1 + (k/k_e)^2 \right)^{17/6}} \dots (2.60)$$

where k_e is a function of time.

c) Similarity and Decay of Turbulence : As already seen, the general theory of turbulent motion cannot lead to specific predictions without auxiliary considerations. For this reason, the concept of self-preservation of correlation functions was introduced by von Karman and Howarth (71). The corresponding hypothesis of similarity of spectra is the work of Heisenberg (44), which states that the spectrum remains similar in the course of time.

A similarity solution of the equation for change of spectrum

$$\frac{\partial E}{\partial t} + W = -2\nu k^2 E \quad \text{can be found out as}$$

follows.

Let V be a characteristic velocity and ℓ a characteristic length. Then from dimensional arguments,

$$F = V^2 \ell \, \psi(\xi) \quad ; \quad W = V^3 w(\xi) \quad ; \quad \xi = k\ell$$

$$\cdots\cdots (2.61)$$

Then the above equation becomes .

$$\frac{1}{V} \frac{d\ell}{dt} \left\{ \xi \psi'(\xi) + \psi(\xi) \right\} + \frac{2\ell}{V^2} \frac{dV}{dt} \psi(\xi) + w(\xi)$$

$$= \frac{-2\nu}{V\ell} \xi^2 \psi(\xi) \qquad \cdots\cdots (2.62)$$

For the similarity solution to be valid we must have

$$\frac{1}{V} \frac{d\ell}{dt} = a_1$$

$$\frac{2\ell}{V^2} \frac{dV}{dt} = a_2 \qquad \cdots\cdots (2.63)$$

$$\frac{\nu}{V\ell} = a_3$$

where a_1, a_2 and a_3 are all constants. Thus eqn. (2.62) becomes

$$a_1 \xi \psi'(\xi) + (a_1 + a_2) \psi(\xi) + 2a_3 \xi^2 \psi(\xi) \, w(\xi)$$

$$= 0 \qquad \cdots\cdots (2.64)$$

Besides the above equations we also have

$$\overline{u'^2} = V^2 \int_0^\infty \psi(\xi) \, d\xi \qquad \cdots\cdots (2.65)$$

$$- \frac{\overline{du'^2}}{dt} = 2\nu \frac{V^2}{\ell^2} \int_0^\infty \xi^2 \psi(\xi) \, d\xi \cdots\cdots (2.66)$$

and the convergence criterion for Loitsianskis' relation as

$$V^2 \xi^5 \lim_{\xi \to 0} \frac{\psi(\xi)}{\xi^4} = J \qquad \cdots\cdots (2.67)$$

The above system of equations presumes that the transfer term in eqn. (2.62) is considered generally of equal importance with the term expressing the viscous dissipation. The above solutions are at variance with eqn.(2.67) i.e. full similarity is only possible if Loitsianskis' theorem is rejected.

Experimental evidence also excludes the possibility of adopting full similarity as a generally valid assumption for all decay processes.

We can consider four different cases, the first two belong to the approach where we consider that the Loitsianski's invariant exists and plays a role in the similarity of spectrum, while in the other two we assume that the similarity of spectrum is occuring only in the eddies contributing appreciably to the dissipation process, and the largest eddies play no role in determining the similarity of the spectrum.

Case I :- Loitsianski's invariant exists and the transfer term is negligible for all frequencies i.e. $w\left(\frac{k}{4}\right) = 0$
This leads to $F = Jk^4 e^{-2k^2 t}$ ......(2.68)

and the law of decay in this case is
$$\overline{u'^2} \ \alpha \ (t-t_0)^{-5/4} \quad ; \quad \lambda^2 = 4\nu(t-t_0)\ldots..(2.69)$$

Case II :- Loitsianski's invariant exists and the influence of viscous dissipation is restricted to high frequencies whereas for low frequencies the transfer term is the prevailing factor . Von Karman and Howarth (71) and Kolmogoroff (36,37,38) have treated this problem. The former authors came to the conclusion that any power law for the decay - time relation may prevail in the decay process while Kolmogoroff gave the law
$$\overline{u'^2} = \text{constant} \cdot t^{-10/7} \quad \text{and} \quad \lambda^2 = 7\nu t \ldots.(2.70)$$

Case III :- Similarity extends over the whole frequency range, with the exception of the lowest. It is assumed that the deviation from similarity shall occur for such small values of k that, whereas the contribution of the deviation is negligible

for computation of ϵ, it enters the calculation of energy.

The above assumption implies that all the higher moments of $F(k)$ are not appreciably influenced by the deviation from similarity. Lin (44) on this assumption derived the decay law.

$$\overline{u'^2} = a\,(t-t_0)^{-1} + b \qquad \ldots\ldots\ldots(2.71)$$

where a and b are constants with $a > 0$

and

$$\lambda^2 = 10\,\nu t\,\left(1 - \frac{10\,u_D^2}{D_0}t\right) \qquad \ldots\ldots(2.72)$$

where u_D^2 is an additive constant giving the departure of the energy content from that in the case of similarity and D_0 is the initial diffusion coefficient.

$$D_0 = \lim_{t\to 0} \frac{\overline{u'^2}\,\lambda^2}{\nu} \qquad \ldots\ldots(2.73)$$

Equation (2.71) can thus be rewritten as

$$\overline{u'^2} = (D_0/10)\,t^{-1} - u_D^2 \qquad \ldots\ldots(2.74)$$

Case IV :- The assumptions in Case III are based on the idea that the low frequency components do not have the time to adjust themselves to an equilibrium state. It is specifically assumed that ϵ may be calculated by a similarity spectrum. Goldstein (22) further generalised the similarity theory and assumed that similarity spectrum might be adequate only for the calculation of higher moments of $F(k)$. He assumed that the statistical properties of turbulence in a range of wave numbers depend not only on the time rate of dissipation ϵ per unit volume and the viscosity ν, but also on the time rate of change $d\epsilon/dt$ of ϵ. Thus the similarity spectrum, according to Goldstein, is only asymptotically correct for a range

of large wave numbers, the range depending on the initial conditions and decreasing as the decay proceeds. He defined the Reynolds Number R as $R = \left\{ \overline{u'^2} \, (t-t_o) \right\}_{t-t_o} / \nu$, where $\left\{ \overline{u'^2} \, (t-t_o) \right\}$ with a suitably chosen origin, is a function of time $(t-t_o)$ and is finite at $t = t_o$. On this basis the general decay law is

$$\overline{u'^2} \, (t-t_o) = R_t \, d(t-t_o) \quad \ldots\ldots\ldots(2.75)$$

where $d(t-t_o)$ is an integral function of $(t-t_o)$ such that $d(o) = 1$ and with an asymptotic value for large $(t-t_o)$, such that it gives the correct law of decay for the final period, i.e. when the viscous dissipation becomes predominant, R becoming very small. The solution for this case is definitely known (Case I). Also $d(t)$ and the number of constants needed to specify it approximately depend on the initial conditions.

If the similarity spectrum is taken as accurate for the calculation of $\int_0^\infty k^4 E(k) dk$ and higher moments, the decay equation is such that $\overline{u'^2} \, (t-t_o)$ is a quadratic expression in $(t-t_o)$ and takes the form

$$\overline{u'^2} \, (t-t_o) = a + b \, (t-t_o) + c \, (t-t_o)^2 \quad \ldots..(2.76)$$

Further generalisation of the above equation is also possible. As the similarity spectrum covers a smaller and smaller range of wave numbers $\overline{u'^2} \, (t-t_o)$ will be expressible as a polynomial of higher and higher degree.

According to the above arguments, a change in initial conditions should bring about a change in the decay law. It should also bring about increasing departures from similarity

spectrum for $F(k)$. These departures from similarity spectrum decreasing for higher moments of $F(k)$.

d) Decay of Isotropic Turbulence :- In practice, isotropic turbulence is generally produced by means of grids placed in a uniform stream and the distances downstream of the grids are taken as corresponding to different times of decay on the basis of Taylor's hypothesis. Based on experimental work, Batchelor and Townsend (7,8) have distinguished three different periods (or zones) of decay. They are (i) the initial period, (ii) the transition period, and (iii) the final period. As mentioned above, these three periods correspond to increasing distances downstream from the turbulence producing grid.

Final Period of Decay :- In the final period of decay, which occurs at a considerable distance downstream from a grid producing turbulence, the Reynolds number of turbulence is very low. The inertial forces are negligible and only the viscous forces are effective. The problem is then amenable to explicit solution and the decay law is given by eqn.(2.69) as discussed in Case I above.

Initial Period of Decay : Much experimental information has been obtained for the initial period of decay . Stewart and Townsend (57) and Batchelor and Townsend (6,7,8) have carried out a very systematic investigation of decay behind grids . Their measurements of the decay as well as turbulence spectra behind grids indicate that a linear decay law prevails during the initial period. The expression given for this decay law by Batchelor (4) in terms of distance from grid is ;

$$\overline{u}_1^2 / \overline{u_1'}^2 = \frac{c}{C_D} \left\{ \frac{x_1}{M} - (x_1/M)_o \right\} \dots \dots (2.77)$$

where C_D is the drag per unit area on the grid, c is a constant depending on grid geometry, x_1 is the distance downstream from the grid and M is the mesh width of the grid, and $(x_1/M)_o$ represents the x_1/M value at some chosen origin of time (or distance).

Equation (2.77) represents a decay law of the type $\overline{u'}^2 (t-t_o) = $ constant which conforms to the recommendations of Karman and Howarth as given in Case II above. According to Lin (44), these authors did not include Case III in their discussions but it fits all their experimental findings. According to him, their measurements of the decay conform to Case III rather than Case II though the variations are very small. The measurements of spectrum by the above authors, however, according to Lin, provide a more definite verification of Case III.

It is to be noted, however, that in the above experiments no change in initial conditions was brought about for studying the decay behind various grids. Experiments by Tsuji and Hama (66) on decay behind grids with change of initial conditions indicate that the decay law depends strongly on the initial conditions, a result which follows from assumptions in case IV. The experimental data obtained by the author has been discussed on the basis of the above assumptions in Chapter V.

CHAPTER - III

METHODS OF TURBULENCE MEASUREMENT

3.1 Preliminary Remarks :

The discussion in this chapter is devoted to a brief review of the different methods of measurement of turbulence and their suitability for measurements of turbulence in liquids . However, attention is focussed primarily on the use of Faraday's law and the associated fundamentals for the development of a turbulence measuring device.

3.2 Methods Other Than Electromagnetic Induction :

There are a number of methods used for measurement of turbulence. Important ones amongst them are discussed in brief under this head.

a) Hot Wire Anemometer :   In its basic form, the hot-wire anemometer is a short length of a fine, temperature-sensitive wire heated by direct electric current. The wire is commonly made up of platinum, nickel or tungsten. When placed in a fluid stream, the hot wire loses heat to the fluid by forced convection. When the hot-wire is in 'equilibrium', the rate of heat loss to the stream by forced convection plus the heat loss to the end supports by conduction equals the rate of heat input to the wire. The equality between heat input and losses is the basis for all equations which relate the electrical parameters of the hot wire to the flow parameters of the fluid.

For the heat loss from an ideal, infinitely long, uniformly heated circular cylinder placed normally in a uniform

stream of a frictionless incompressible flow, King (34) experimentally found

$$\text{Heat loss} = I^2 R_W = (A' + B'\sqrt{\rho U})(T_W - T_a) \quad ....(3.1)$$

where I — Electrical current flowing through the wire,

T_W — Temperature of heated wire.

T_a — Temperature of the fluid

U — Fluid velocity

A', B'— Constants depending on wire and fluid characteristics.

Since the electrical resistance of a wire is a function of the temperature , one has

$$R_W = R_o \left\{ 1 + \alpha(T_W - T_o) \right\}$$

and $$R_a = R_o \left\{ 1 + \alpha(T_a - T_o) \right\}$$

or $$T_W - T_a = \frac{R_W - R_a}{\alpha R_o} \quad ....(3.2)$$

where, R_W — Wire resistance at temperature T_W

R_a — Wire resistance at temperature T_a

R_o — Wire resistance at reference temperature T_o (usually 32° F) at which α is evaluated

α — Temperature coefficient of electrical resistivity of the wire.

Combining equations (3.1) and (3.2) one gets ;

$$\frac{I^2 R_W}{R_W - R_a} = \frac{A'}{\alpha R_o} + \frac{B'\sqrt{\rho}}{\alpha R_o}\sqrt{U} = A + B\sqrt{U} \quad ....(3.3)$$

In hot-wire anemometer equation (3.3) is used to relate the heat input to the fluid velocity where the constants

A and B are found experimentally from the linear curve of I^2 versus $\sqrt{U}$ as shown in the following figure.
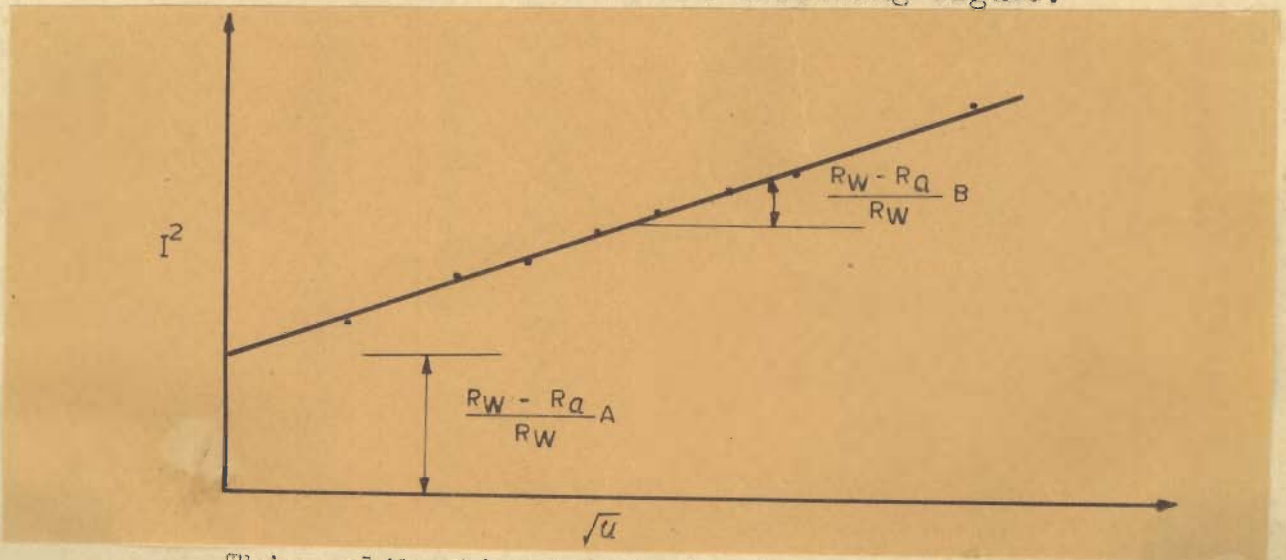
This calibration has to be done in a gas flow with a turbulence intensity as low as possible. It has been found that such a static calibration may be satisfactorily used in turbulence measurements.

Two different methods are used for carrying out the turbulence measurements .

The Constant Current Method : -   Here the current I is kept constant; the temperature and hence the resistance changes with the fluctuating velocity. The hot-wire is built into a Wheatstone bridge as shown schematically in the figure below. To maintain the constant wire current, the Wheatstone
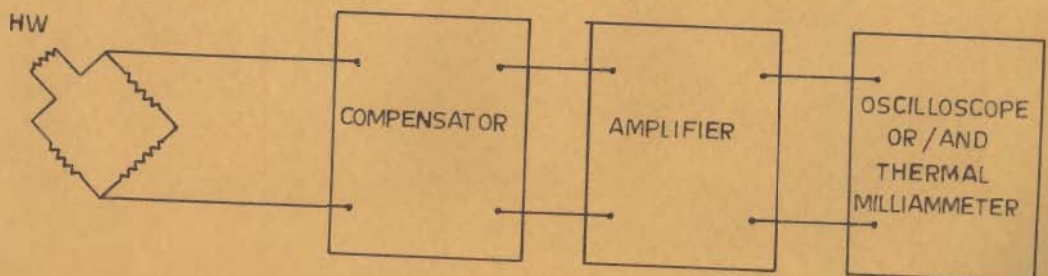
bridge is supplied with current from a high voltage source and passes through a large current control resistor which is much larger than the bridge resistance. Therefore changes in the hot wire resistance will have very little effect on the current flowing from the battery, thus preserving the constant current condition.

The Constant Temperature Method : In the constant temperature anemometer system, the wire resistance (hence the temperature) is held constant. A velocity fluctuation $\triangle u$ in the stream will cause a fluctuation in the current passing through the hot-wire $\triangle I = \dfrac{\triangle e}{R_W}$. The hot wire which is again built into a Wheatstone bridge, as schematically shown in the following figure, is automatically supplied by the amplifier, through a feedback system, with the exact amount of current necessary. to keep it at a constant resistance R_W
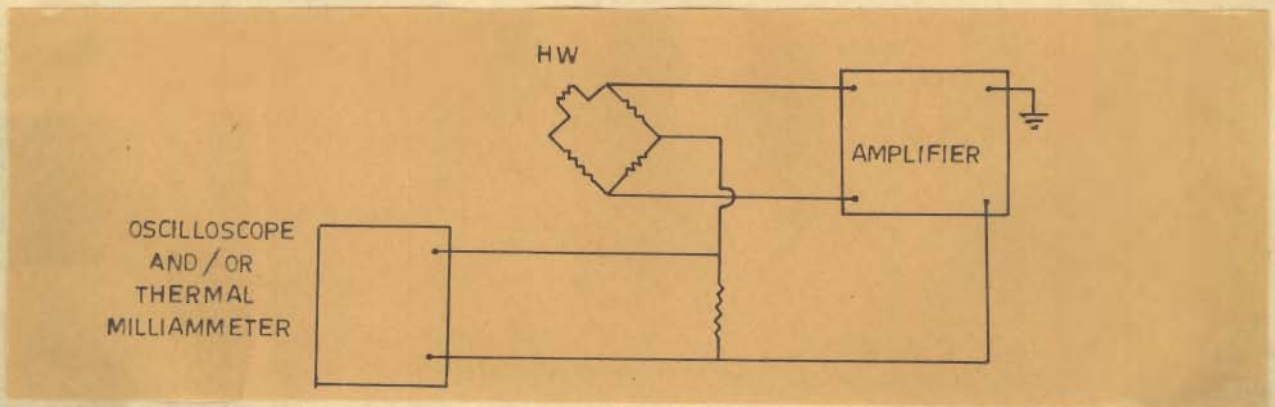
For the constant current set, if one intrduces $u_1 = \bar{u}_1 + u_1'$ and $R_W = \bar{R}_W + r_W'$ in eqn. (3.3) then one can write the equation as

$$ - \frac{I^2 r_W R_a}{(\bar{R}_W - R_a)^2} = B \sqrt{\bar{u}_1} \, \frac{u_1'}{2\bar{u}_1} \qquad \ldots\ldots(3.4)$$

provided $\dfrac{u_1'}{\bar{u}_1} \ll 1$ so that $\dfrac{r_w}{\bar{R}_W - R_a} \ll 1$.

Thus the change e in voltage across the wire, corresponding to the turbulence-velocity change u_1' is

$$e = I r_w = - \frac{(\bar{R}_W - R_a)^2}{2 I R_a} \, B \sqrt{\bar{u}_1} \, \frac{u_1'}{\bar{u}_1}$$

or $e = - S_{cc} u_1'$ ......(3.5)

where $S_{cc} = \dfrac{(\bar{R}_W - R_a)^2}{2 I R_a} \, \dfrac{B \sqrt{\bar{u}_1}}{\bar{u}_1}$ is the sensitivity of the wire.

Equation (3.5) then governs the response of the hot wire. u_1' can thus be measured by leading the voltage signal e via an amplifier to a thermal milliammeter - u_2' and u_3' can be measured by making use of the direction - sensitivity of the hot-wire. The ratio of cooling is determined mainly by the velocity component perpendicular to the wire. The effect of the velocity component parallel to the wire becomes noticeable only when the normal velocity component is very small or zero.

For measurement of shear stresses, two wires in an X-array (as shown below) are used.
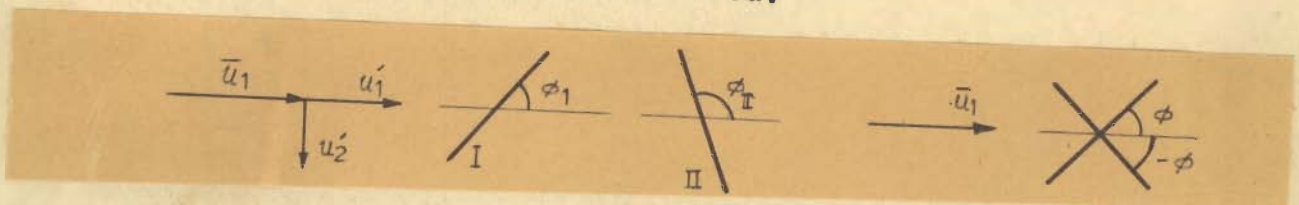
The response of the two hot wires can be worked out by considering the response of a wire in positions I and II as shown in the figure. If the wires are placed in the

$\bar{u}_1 - u_2'$ plane, the responses are

In position I : $(e)_1 = -(S_1)_1 u_1' - (S_2)_1 u_2'$

In position II: $(e)_2 = -(S_1)_2 u_1' + (S_2)_2 u_2'$

The wires in the X-array are matched so that $(S_1)_1 = (S_1)_2$ and $(S_2)_1 = (S_2)_2$. The signals obtained through the two wire can then be lead to a thermal milliammeter (i) directly and (ii) through an adding and subtracting circuit resulting in readings for $\overline{e_1^2}$, $\overline{e_2^2}$, $\overline{(e_1+e_2)^2}$ and $\overline{(e_1 - e_2)^2}$ from which $\overline{u_1'^2}$, $\overline{u_2'^2}$ and $\overline{u_1'u_2'}$ can be computed. By changing the plane of the wires in the X-array one can compute the other shear stresses also.

For a constant temperature set, the equation governing the response of the hot wire is

$$e = S_{ct} - u_1' \qquad \dots\dots(3.6)$$

where $\quad S_{ct} = \dfrac{\overline{R}_W \cdot R_a}{4\,\overline{I}} \quad \dfrac{B\sqrt{\overline{u}_1}}{\overline{u}_1}$

which is similar to eqn. (3.5) except that the sensitivity S_{ct} is different. Measurements are made in a manner similar to that of the constant current set.

<u>Limitations of Hot Wire</u> : Although linear response equations have been used in the above analysis, in practice the response of the wires is affected by ;

i) Finite thermal inertia of the wire, causing a time lag between the rapid fluctuations of the air and the corresponding fluctuations of the wire temperature. Compensation for this thermal lag can be made

electronically, though the compensation is for amplitude only and not for the phase shift.

ii) Cooling action of wire supports. This effect can be minimised by keeping the thermal conductivity of the support material lower than that of the wire. This effect has been studied in detail by Betchov (28) and Lowell (28).

iii) Non uniform velocity distribution along the wire. This effect can be minimised by a thin, short wire, although stability must be reckoned with in deciding upon the ℓ/d ratio of the wire. Generally wires of 2.5 - 5.0 μ dia. and 0.5 - 1 mm length are used.

The hot-wire has become an almost standardised technique for turbulence measurements in air flow. The development has come through its extensive use by various investigators such as Townsend, Stewart, Dryden, Laufer, Batchelor, Corrsin, Vander Hegge Zijnen and others (28). The use of hot wire anemometer in water has been reported by Richardson, Stevens, and Patterson (11) though the success has been limited.

The main limitations of the hot-wire anemometer as a turbulence measuring device in liquids are :-

i) Deposition of impurities on the wire, requiring frequent cleaning of the wire and recalibration.

ii) Low operating temperatures are needed to prevent evaporation, electrolysis, formation of scales and algae etc.

iii) Formation of air bubbles round the wire.

iv) Thicker and longer wires are needed to fulfill
strength requirements, having an adverse effect
on the sensitivity of the wire.

b) Hot Film Anemometer :   The hot-film anamometer - a
modified version of the hot-wire - was introduced by Hubbard
and Ling (46) for liquid turbulence measurements. It is
similar to the hot-wire , except a heated, very thin plati-
num film is used as the sensing element. This film, which
has a length of 1 mm and a width of 0.2 mm, is fused onto
the wedge-shaped end of a glass or ceramic support. The rest
of the components are the same as for a hot-wire.

The hot-film has the advantage of being more
rugged and stable compared to the hot wire. Later applica-
tions of the hot film were reported by Cohn (10) and Tan and
Ling (58) . This method, however, shares some of the draw-
backs of the hot-wire, such as the formation of bubbles,
evaporation , electrolysis etc., requiring low operating
temperatures. Sensitivity to surface contamination, however,
as claimed by Hubbard and Ling (46) is low. They also claim
a superior signal to noise ratio compared to the hot-wire,
under similar operating conditions, particularly for the
constant temperature method.

c) Electric Discharge Anemometer : This method, useful for
turbulence measurements in gases only, is based on the poten-
tial-electric-current characteristic of an electric discharge
between two electrodes. For electrodes of a given shape and

gap, the characteristic depends on the nature of the gas, the pressure, temperatures, humidity and velocity. It is the dependence on velocity that makes the electric discharge applicable to turbulence measurements. Differences in discharge potential of the order of 1 volt are obtainable for velocity differences of 1 m/sec which need little amplification. Also the effects corresponding to the thermal-inertia effects of the hot-wire are insignificant. Applications of this method for turbulence measurements have been reported by Lindwall, Fucks, Agostini, and Werner (28).

d) Total Head Tube : A device, making use of a total head tube in combination with a capacitance type pressure transducer, was used by Ippen (30) for turbulence measurement in liquids. A sketch showing the instrument in principle is as shown below .
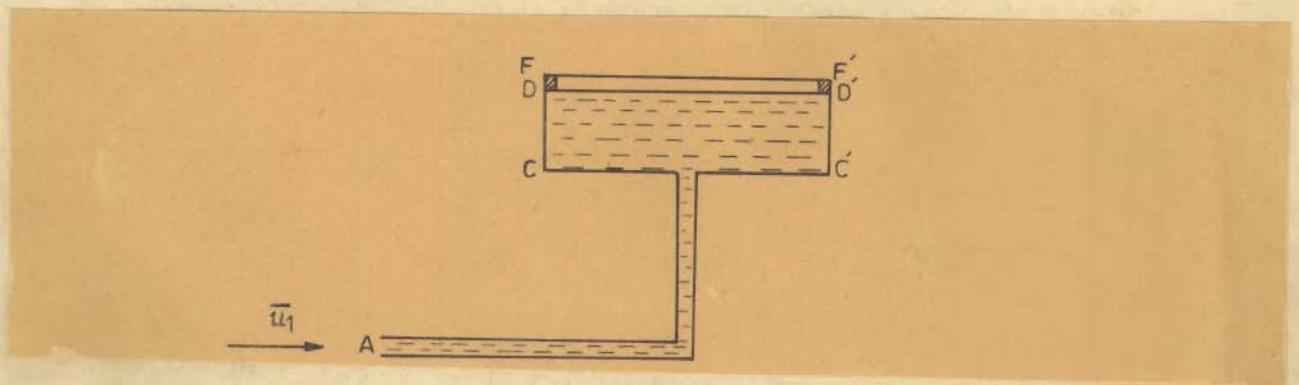
A total head tube is connected at one end to a pressure chamber of larger cross-section area CDD'C'. The other end of the chamber is closed by a thin diaphragm DD'. This diaphragm is placed at a short distance from another fixed plate FF' as shown and electrically insulated from it. The tube and the pressure chamber are filled with the liquid

in the beginning and the tube placed at the point where the
measurements are to be made. Any fluctuations in the velo-
city at the point A give rise to a corresponding change in
pressure in the chamber, which in turn gives rise to dis-
placements of the diaphragm DD'. When the diaphragm DD'
moves, the air gap between DD' and FF' changes resulting in a
change of capacitance between the two plates (i.e. DD' and FF')
This capacitance change is measured electronically and from
this the turbulent fluctuations can be obtained. For better
frequency response, the resonance frequency of the diaphragm
DD' should be much larger than the frequency of the fluctua-
tions to be measured. Eagleson (19) used a quartz crystal
as the pressure transducer instead of the capacitance between
DD' and FF' and claims better frequency response. Other
pressure tranducers such as barium titanate ceramic have also
been used (50).

The total head tube in combination with the
pressure transducer gives a stable instrument with repro-
ducible results, but its versatility is limited. It can
measure turbulent velocity fluctuations provided the turbu-
lent pressure fluctuations are negligible. Further it can
measure the velocity fluctuations, only when there is an
appreciable mean velocity of flow, and that too in the direc-
tion of the mean velocity only. No transverse velocity fluc-
tuations can be measured.

e) Methods Based on Flow Visualisation : Certain methods for measurement of turbulence in liquids based upon flow visualisation have also been used by various experimenters. These consist mostly of introducing some very tiny insoluble particles in the fluid and then observing their paths cinematographically (28). Use of emulsions - which are mixtures of benzene and carbon tetrachloride or olive oil and ethylene dibromide - has been made for applying these methods to water. The emulsion can be made such as to have the same density as water and tiny droplets of it introduced in the flow field. Sometimes a suitable material miscible with the flowing fluid can be introduced continuously in the flow and its dispersion measured downstream from the injection point. Sometimes the tracer can be introduced electrically as well which is especially useful in observations of the boundary layer (29).

These methods have the drawback that they give only limited information about the flow field and quantities such as correlation or spectra cannot be measured.

f) Electrokinetic Transducer : Recently Cermak and Baldwin (10) have reported the use of electrokinetic transducers for measurement of turbulent flow in water. The method, still in the development stage, makes use of Helmholtz's theory of streaming-potential for turbulence measurements. Helmholtz's theory predicted that a d.c. potential difference would be generated by the laminar flow of liquids through capillary tubes made of materials which are electrical insulators. Bocquet (10) was the first to report instantaneous fluctua-

tions of streaming-potential, due to turbulent flow, at solid-liquid interfaces. Binder (9), measured the streaming-potential fluctuations by using copper electrodes flush with the wall of a glass pipe while, Chuang (10) and Duckstein(10) succeeded in adapting the electrokinetic electrodes to the study of fully developed pipe flow and two-dimensional wall jets respectively. The transducer used by the latter workers being in the form of a probe with two closely spaced electrodes, the instantaneous potential difference signal from which is related to the component of the turbulent velocity fluctuation along the line between electrode centres.

This method holds a lot of promise, though more knowledge must be obtained on the effect of mean velocity level upon response to velocity fluctuations, the selectivity of various electrode configurations to velocity fluctuation direction and the effect of fluctuation magnitude on signal output. A sound theoretical analysis relating turbulent velocities in the oncoming flow to the potential differences sensed by the electrode pair is also wanting.

3.3 Method of Electromagnetic Induction :

The method which is intrinsically most nearly perfect for measuring velocities (turbulent fluctuations included) is that of electro-magnetic induction (26,35). 'It is capable of indicating over an extremely wide range (of frequencies) has zero lag, is practically independent of conductivity, temperature, pressure and gaseous or solid impurities and indicates the true vector components of velocity' (29). Based on Faraday's law of electromagnetic induction, this method

has tremendous potential, though some problems need to be overcome before it can find widespread application.

a) Electromagnetic Induction in a Fluid in Motion : The treatment here follows that given by Day (14). When a force F_e (of electric origin) is exerted on a charged particle at a point, an electric field E is said to exist. Then,

$$\underline{E} = \underline{F_e}/q \qquad \dots\dots(3.7)$$

where q is the charge of the particle.

When the charged particle is stationary, an electrostatic field of intensity E is the only field present. If the particle moves, an electromagnetic field is superposed on the electrostatic field. When the charged particle moves through an electromagnetic field, the additional force per unit charge exerted upon it will be

$$\underline{Fm}/q = \underline{V} \times \underline{B} \qquad \dots\dots(3.8)$$

where V = velocity of the moving charged particle

B = strength of the electromagnetic field

The total force acting on the moving charged particle will be the sum of the above two. Therefore

$$\underline{F}/q = (\underline{F_e} + \underline{Fm})/q = \underline{E} + \underline{V} \times \underline{B} \quad \dots\dots(3.9)$$

When this force acts on the charged particle over a distance, work is done. The electrical potential energy of a unit charged particle at a point is called the potential at that point. It is in fact the work done or the electrical potential energy gained when moving a unit charge from infinity to the point under consideration. The potential difference between any two points is thus the change in the

amount of electrical potential energy per unit charge between the two points.

An electromotive force (e.m.f.) ε is defined as that portion of an electrical circuit in which non-electrical energy is converted to electrical energy.

Faraday discovered that a source of e.m.f. results when there is a change of magnetic flux through a conductor placed in a magnetic field. The law that bears his name is

$$\varepsilon_{induced} = -\int \frac{d}{dt} (\underline{B} \cdot \underline{n}) \, dA \qquad \ldots\ldots(3.10)$$

where n = unit normal vector

A = Surface area of the conductor

This equation states that the induced e.m.f. in a circuit is equal to the negative time rate of change of the magnetic flux through the conductor. Lenz's law states that the polarity of the e.m.f. is such that it tries to oppose the field causing it.

The change in magnetic flux may be caused either by a change in magnetic field (transformer action) or by a movement of the conductor with respect to the magnetic field (motional induction). In the case of a fluid flow steady in time relative to a constant external magnetic field, it is the motional induction which is operative.

Any e.m.f. may be defined by the integral

$$\varepsilon = \oint \underline{F}/q \, \underline{d\ell} \qquad \ldots\ldots(3.11)$$

where ℓ is an arbitrary line enclosing the source.

But for moving charges, the value of $\underline{F}/q$ can be substituted from equation (3.9) yielding;

$$\varepsilon = \oint \underline{E} \cdot d\underline{l} + \oint \underline{V} \times \underline{B} \cdot d\underline{l} \qquad \ldots\ldots\ldots(3.12)$$

$$= 0 + \oint \underline{V} \times \underline{B} \cdot d\underline{l} \qquad \ldots\ldots\ldots(3.13)$$

Then equating (3.10) and (3.13) we obtain

$$\varepsilon_{induced} = -\int_A \frac{d}{dt}(\underline{B} \cdot \underline{n})\, dA = \oint \underline{V} \times \underline{B} \cdot d\underline{l}$$

$$\ldots\ldots(3.14)$$

The potential difference between two points in an electric field is

$$\emptyset_{ab} = -\int_a^b \underline{E} \cdot d\underline{l} \qquad \ldots\ldots\ldots\ldots(3.15)$$

Since the electrostatic vector is irrotational, the potential $\emptyset$ and electric field intensity are further related,

$$\nabla \emptyset = -\underline{E} \qquad \ldots\ldots\ldots\ldots(3.16)$$

b) Induced Voltage - Turbulence Intensity Equations : The equations mentioned above can be used to develop the relationships for measuring turbulence with electromagnetic induction, as discussed by Grossman (26).

The current density $\underline{J}$ for a conductor of area A carrying a current $\underline{i}$ is given by

$$\underline{J} = \underline{i}/A = \sigma \underline{F}/q \qquad \ldots\ldots\ldots(3.17)$$

where σ = electrical conductivity

This gives

$$\underline{i}/\sigma A = \underline{F}/q = \underline{E} + \underline{V} \times \underline{B} \qquad \ldots\ldots\ldots(3.18)$$

from equn. (3.16) this yields,

$$-\nabla \emptyset = \underline{B} \times \underline{V} + \underline{i}/\sigma A \qquad \ldots\ldots(3.19)$$

Considering the following orientation of flow and

magnetic field in a rectangular coordinate system ;
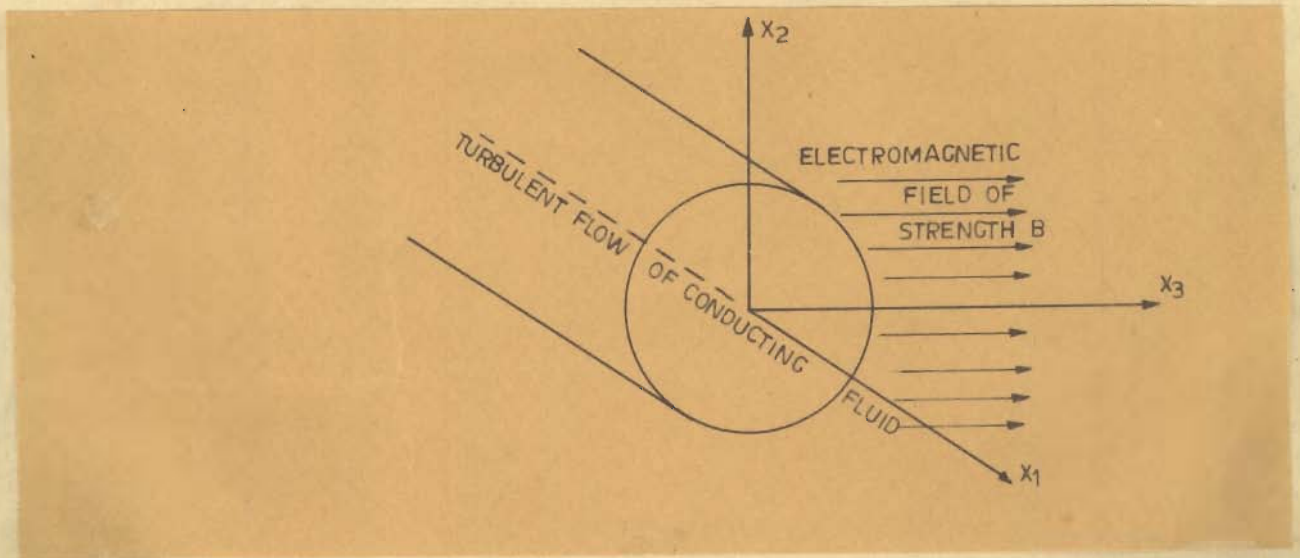
The three components represented by equation (3.19) are then

$$- \frac{\partial \phi}{\partial x_1} = - B.u_2 + \frac{i_{x1}}{\sigma A} \qquad \ldots\ldots\ldots(3.20)$$

$$- \frac{\partial \phi}{\partial x_2} = - Bu_1 + \frac{i_{x2}}{\sigma A} \qquad \ldots\ldots\ldots\ldots(3.21)$$

$$- \frac{\partial \phi}{\partial x_3} = i_{x3} / \sigma A \qquad \ldots\ldots\ldots\ldots(3.22)$$

The above equations relate the potential gradient velocity and magnetic field in case of a fluid moving through a magnetic field.

In turbulent flow, the instantaneous velocity may be replaced by the sum of the mean and the fluctuation. Doing the same for the induced e.m.f. and the currents we get for eqn. (3.20)

$$\frac{\partial}{\partial x_1} (\bar{\phi} + \phi') = B (\bar{u}_2 + u_2') - (\frac{\bar{i}_{x_1} + i'_{x_1}}{\sigma A})$$
$$\ldots\ldots\ldots(3.23)$$

Squaring, averaging and separating into the mean and deviation equations we get for fluctuations u_2'

$$\overline{\left(\frac{\partial \phi'}{\partial x_1}\right)^2} = B^2 \overline{u_2'^2} - \frac{2B}{\sigma A}\overline{u_2' i'_{x_1}} + \frac{\overline{i'^2_{x_1}}}{\sigma^2 A^2}$$

$$\dotfill(3.24)$$

and for other directions,

$$\overline{\left(\frac{\partial \phi'}{\partial x_2}\right)^2} = B^2 \overline{u_1'^2} - \frac{2B}{\sigma A}\overline{u_1' i'_{x_2}} + \frac{\overline{i'^2_{x_2}}}{\sigma^2 A^2}$$

$$\dotfill(3.25)$$

and

$$\overline{\left(\frac{\partial \phi'}{\partial x_3}\right)^2} = \frac{\overline{i'^2_{x_3}}}{\sigma^2 A^2} \qquad \dotfill(3.26)$$

If the induced currents i'_{x_2} are neglected and the partial derivatives replaced by finite increments, eqn. (3.25) can be written as

$$\frac{\overline{\Delta \phi'^2}}{\Delta x_2^2 \, B^2} = \overline{u_1'^2} \qquad \dotfill(3.27)$$

Thus equation (3.27) gives the value of the fluctuations in terms of the potential difference between two points and the magnetic field strength. A measurement of the e.m.f. between two points separated by a distance Δx_2 along the X_2-axis therefore gives the value of the velocity fluctuation along the $X_\perp$ - direction , if the magnetic field strength B is known. Similarly ' Eqn. (3.25) can give the fluctuations along the X_2-axis while a different orientation of magnetic field will yield the same values along X_3 - axis.

One of the shortcomings in using the above
equations is the neglecting of induced currents. A proper
evaluation of induced currents can be made if the orientation
of magnetic field can be changed keeping other quantities the
same. Thus while equ.$'$ (3.26) gives the value of i'_{x_3} , the
values of i'_{x_1} and i'_{x_2} can be obtained with different
orientations. This calls for a lot of flexibility in the
experimental set up and work in this direction is necessary
before a proper decision about the effect of induced currents
can be made. In the present work, however, the data has been
presented without taking into account these currents.

-:o:-

CHAPTER - IV

EXPERIMENTAL PROGRAMME

4.1 Preliminary Remarks :

The experimental programme consisted of the analog spectrum measurements for fluctuations of velocity in the x_1 direction. The e.m.f. generated between two points along the x_2 axis due to the passage of water through a uniform magnetic field (in x_3 direction) was measured and analysed. The experiments were carried out in a 2''dia. Lucite pipe with mean velocity of flow in the x_1-direction only. The measurements were made for turbulence in the pipe flow and that generated by various grids singly as well as in combination. The experimental programme is considered in four parts :

Experimental Set Up

Experimental Methods

Scope of Tests

Typical Record and its Interpretation

4.2 Experimental Set Up :

a) Non Electrical System :- A schematic diagram of the system is shown in Fig. 4.1. Water was provided from a recirculatory system. A centrifugal pump with a capacity of 500 g.p.m. against a head of 100 ft. supplied water to the overhead distribution lines. Flow rates were measured by an 'A.O.Smith' turbine-meter connected to a pulse rate integrator. Water passed from the distribution lines to the approach section through a 2'' galvanised pipe. The approach section, 20 ft of 2'' galvanised pipe, was preceded by a valve,
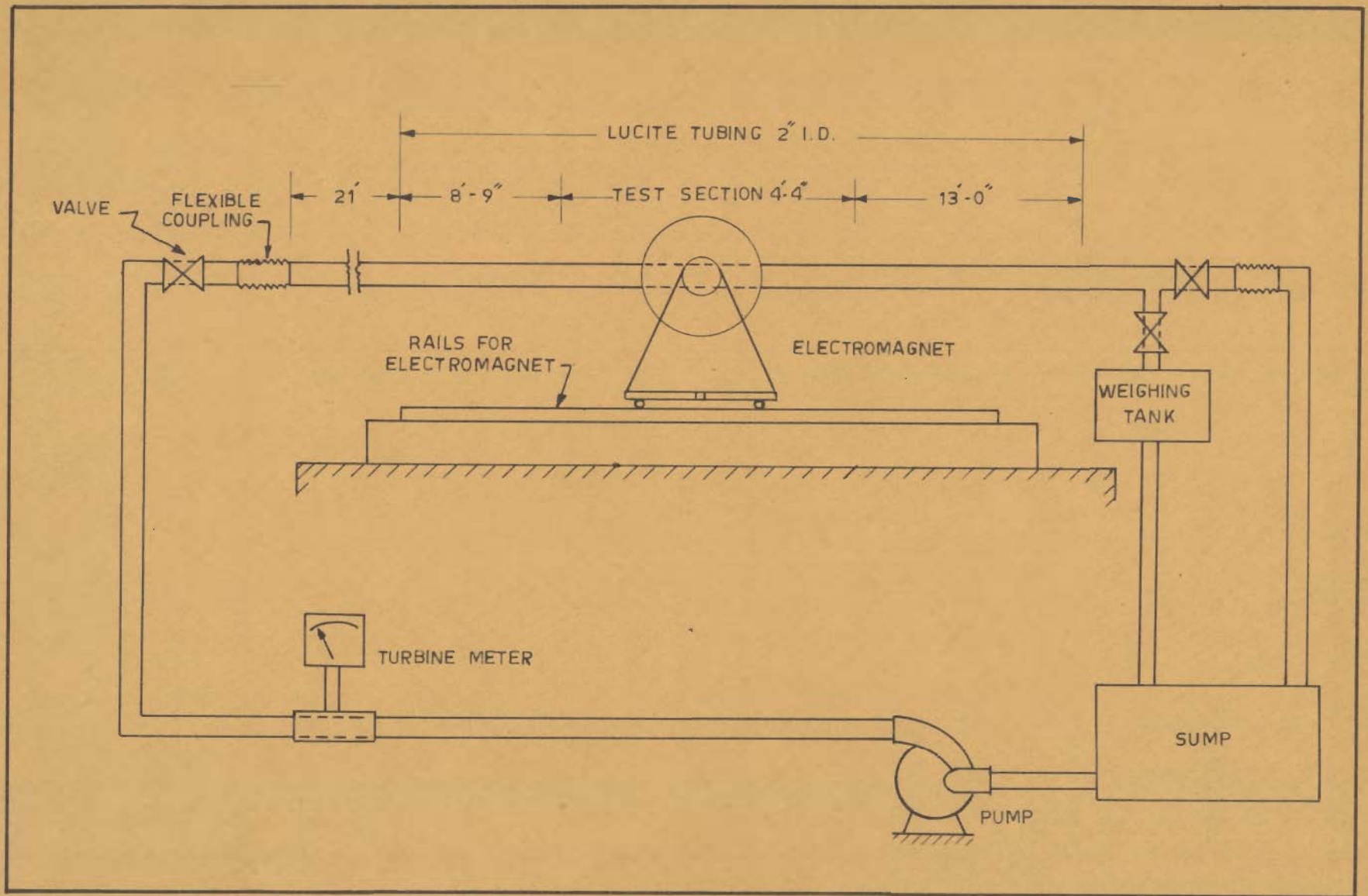
FIG. 4.1. WATER SUPPLY SYSTEM (SCHEMATIC)

a pressure gauge and a rubber pipe section. The rubber
section was used to isolate the approach and the test sections
from the vibrations in the distribution lines. The approach
section was followed by six lengths of 2" diameter lucite
tubing. Each length was 4 ft. 4 in. long and was fitted with
a set of wall to wall probes. The tubing passed between the
pole faces of an electromagnet and the third length contained
the test section where the radial traverse measurements could
be made. The lucite tubing was followed by another rubber
section and a 'tee' with a 2'' and a 0.75'' outlet. The
smaller outlet was used for low discharges. The water from
the larger outlet passed directly to the sump, while the water
from the smaller outlet could be diverted to a weighing tank
for discharge measurements. For larger discharges, the
readings were taken directly from the 'A.O.Smith' turbine-
meter. The approach section and the lengths of the lucite
tubing were supported on angle iron. A frames and were seated
on sponge rubber cushions to further minimise vibrations.

       The test section in the lucite tubing had provision
for the location of screens and access holes for the inser-
tion of the traverse probe. The screens used were of the
type shown below.

The values of 'M' and 'd'   used were

        Screen No. 1 $M = 3/16''$ $d = 1/16''$

        Screen No. 2 $M = 3/8\ ''$ $d = 1/8''$

        Screen No. 3 $M = 3/4''$ $d = 1/4''$

The screens were machined from brass discs of thickness 2 d. They were bi-plane screens made by milling grooves on the discs halfway through from either side and at right angles to each other. They were then turned on a lathe to fit the inside of the lucite pipe. Two small brass rods at right angles held the screens in position.

Access to the interior of the pipe was provided by a lucite boss which was cemented to the top of the pipe downstream from the grids. The boss is shown in Fig. 4.2. There were sixteen access holes, the first eight at 1'' spacing and the next eight at 2'' spacings. The holes were threaded to accept the O-ring seal shown in Fig. 4.2. The stem of the probe was inserted through the O-ring seal and into the pipe. A special wall to wall probe could also be installed in the access holes.

b) Electrical and Electronic System :- The magnetic field was developed by a model L 12-A electromagnet manufactured by the Spectromagnetic Industries Inc., of Hayward, California. The pole faces were 12'' dia. and were set at a 3'' gap. The d.c. power for the magnet was obtained directly from the wall outlets in the laboratory, which in turn were supplied by a silicon controlled rectifier. Approximately 250 volts d.c. was necessary to provide 15 amps. which developed a magnetic

4.75″

1.5″ O.D. BRASS TUBING

PROBE

LUCITE BUSHING WITH
O-RING SEALS
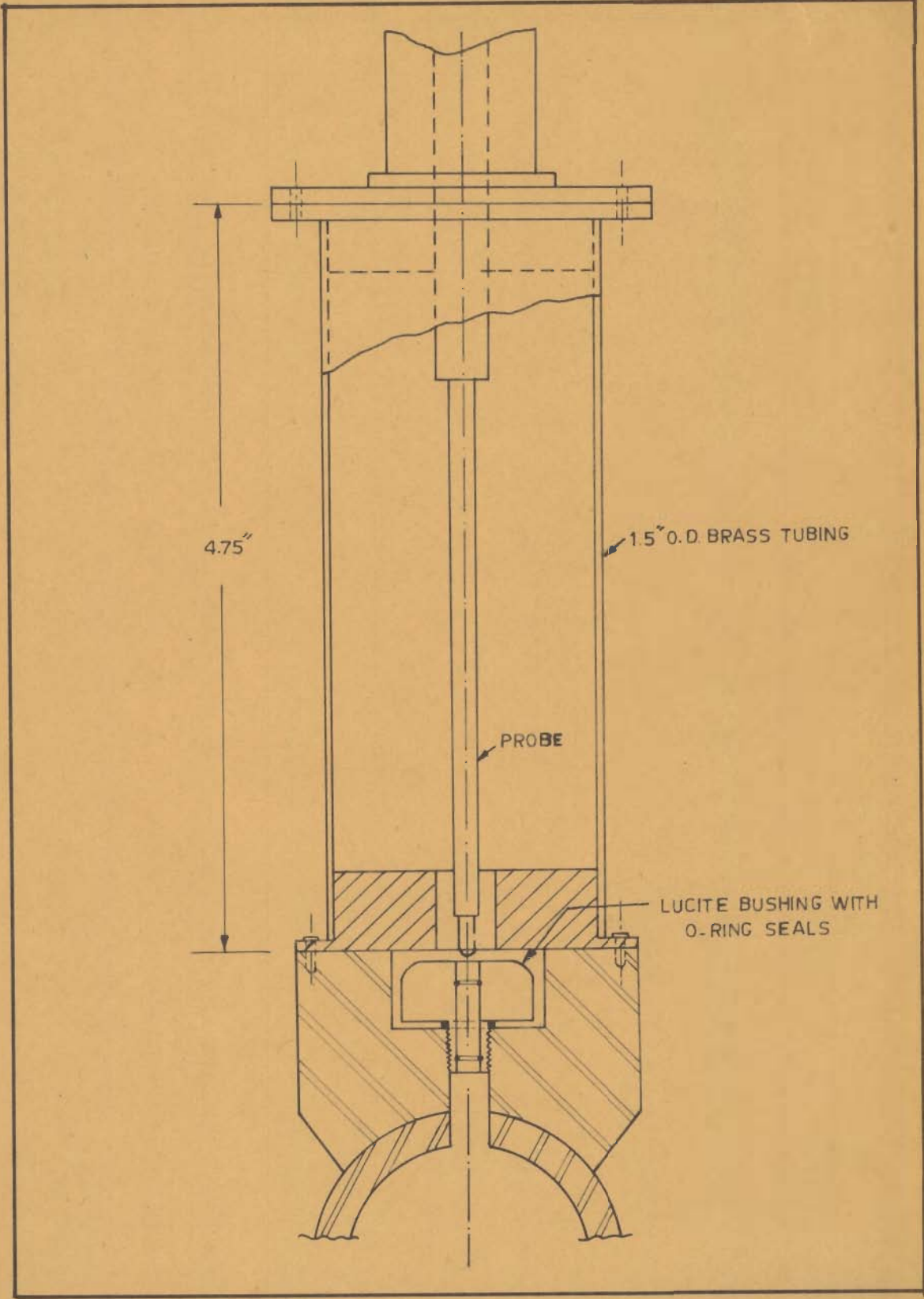
FIG.4.2 _ TRAVERSE PROBE HOLDER AND LUCITE
BOSS DETAILS

field strength of 9700 gauss. A calibration curve for the
magnet is given in Fig. 4.17. Figure 4.3 is a schematic
diagram of the power supply,wiring and cooling water for the
electromagnet. The supply to the magnet could be controlled
from a control rack, which also contained a voltmeter and an
ammeter in the circuit. Reversal of the polarity of the
magnetic field was brought about by a double-pole, double-
throw switch mounted on the electromagnet. Because of the
high inductance of the windings of the magnet, it was necess-
ary to install a device to check objectionable arcs caused
by magnetic field collapse when the supply was shut off.
This was achieved by connecting a selenium rectifier in series
with a 10 ohm 100 watt resistor in parallel with electromag-
net coils. To provide proper heat transfer near the electro-
magnet coils, cooling water was circulated through copper tub-
ing, installed within the magnet housing by the manufacturer.
A 'Shur-Flow' automatic interlock was installed in the
cooling water supply line so that a horn sounded if the
supply to the magnet was put on without opening up the cool-
ing water supply valve or if the quantity of the cooling
water was inadequate. The magnet could be rotated on both
its horizontal axis as well as its vertical axis. It was
mounted on tracks parallel to the lucite tubing so that it
could be positioned at any location along the lucite section.

The e.m.f. induced, due to the flow of water in
the lucite tubing through the magnetic field, was picked up
by means of two types of probes. A set of wall to wall probes
is shown in Figs. 4.4 and 4.7. These probes were furnished by

the Foxboro Corporation and were mounted diametrically oppos-
ed and flush with the inside of the lucite pipe. The wall to
wall probes picked up the potential across the entire pipe
diameter. A wall probe was also installed opposite each
access hole and, used with the special wall probe shown in
Fig. 4.5, provided wall to wall measurements throughout the
test section.

Traverse probe measurements were made with the probe
and holder shown in Figs. 4.2 and 4.5. This probe measured
the potential developed across a gap of 0.08" at any point
along the vertical diameter of the pipe at an access hole. A
close up view and the detailed drawing of the probe are shown
in Figs. 4.6 and 4.8 . The stem of the probe was 1/8" O.D.
type 302 stainless steel tubing, insulated with shrinkable
Teflon tubing. The Teflon tubing was placed over the stem
and the two put in a furnace. At a temperature of 950° F,
the Teflon tubing shrunk onto the stem forming a watertight
and electrically insulated coating. The lower 1/4" of the
stem was left bare and was used to connect the floating in-
put ground of the amplifier to the water. The wires inside
the stem were 0.017" dia. type 302 spring temper stainless
steel. They were also insulated with the help of Teflon
tubing. The two wires extended through the stem and up
through the holder to connect with the impedance isolator in-
put cable. On the other end of the stem they extended out
to a very small distance. The Teflon insulation was removed
from the portions of the wire extending out and these portions
were insulated with several coats of duPont 'Formvar' wire

COOLING WATER

CONTROL RACK
RECEPTACLES

HORN

110V A.C.

PRESSURE OPERATED
MICROSWITCH

0 - 20A

CONSTANT
CURRENT
INDICATOR

ELECTROMAGNET COILS
AND COOLING SYSTEM

ARC
SUPPRESSOR

POLARITY CHANGE
SWITCH

250V D.C.

V   0 - 300V D.C.

−

+
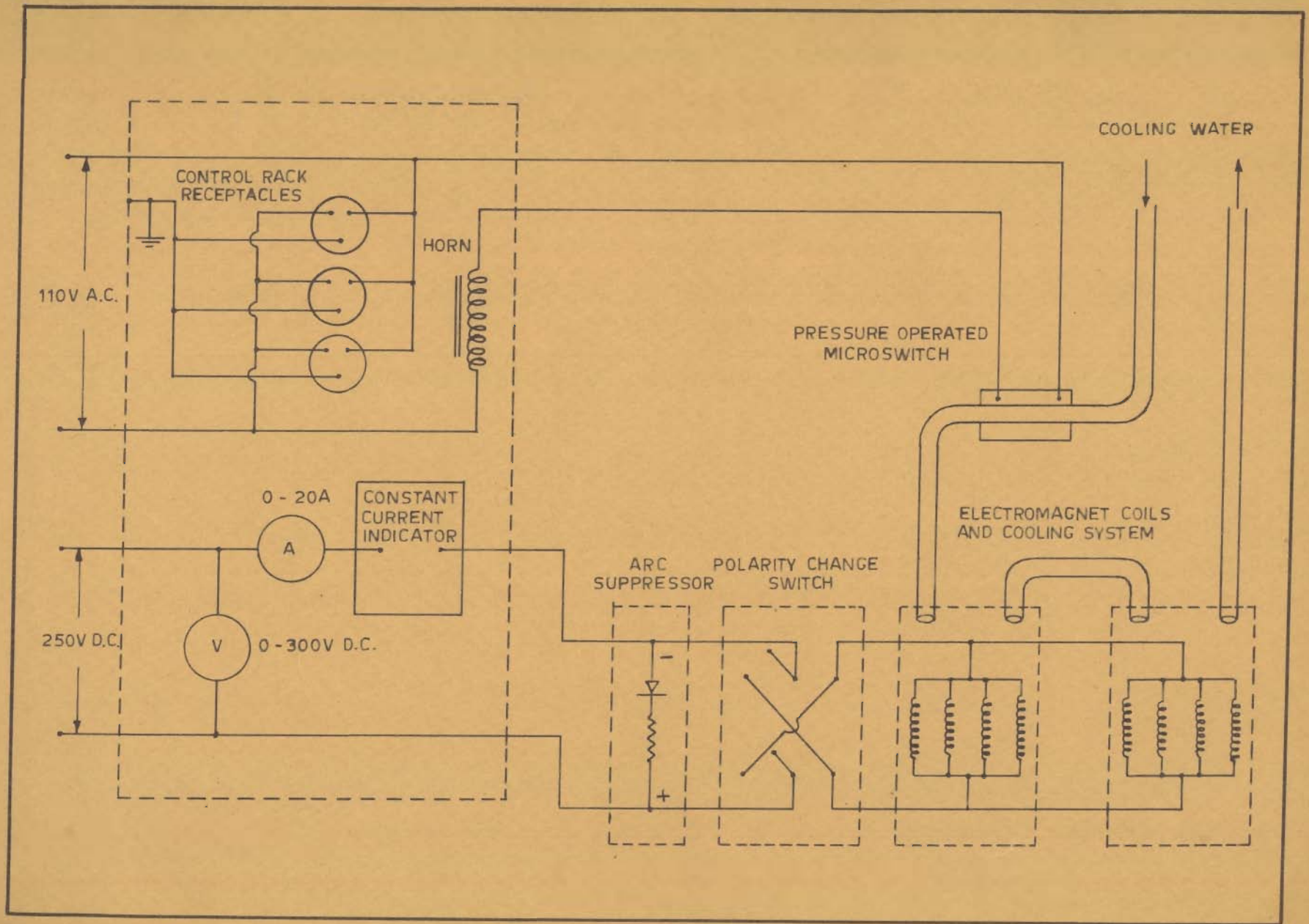
FIG.4.3_SCHEMATIC DIAGRAM OF ELECTROMAGNET POWER SUPPLY
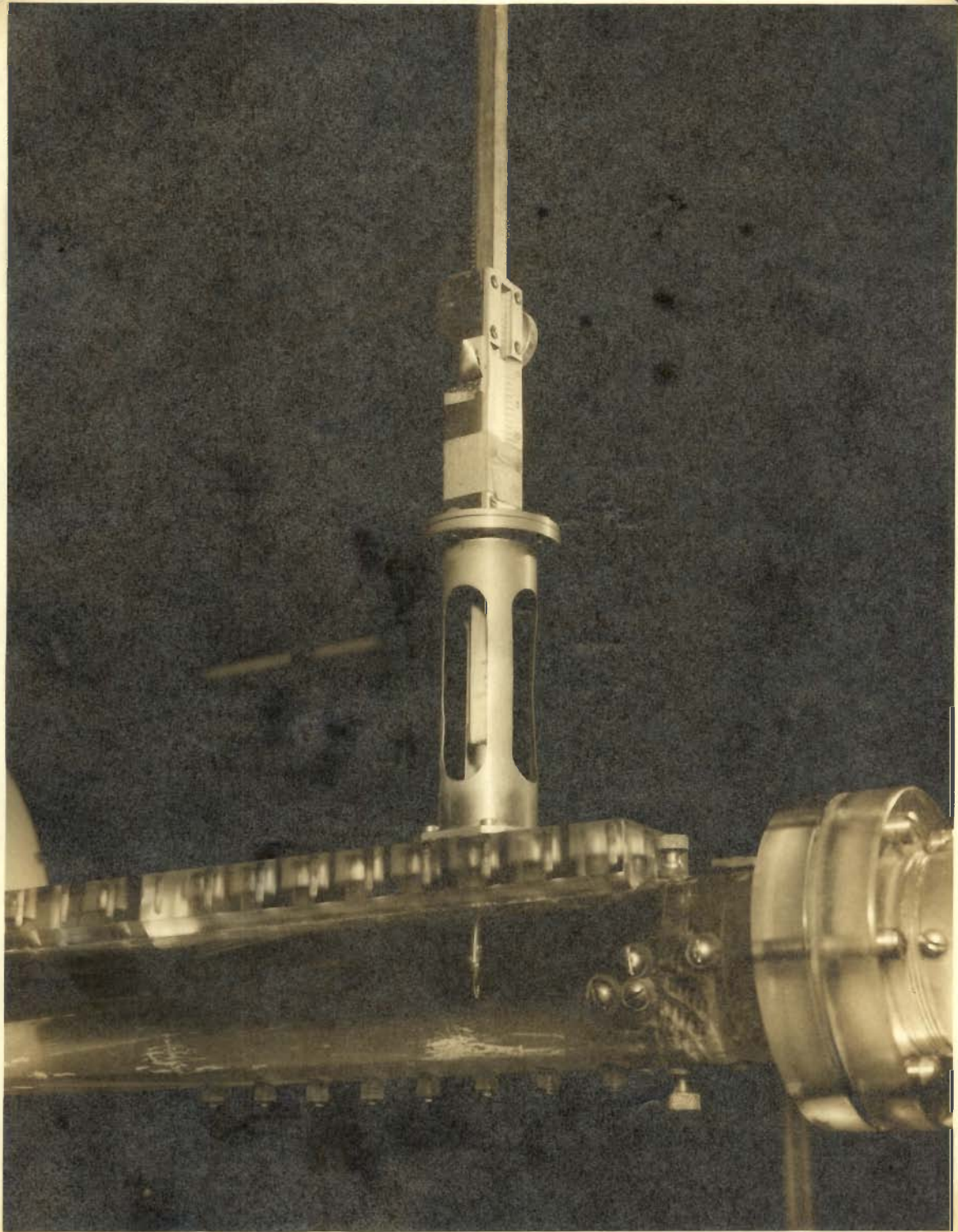
FIG. 4.4   TEST SECTION SHOWING TRAVERSE AND WALL TO WALL PROBES
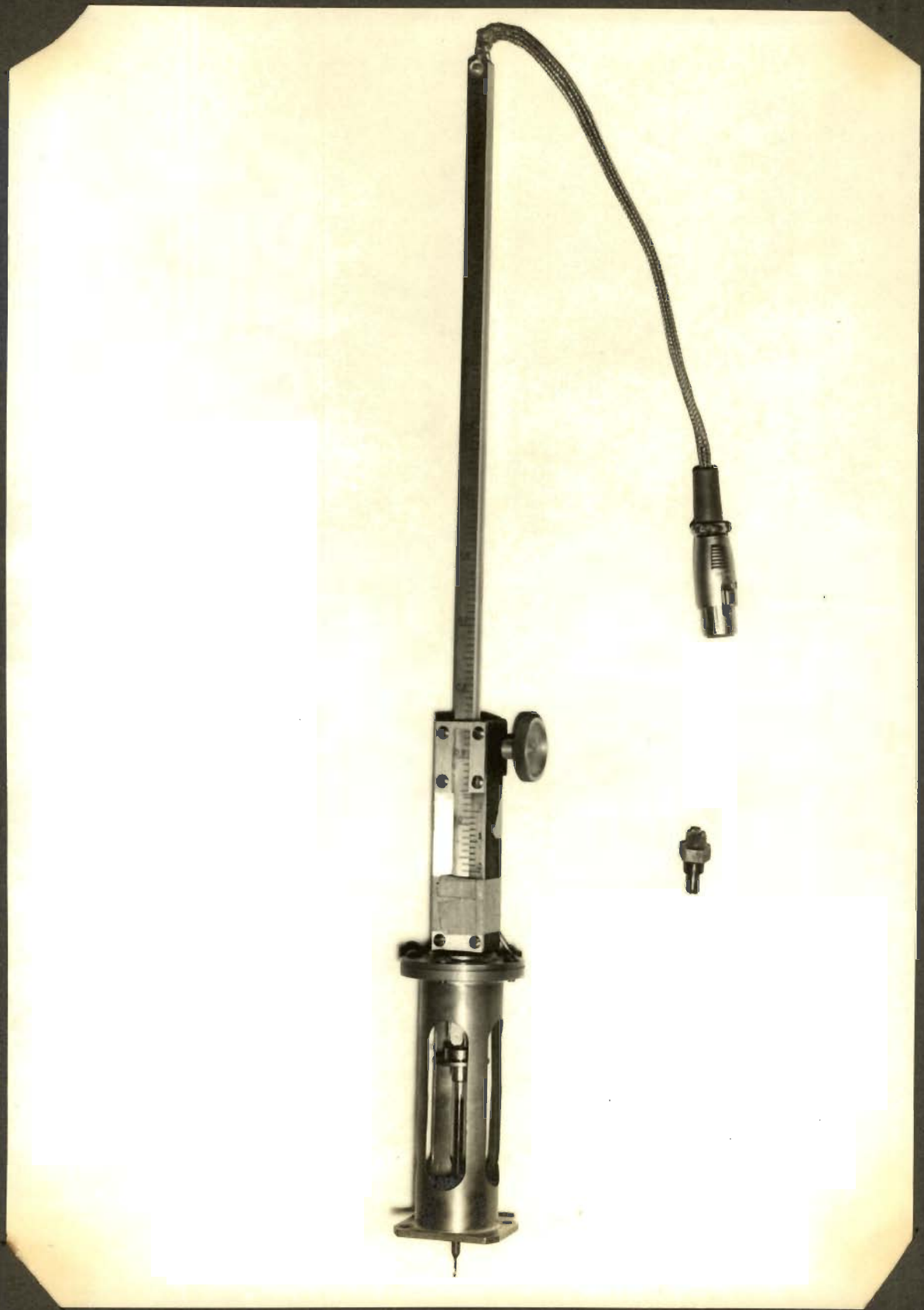
FIG. 4.5   TRAVERSE PROBE WITH HOLDER AND WALL TO WALL PROBE

FIG. 4.6 CLOSE UP VIEW OF TRAVERSE PROBE

SHRINKABLE 'TEFLON' TUBING
0.009" WALL

SHRINKABLE 'TEFLON' TUBING
0.015" WALL

4.5"

TYPE 302 STAINLESS STEEL
TUBE 0.125" OD. 0.070" ID.

1/4"

EPOXY CEMENT SEALER

3/8"

0.08"

TYPE 302 STAINLESS STEEL
WIRE 0.017" DIA. INSULATED
WITH COAT OF 'FORMVAR'
WIRE ENAMEL

TIPS WITH INSULATION
REMOVED
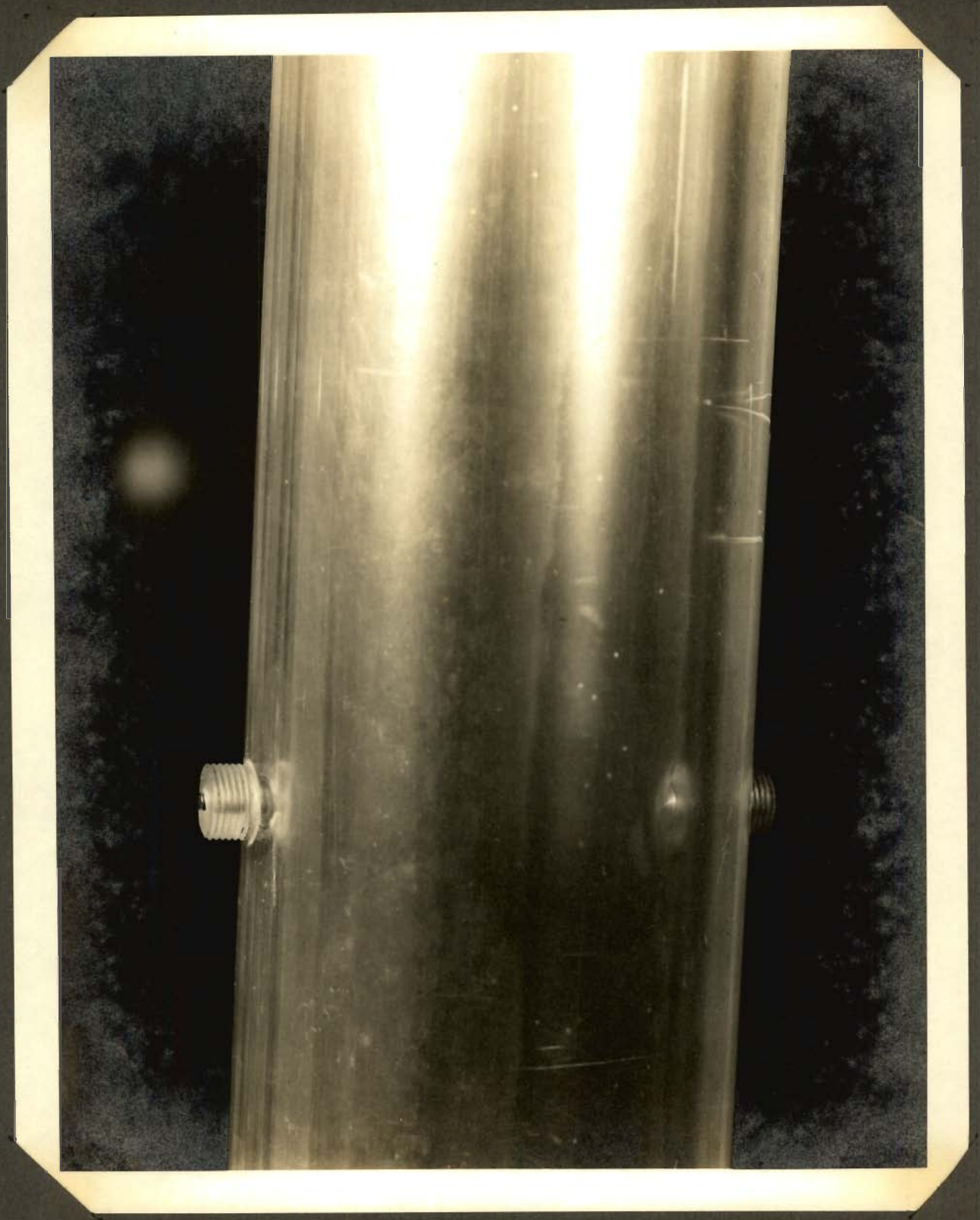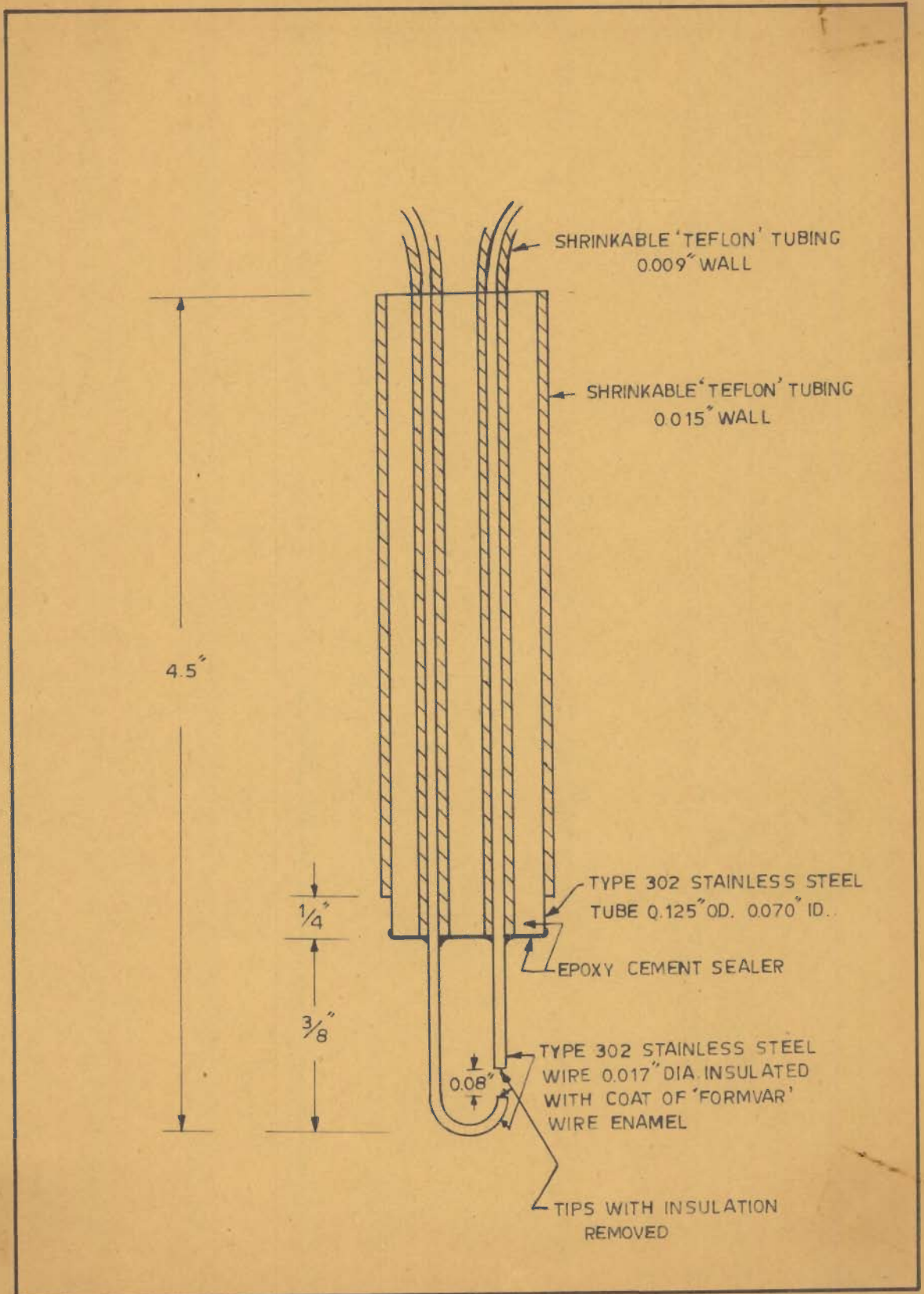
FIG. 4.8_TRAVERSE PROBE DETAILS

enamel. The wires were dipped into 'Formvar' and each coat
was baked at 180° F, for 30 mins. The enamel was removed
from the two tips, furnishing two conducting surfaces
separated by a gap of 0.08".

The traverse probe was positioned with a holder,
shown in Figs. 4.2 and 4.5, adapted from a 'Lory Type A' point
gauge manufactured by the A.B.McIntyre Instruments. The
vernier on the holder could read to 0.001 ft.

Figure 4.9 shows the two stacks of electronic
equipment used in the measurement of the induced voltages.
The signal path is shown in Fig. 4.10 . The signal picked
up by the probes was carried through a double shielded in-
put cable. The double shielding prevented the input leads
from acting as antenna and prevented any voltage which was
common to both probe tips such as 60 cps pick up from being
transformed into a differential signal. In case of the wall
to wall probes, the outer shield was connected to the inner
shield and both were floating at the probe end of the input
cable. For the traverse probe, the inner shield was connec-
ted to the probe stem and the outer shield was floating at
the probe. For both cases, at the amplifier end, the outer
shield was connected to the earth ground and the inner
shield was connected to the floating input ground.

The signal was first fed into a 'Philbrick' P 55A
all silicon operational amplifier hooked up as a voltage
follower (Fig. 4.11). The operational amplifier circuit was
designed to provide a gain of unity alongwith a very high
input impedance and a low output impedance. Thus it acted as
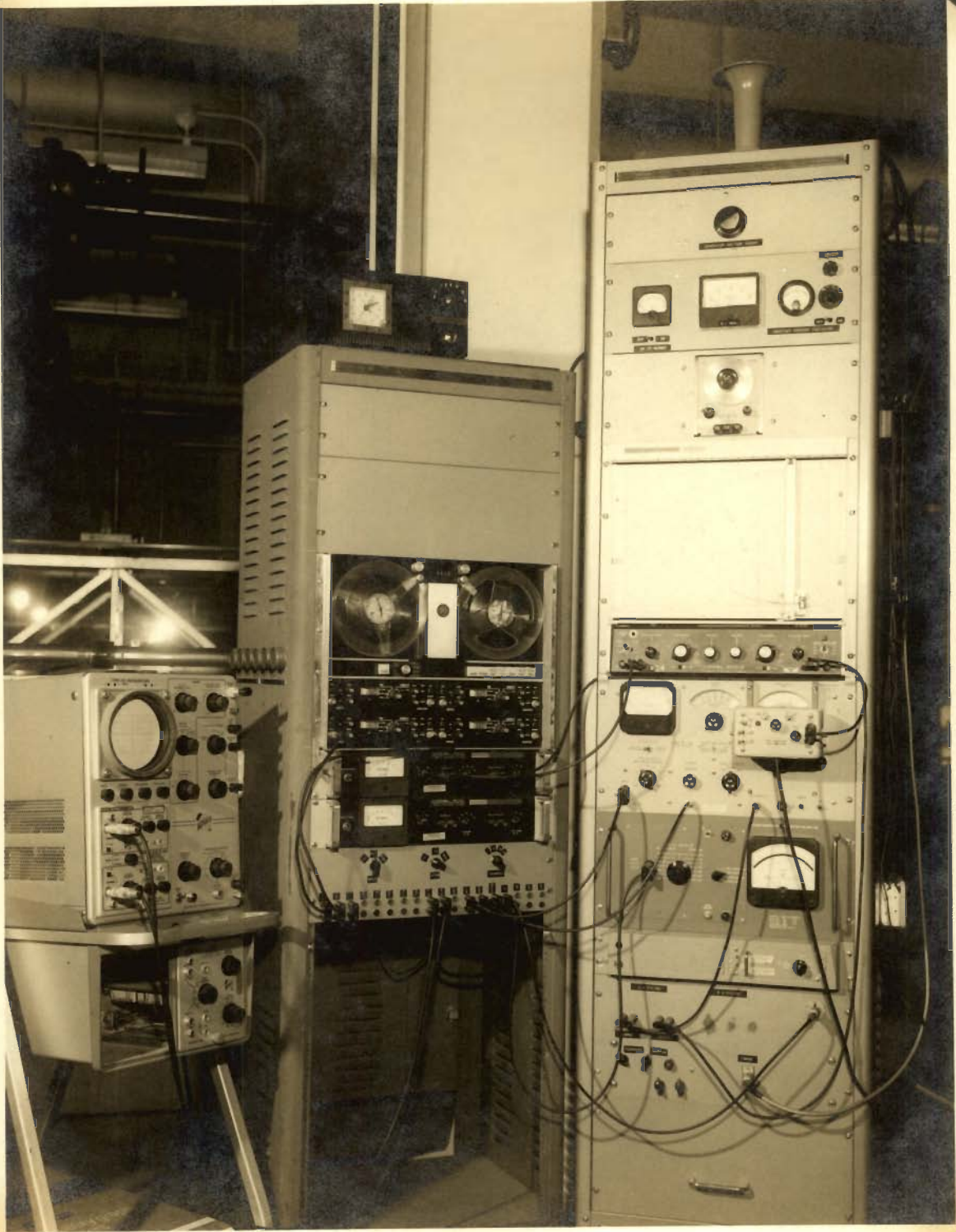
FIG. 4.9 ELECTRONIC EQUIPMENT
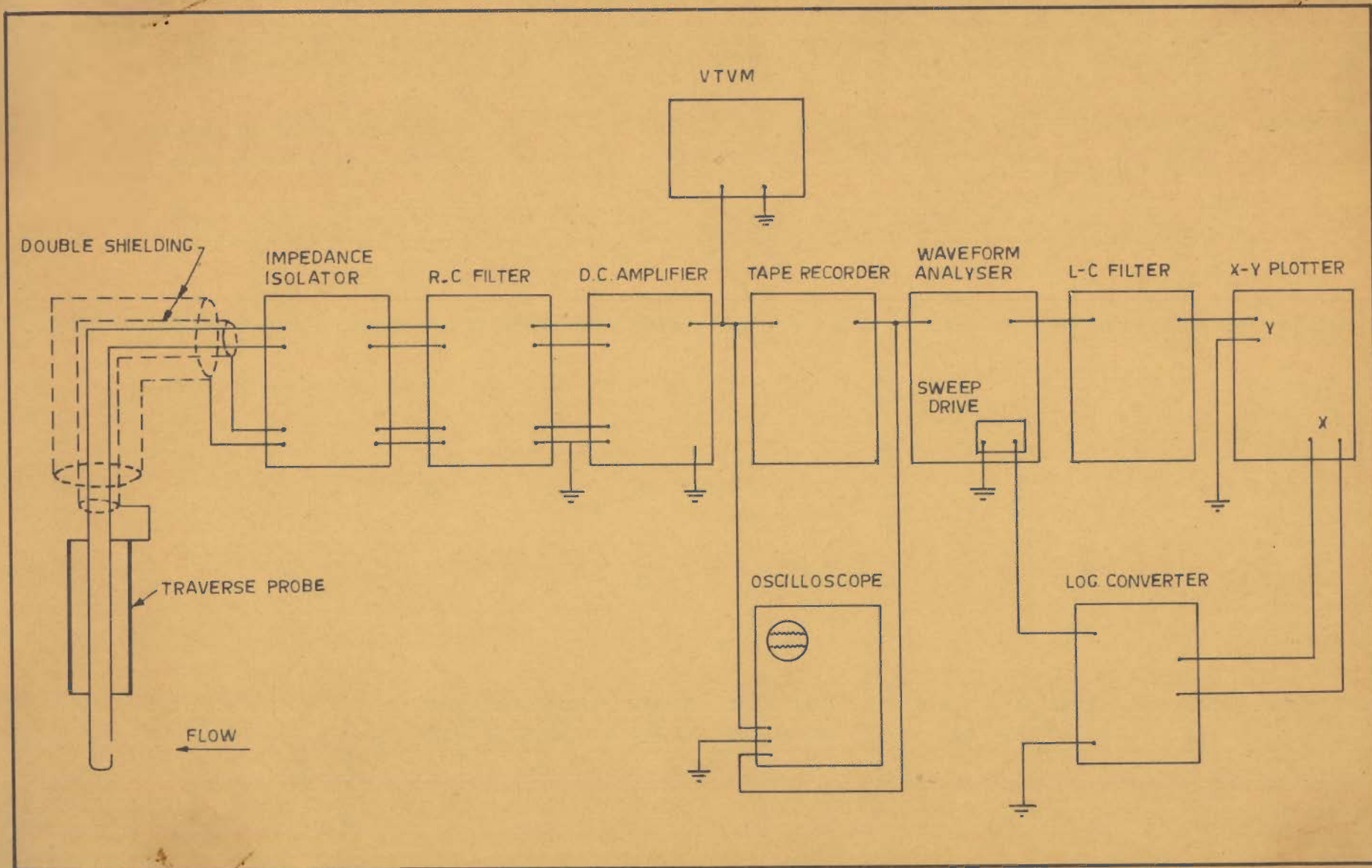
FIG. 4.10 _ SIGNAL ANALYSIS PROCESS

an impedance isolation between the high impedance probe
and the rest of the system, thereby improving the frequency
response of the system, and decreasing noise level.

The output of the operational amplifier was filtered
by the R-C filter shown in Fig. 4.12. This removed the d.c.
component of the signal which would otherwise have overloaded
the amplifier. In some of the runs, the operational amplifier
was not used and the R-C filter used had different component
values. The data for this case was later corrected by
comparison with the data obtained while using the operational
amplifier.

A 'Sanborn' 860-4000 amplifier increased the
strength of the signal upto 1000 times. The amplifier has
the features of floating input and output, chopper stabilisa-
tion for low frequencies and, when used with the double shiel-
ded input cable, a high degree of common mode rejection.

The filtered and amplified signal was then subjec-
ted to further analysis by

    i)   feeding it into a 'Ballantine' true R.M.S. vacuum
         tube voltmeter.

   ii)   feeding it into a 'Hewlett Packard' model 302 A wave-
         form analyser

  iii)   recording it in a 'Precision-Instruments' 4 channel
         FM taperecorder.

   iv)   displaying it in a 'Tektronix' Type 531 Oscilloscope.

The vacuum tube voltmeter gave the total strength
of the signal from which $\sqrt{u_1'^2}$ could be found out.

The wave form analyser, which was actually used as a tunable voltmeter measured the voltage contained in a 7 c.p.s. segment of the signal. The analyser was continuously tuned at a constant rate by a 'Hewlett-Packard' 297-A sweep drive. The analyser provided an r.m.s. output voltage of the frequency component being analysed for a wide variety of stages of attenuation. Because this output was not constant, an L-C filter (Fig. 4.13) was used to dampen out the fluctuations. The filtered output was applied to the Y -axis of a 'Moseley' 2 DR-2 X-Y plotter. The sweep drive had a d.c. output proportional to the frequency of the sweep. A 'Moseley' 60-D logarithmic converter took the logarithm of the sweep drive output and applied it to the X-axis of the plotter. Thus a plot of frequency vs r.m.s. voltage was obtained.

The signal recorded on the taperecorder was played back at ten times the original speed into the wave form analyser. This was done because the analyser could not be used accurately for frequencies below 20 c.p.s. Playing back at 10 times the speed had the effect of making every frequency appear ten times larger to the analyser thus reducing its search bandwidth to 0.7 c.p.s. The waveform analyser could then be used for frequencies as low as 2 c.p.s. The region of the plot between 2 c.p.s. and 20 c.p.s. was thus filled up using the taperecorder after a proper adjustment of the scales.

The oscilloscope was used to monitor the signal at any stage of analysis and detect any 'spikes' etc. in the signal.
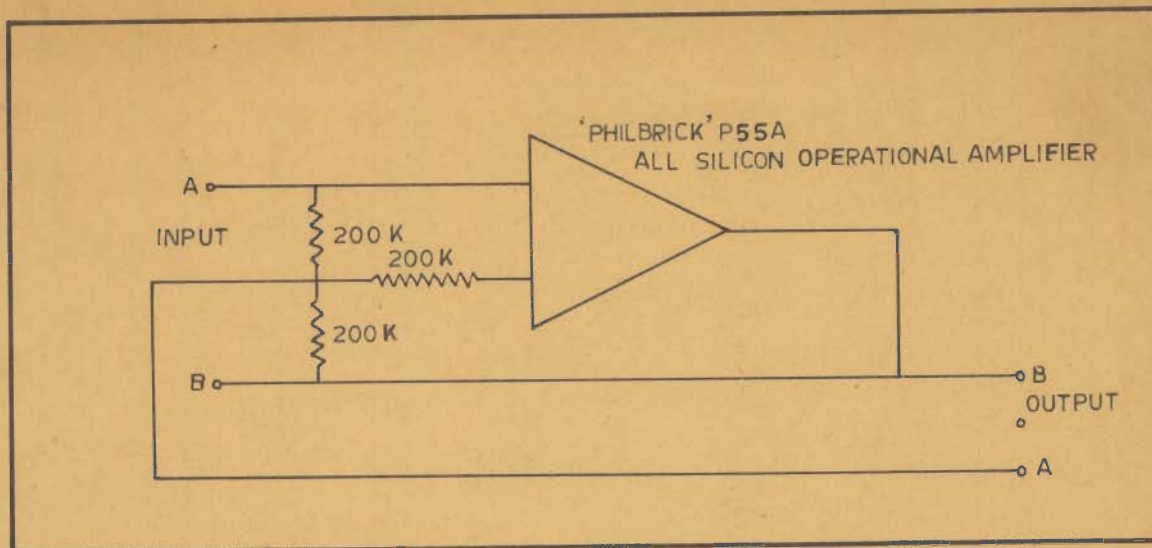
FIG. 4.11 _ IMPEDANCE ISOLATOR CIRCUIT
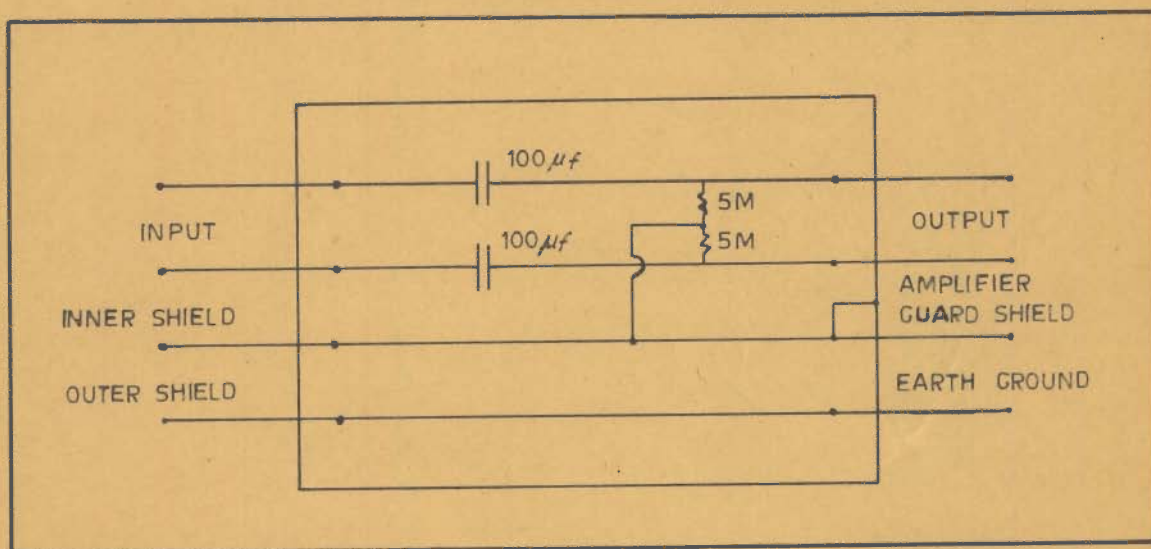
FIG. 4.12 _ R.C. FILTER CIRCUIT
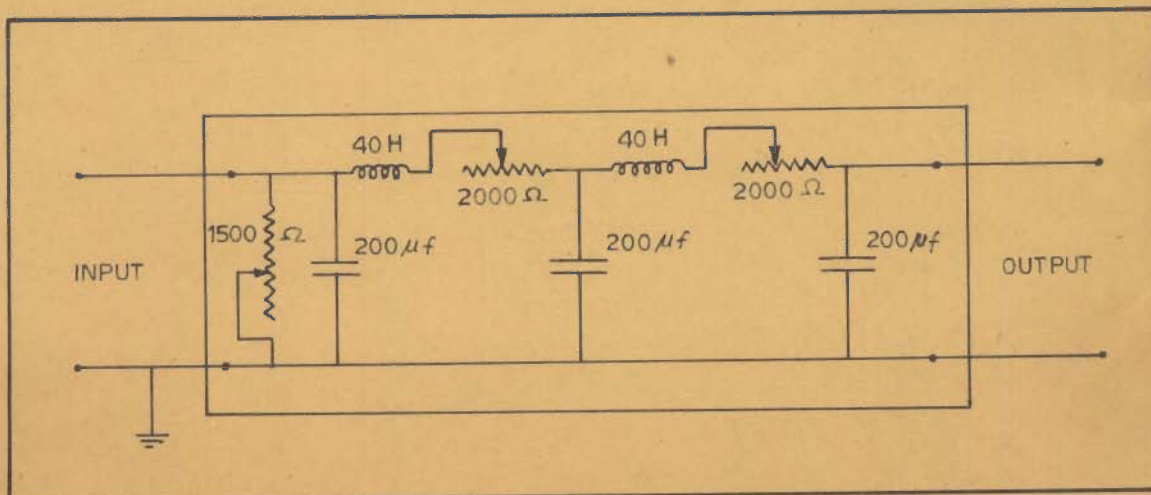
FIG. 4.13 _ L - C FILTER CIRCUIT
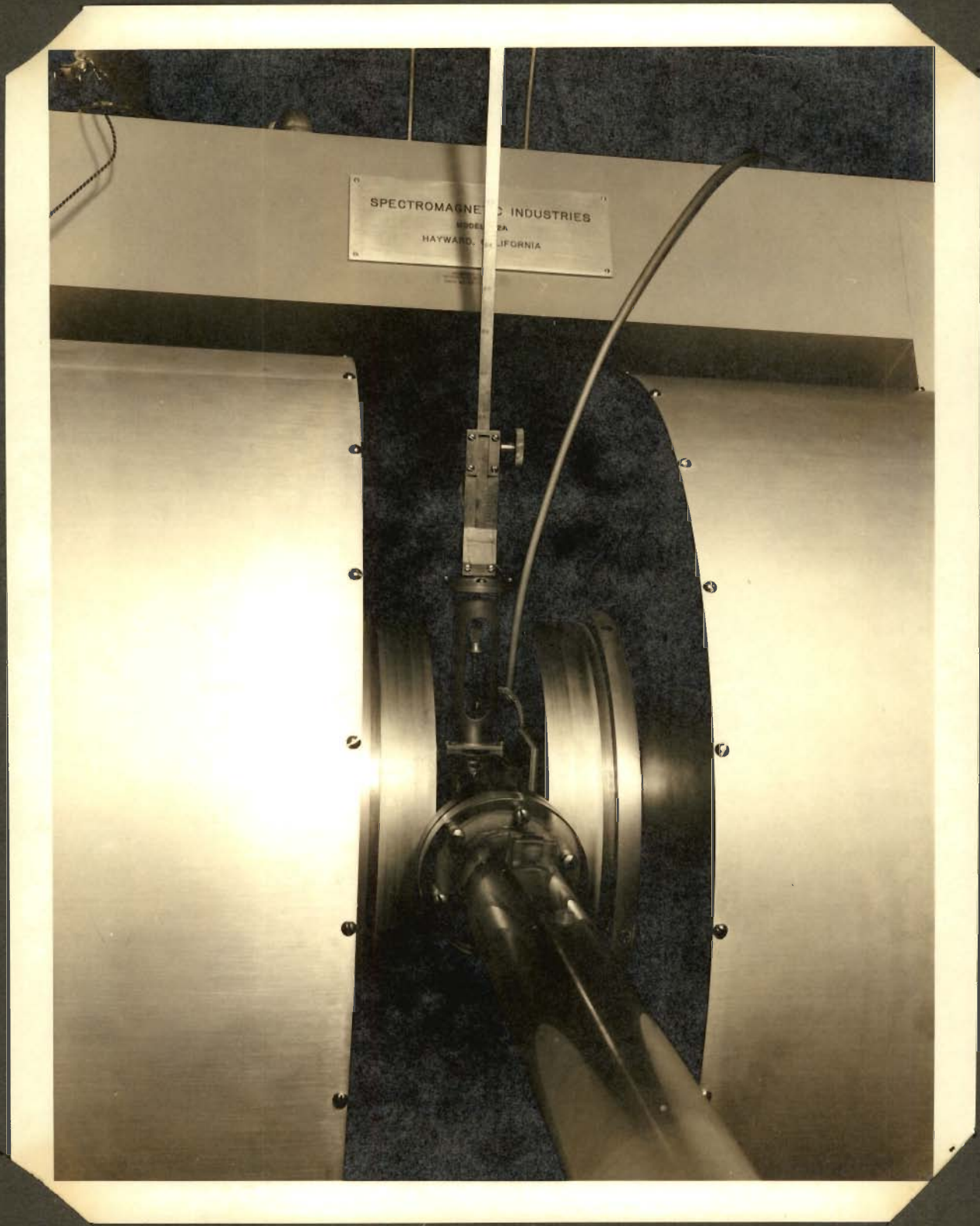
FIG. 4.14 TRAVERSE PROBE IN POSITION WITH ELECTROMAGNET
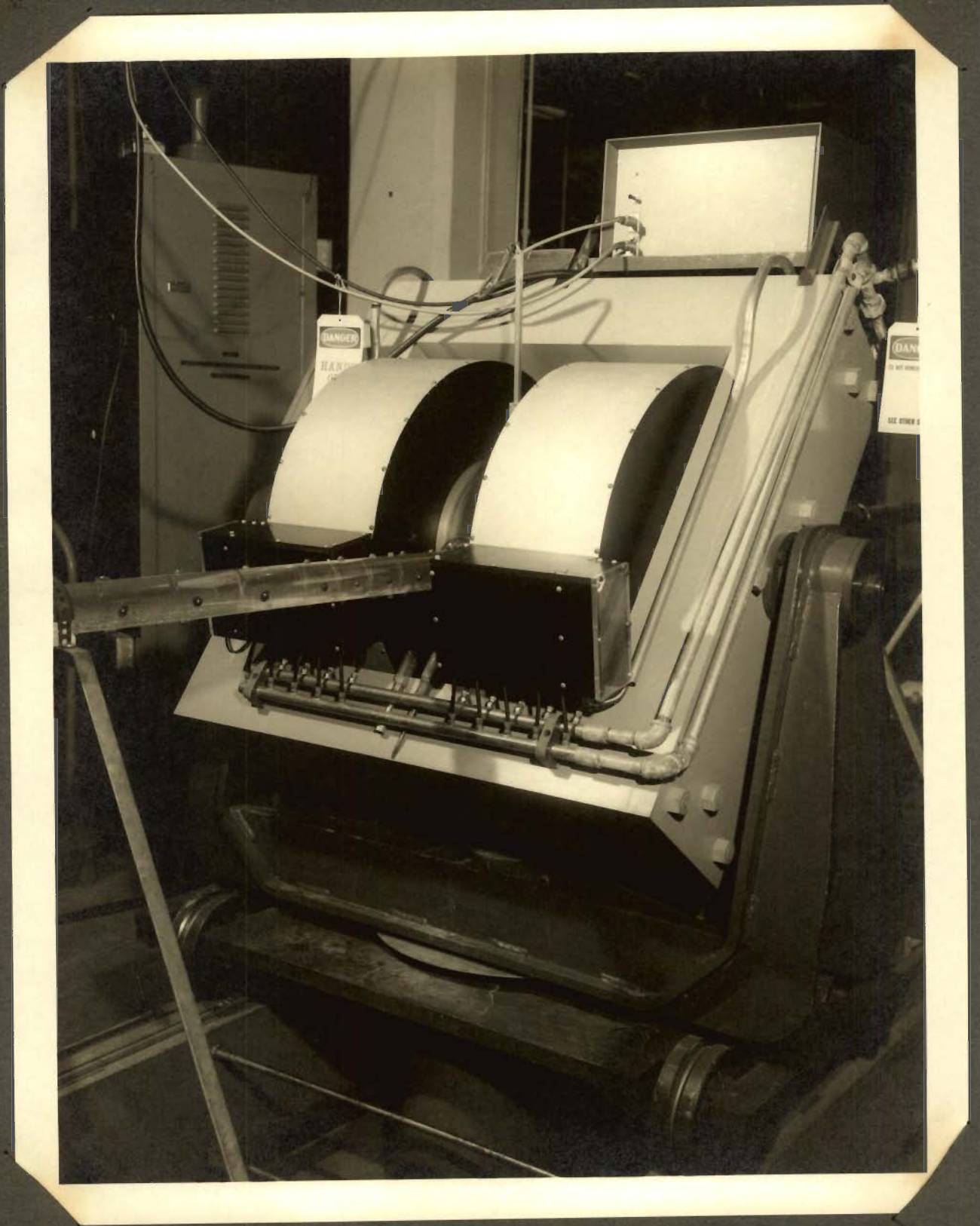
FIG. 4.15   ELECTROMAGNET & IMPEDANCE ISOLATOR

The final result of the signal analysis was an
analog spectrum plot of r.m.s. voltage versus the log-
arithm of the frequency.

4.3 Experimental Methods :

After some preliminary work, the following pro-
cedure was developed for the collection of the experimental
data.

At the beginning of each series the probe and
screens were checked for cleanliness, the electronic equip-
ment was turned on for warming up, the flow rate was adjusted
and the X-Y recorder pens were cleaned and filled with ink.
After this, the tape-recorder was calibrated according to
'P.I.Manual'. With the 'MODE' selector, on the control
panel, in the 'CAL' position, the tape recorder input and
output voltages were matched by switching the 'VTVM' selector
from 'TI' to ' TO' .

At the beginning of each run, the probe was set
to the desired location and the electromagnet turned on.
The signal from the probe was amplified to such an extent
that it did not overload the tape recorder and the tape
recording of the magnet-on signal was started at 3.75 i.p.s.
For the recording, the 'MODE' selector was kept in 'REC'
position and the 'CHANNEL' selector set for the tape channel
being used. The waveform analyser was then calibrated
according to the 'Hewlett-Packard' Manual. With the analyser
meter reading 1.00 volts and the 'Y-range' selector of the
X-Y recorder on 0.1 volts/div., the L-C filter potentiometers
were adjusted to give full scale deflection on the X-Y recorder

for both 'RESPONSE' and 'DAMPING' positions. The signal, being recorded in the tape recorder was then applied to the analyser input also and the range selector set to give maximum resolution on the analyser meter. The sweep drive output level control was turned fully clockwise, the frequency dial set to zero and the sweep lever was engaged in the short sweep position. The 'X-Zero' of the X-Y recorder was adjusted to give an X-deflection of eight inches for a frequency dial reading of 100 with the logarithmic converter on d.c. and the attenuator and scale factors at 10 and 5 respectively. The frequency dial was turned back to 10 c.p.s the low speed lever was engaged and the c.c.w. sweep turned on. The pen was lowered when the dial reached 20 c.p.s. and the spectrum plotted between 20 to 2000 c.p.s. The necessary information to describe the run number and conditions were recorded on the X-Y recorder sheet.

After the above spectrum had been plotted and about 800 ft of the tape recorded, the electromagnet was turned off. The tape footage counter reading was noted at this point. The colour of the recorder ink was changed and the magnet -off spectrum between 20 to 2000 c.p.s. plotted by repeating the procedure followed for the magnet on spectrum. About 800 ft of tape was recorded for this case also.

The spectrum between 2 - 20 c.p.s. for both the magnet-on and magnet-off conditions was then plotted by playing back the tape recorded signal for each case into the waveform analyser at a speed of 37.5 i.p.s. For this the 'MODE' selector was set to 'PBK' position, the analyser range was

switched one step counterclockwise from the original and the pen of the X-Y recorder was made to coincide with the 20 c.p.s. mark on the recording sheet for a frequency dial reading of 200. A frequency dial reading of 20 then corresponded to 2 c.p.s.

After thus having recorded the magnet-on and magnet-off spectra for any one run between 2 to 2000 c.p.s. the magnet field polarity was reversed and another run started.

The run numbers were coded to contain information about probe location, grids, flow rate and the number of the run at the specified condition e.g. run no. d - (1-7-2)-90-1.

$\underline{d}$ -(1-7-2)-90-1 ----→ ·   'd' designates the fourth access hole downstream from the disturbance.

d-(1-7-2)90-1 ----→   '1-7-2)designates the grid placement

($\underline{1}$-7-2) ----→   '1' is the downstream grid number.

(1-$\underline{7}$-2) ----→   '7' represents the spacing between grids in inches.

(1-7-$\underline{2}$) ----→   '2' represents the number of the upstream grid

d-(1-7-2)-$\underline{90}$-1 ----→   '90' is the mean flow rate in gallons per min.

d-(1-7-2)-90-$\underline{1}$ ----→   '1' is the number of the run made under the specified conditions.

When there was only one screen, the whole quantity within the brackets i.e. (1-7-2) etc., was replaced just by the number of the grid.

4.4 Scope of Tests :

The testing programm may be considered in two phases - preliminary and final. The preliminary phase consisted of developing the techniques of measurement, the proper design of traverse probe, shielding and cable arrangements to reduce 60 c.p.s. pick up and the use of the tape-recorder to cover the low frequency range. Some work was done to measure the wall to wall turbulence level at all sections of the pipe. Various R-C filter arrangements were tried and so were various speed ratios for the playback of the tape-recorded data. The ability to reproduce data was confirmed. Certain arrangements were tried to eliminate the effect of the high source (probe) impedance. After gaining confidence in the equipment, the final phase of the test program was conducted.

The second phase of the work consisted of the measurement of analog spectra under various conditions. The total area under the curve recorded at the output of the harmonic analyser (plot of r.m.s. voltage vs frequency) also gives $\sqrt{u_1'^2}$ which was checked with the value read from the r.m.s. vacuum tube voltmeter. Spectral measurements were made for the following cases :

a) Traverse Probe . Mean discharges 90 and 45 gallons per min which correspond to velocities of 9.25 ft/sec and 4.625 ft/sec, and R of 1.54×10^5 and 7.7×10^4 respectively.

No screens — various radial and longitudinal positions

Screen Nos. 1 to 3 – One screen at a time, various
radial and longitudinal positions

Screen Nos. 1 and 2– No.2 upstream of No.1 at 1"
and 4" spacing, various radial
and longitudinal positions.

Screen No. 1 and 3– No.3 upstream of No.1 at 1", 4"
7", spacing, various radial and
longitudinal positions.

b) Wall to Wall Probe : The same observations as above
were repeated at the same discharges. Only one observation
at one longitudinal position is possible in this case.

4.5   Typical Record and Its Interpretation :

Figure 4.16 shows a typical record of the analog-
spectrum curve as obtained from the set-up . The upper plot
represents the magnet-on spectrum while the lower one is the
magnet-off spectrum or noise. An average line has been
drawn through both the magnet-on and magnet-off spectra.
Along the abscissa are the frequencies on a logarithmic
scale, while the ordinate gives the r.m.s. value of voltages.

From the plot in Fig. 4.16 the various parameters
used later, in discussions, can be obtained in the following
manner.

a) Determination of Turbulence Intensity and Taylor's
One Dimensional Spectrum :– The ordinates at various fre-
quencies are read, both for the magnet-on and magnet -off
spectrum. The square of these give the corresponding mean-
square voltages in a 7 c.p.s. wide band at the indicated

frequency. The difference between the mean-square voltages for the magnet-on and magnet-off spectrums gives the net signal in the 7 c.p.s. band at the indicated frequency. Dividing the net signal at each frequency by the band-width (7 c.p.s) we get the signal in mean-square volts/c.p.s. Thus a plot of mean-square volts/c.p.s. vs the frequency can be prepared. The area under the curve thus prepared gives the total signal in mean-square volts, while by dividing the ordinate at each frequency for this curve by the total area we get a normalised spectrum, which is the same as Taylors' one dimensional spectrum. The turbulence intensity $\overline{u'^2_1}$ can be obtained from the total signal in mean-square volts by using equation (3.27). Sample computations for the analog-spectrum shown in Fig. 4.16 are presented in Table 4.I. These computations were, however, carried out on an IBM 1620 Digital Computer.

Using the relations $k = \dfrac{2\pi n}{\overline{u}_1}$ and $F_1(k) = \dfrac{\overline{u}_1}{2\pi} F_1(n$ the spectrum in terms of wave number was also obtained. Here k represents the wave number, n the frequency, $\overline{u}_1$ the mean velocity of flow and $F_1(n)$ is the Taylor's one-dimensional spectrum function at a frequency n, $F_1(k)$ being the corresponding spectrum function at a wave number k such that

$$\int_0^\infty F_1(k)\,dk = \int_0^\infty F_1(n)\,dn = 1$$

b) Determination of Micro Scale and Spectra of Vorticity :
From the $F_1(k)$ vs k curve as obtained above, the microscale of turbulence λ was computed making use of the relationship ;

$$\frac{1}{\lambda^2} = \frac{1}{2} \int_0^\infty k^2 \, F_1 \, (k) \, dk$$

From the values of λ , so computed, the spectra were non-dimensionalised by computing F_1 (k) $/\lambda$ and λk . The spectra of vorticity was also obtained in the non-dimensional form by computing $\lambda k^2 F_1 (k)$ corresponding to various values of λk. Sample computations are presented in Table 4 II . These computations were also carried out on an IBM 1620 Digital Computer.

−:o:−
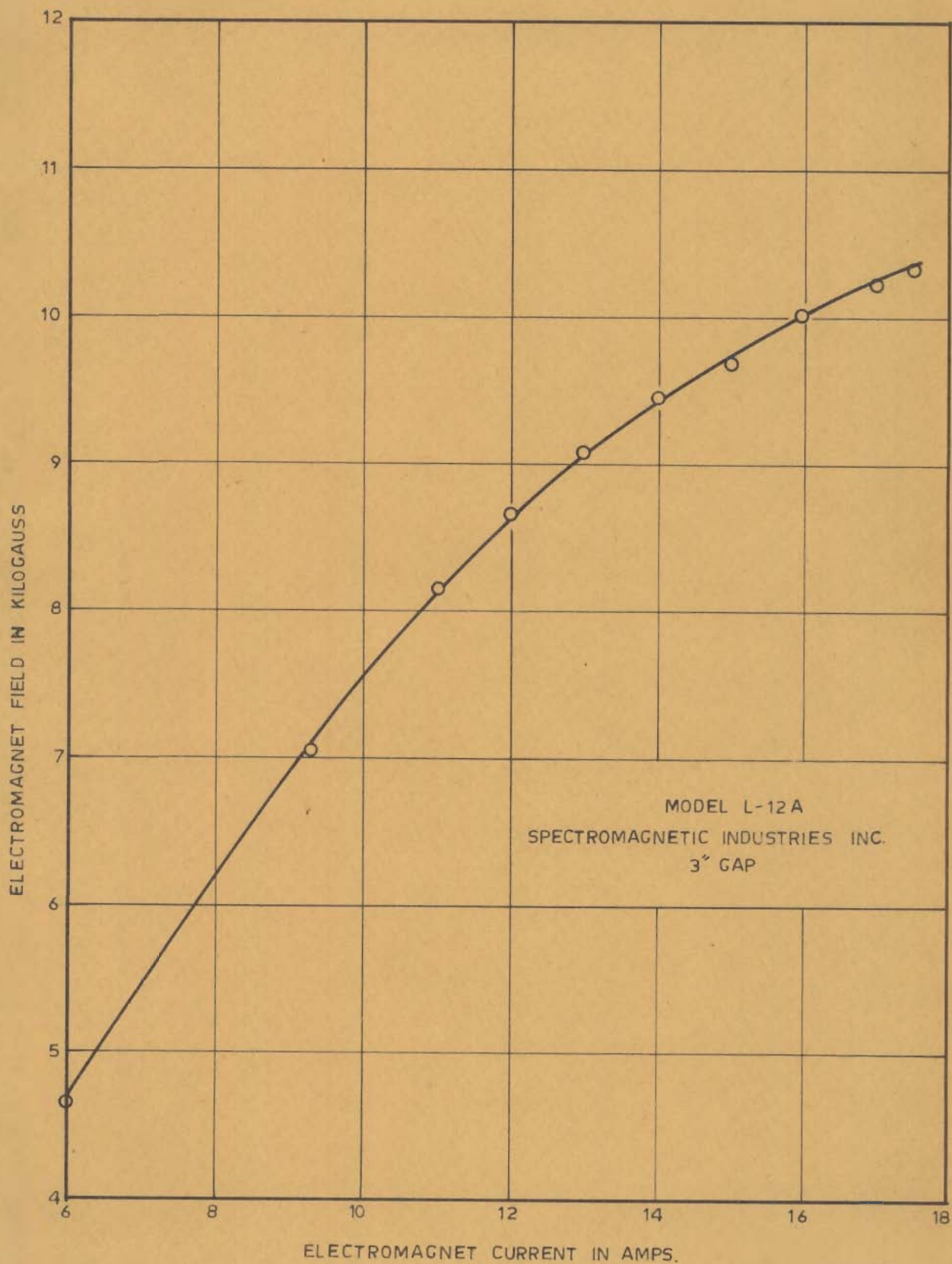
FIG.4.17 CALIBRATION CURVE FOR ELECTROMAGNET

TABLE - 4 I
SAMPLE COMPUTATIONS

Run No. b-1-90-1;   Grid 3/16 '' only; $\bar{u}_1 = 9.25$ ft/sec;   R = 1.54×10^5; $x_1 = 2$ ''

Frequency c.p.s.	Signal RMS, μV	Noise RMS, μV	Signal MS, μV	Noise MS, μV	Net Signal MS, μV	Mean Signal MS, μV	n c.p.s.	$x = \frac{\text{Mean signal}}{n}$ MS μV c.p.s	Wave Number $k = \frac{2\pi n}{\bar{u}_1}$ ft^{-1}	$F_1(n) = \frac{\text{Net Signal}}{\text{Signal sum}}$	$F_1(k) = \frac{u_1 F_1(n)}{2\pi}$ ft
1	2	3	4=2^2	5=3^2	6=4−5	7	8	9	10	11=6/Σ 9	12
2	54	7.5	2916	56.25	2854.75				1.36	.537x10^{-1}	.78792x10^{-1}
						2293.87	3	6881.61			
5	42	6.0	1764	36	1728.00				3.4	.3541x10^{-1}	.52038x10^{-1}
						1252.87	5	6264.35			
10	28	2.5	784	6.25	777.75				6.8	.1595x10^{-1}	.23373x10^{-1}
						684.55	10	6840.55			
20	24.4	2.0	595.36	4.0	591.36				13.6	.121x10^{-1}	.17787x10^{-1}
						449.43	30	13482.9			
50	17.6	1.5	309.76	2.25	307.51				34	.630x10^{-2}	.92610x10^{-2}
						191.97	50	9598.5			
100	8.8	1.0	77.44	1.0	76.44				68	.156x10^{-2}	.22932x10^{-2}
						41.86	100	4186.0			
200	2.88	1.0	8.29	1.0	7.29				136	.149x10^{-3}	.21903x10^{-3}
						4.04	300	1212.0			
500	1.02	0.5	1.04	0.25	0.79				340	.162x10^{-4}	.23814x10^{-4}
						0.43	500	205.0			
1000	0.4	0.3	0.16	0.09	0.07				680	.144x10^{-5}	.21168x10^{-5}
						0.046	1000	46.0			
2000	0.18	0.1	0.032	0.01	0.022				1360	.453x10^{-6}	.665591x10^{-6}
							SUM=	48716.91			

$$\overline{u_1'^2} = \frac{\overline{\triangle\phi'^2}}{\triangle x_2^2 \cdot B^2}$$

Bandwith of Analyser = 7 c.p.s.

Area under Curve = $\dfrac{\Sigma\ 9}{7.0}$ = $\dfrac{48716.91}{7.0}$

= 6959.56 Ms μV

B = 9700 Gauss = 9700 x10^{-4} volts-sec/m^2

x_2 = 0.08 '' (Probe gap)

$$\overline{u_1'^2} = \frac{6959.56 \times 10^{-12}}{\left\{\dfrac{(9700\times10^{-4})^2}{(3.28)^2}\right\}\left(\dfrac{0.08}{12}\right)^2}$$

$$= \frac{6959.56}{3.61\times10^5} = 1.9166 \times 10^{-2} \quad ft^2/sec^2$$

$$\therefore \quad \frac{\overline{u_1^2}}{\overline{u_1'^2}} = \frac{(9.25)^2}{1.9166 \times 10^{-2}} = 44.46 \times 10^2$$

TABLE 4 II

SAMPLE COMPUTATIONS

k	$F_1(k)$	k^2	$k^2F_1(k)$	Mean $k^2F_1(k)$	k	Mean x Δk	λk	$F_1(k)/\lambda$	$\lambda k^2F_1(k)$
	2	3	4	5	6	7	8	9	10
1.36	$.7879 \times 10^{-1}$	1.8496	.1457				.03790	$.2849 \times 10^{1}$	$.4060 \times 10^{-2}$
3.4	$.5203 \times 10^{-1}$	11.56	.601	.7467/2	2.04	1.5232/2	.09531	$.1865 \times 10^{1}$	$.2684 \times 10^{-1}$
6.8	$.2337 \times 10^{-1}$	46.2	1.079	1.680/2	3.4	5.712/2	.19410	$.8310 \times 10^{-1}$	$.3021 \times 10^{-1}$
13.6	$.1778 \times 10^{-1}$	184.96	3.288	4.367/2	6.8	29.695/2	.3790	$.3310 \times 10^{-1}$	$.9201 \times 10^{-1}$
34	$.9261 \times 10^{-2}$	1156	10.705	13.993/2	20.4	285.472/2	.5931	$.3310 \times 10^{-1}$	$.2991 \times 10^{0}$
68	$.2293 \times 10^{-2}$	4620	10.59	21.295/2	34	724.03/2	1.9410	$.8161 \times 10^{-2}$	$.2960 \times 10^{0}$
136	$.2190 \times 10^{-3}$	18496	4.05	14.559/2	68	990.012/2	3.790	$.7781 \times 10^{-3}$	$.1130 \times 10^{0}$
340	$.2381 \times 10^{-4}$	115600	2.752	6.802/2	204	1387.6/2	9.531	$.8490 \times 10^{-4}$	$.7681 \times 10^{-1}$
680	$.2116 \times 10^{-5}$	462000	.9775	3.729/2	340	1267.86/2	19.410	$.7520 \times 10^{-5}$	$.2731 \times 10^{-1}$
1360	$.6659 \times 10^{-6}$	1849600	1.231	2.208/2	680	1501.44/2	37.90	$.2378 \times 10^{-5}$	$.3433 \times 10^{-1}$
					Sum	3096.66			

$A = 3096.66/2 = 1548.33$; $\quad B = \sqrt{A} = 39.4$; $\quad \lambda = 1/B = 0.0254$ ft

CHAPTER - V

DISCUSSION OF RESULTS

5.1 Preliminary Remarks :

The present chapter is devoted to analysis of the data obtained from the analog set up and discussion of the results obtained therefrom in the light of existing theoretical and experimental notions regarding turbulence. The method of interpretation of a typical record obtained from the analog set up has already been described in Chapter IV. The data have been used for the proving of the analog set up and for studying the characteristics of decay of turbulence behind grids, the energy spectra and their similarity and the similarity of dissipation spectra (or the spectra of vorticity). Some qualitative observations regarding the effect of probe gap on the measurements of spectra have also been made making use of the spectra obtained with the wall to wall probes.

5.2 Measurement of Velocity Fluctuations in the Pipe Cross Section :-

As already mentioned, measurements of the one dimensional energy spectrum were made in the pipe without any grid, from which velocity fluctuations $\overline{u_1'^2}$ at that level were computed. The measurements were made at any cross section, along a diameter of the pipe at various radial positions. This was done primarily for checking the behaviour of the set up by comparison of the results with published work. Figure 5.1 shows a plot of ($\sqrt{\overline{u_1'^2}}/u_*$) vs ($r'/a$) . Here u_* represents the shear velocity, r' represents the distance of the point of observation from the pipe wall and $2a$ is the dia-

meter of the pipe. Since no pressure measurements were taken along the pipe length to find the hydraulic gradient, u_* could not be computed directly using the formula $u_* = \sqrt{\dfrac{p_1-p_2}{\rho}} \cdot \dfrac{2a}{4L}$. Hence the value of u_* has been computed on the assumption that the pipe behaves as a hydrodynamically smooth pipe and hence 'f' can be estimated by the Blassiu's equation $f = \dfrac{0.316}{IR^{1/4}}$.
The term u_* is related to f by the equation $u_* = \bar{u}_1 \sqrt{f/8}$. Here 'f' is the Darcy-Weisbach resistance coefficient and IR is the Reynold's number of flow $\bar{u}_1 2a/\nu$.

For a discharge of 90 g.p.m. ($IR = 1.54 \times 10^5$), the results are as shown in Fig. 5.1. Also plotted there are the curves obtained by Laufer (39) for R = 50,000 and 500,000. The data points conform well to the curve given by Laufer for R = 50,000, except for r'/a values less than 0.2. This is probably because of the disturbance created near the walls by the access-holes made in order to introduce the traverse probe.

Figure 5.2 gives the u_1' spectra for the various radial positions of the pipe flow at a Reynolds number of 1.54 $\times 10^5$. The spectra obtained by Laufer are reproduced in Fig. 5.3, for comparison. As is evident from the two figures, the spectra also show the same trend as those given by Laufer.

The same spectra have been replotted in Fig. 5.4, using $\bar{u}_1 F_1(n) \Lambda_f$ and $n \Lambda_f / \bar{u}_1$ as the parameters, Λ_f being the integral scale as determined from the energy spectra. The reference curve shown in the figure is $\dfrac{\bar{u}_1 \, F_1(n)}{\Lambda_f} = \dfrac{4}{1 + \dfrac{4\pi^2 n^2 \Lambda_f^2}{\bar{u}_1^2}}$
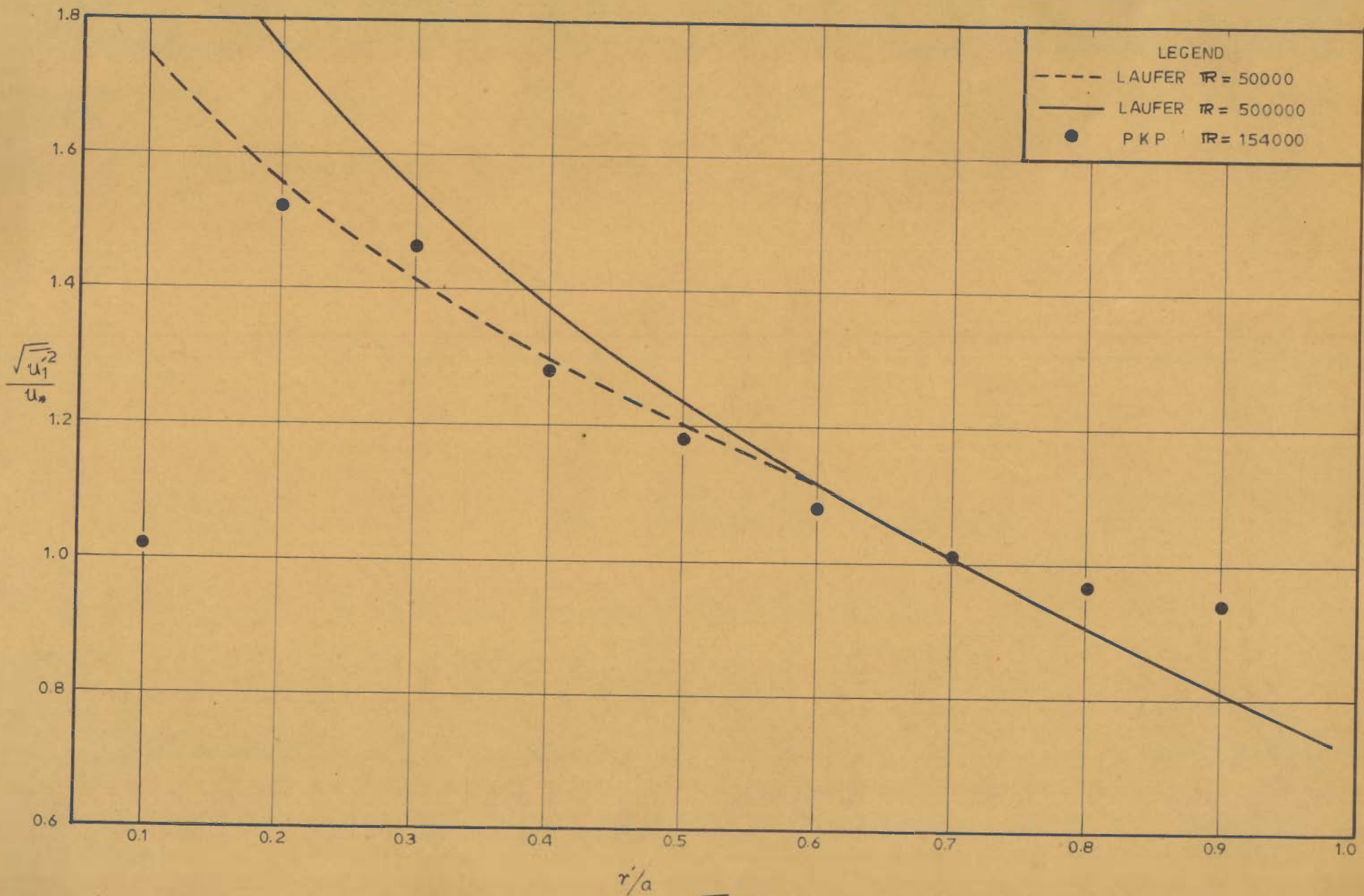
FIG.5.1_VARIATION OF $\sqrt{\overline{u_1'^2}}/u_*$ VS. r/a IN PIPE

LEGEND

- - - - LAUFER $\text{R} = 50000$

———— LAUFER $\text{R} = 500000$

● P K P $\text{R} = 154000$

which is the expression obtained if the correlation curve is approximated by the exponential function exp $(- x_1 / \Lambda_f)$. The agreement with the curve is not very good, specially away from the central portion, indicating that the correlation curve deviates from an exponential shape as one moves towards the wall.

5.3 Decay Behind a Single Grid :

The decay of turbulence behind single grids has been the subject of many theoretical and experimental studies. Most of the studies having been carried out in wind tunnels. Measurements are made at various distances downstream of the grid; according to Taylor's hypothesis, the rate of decay of turbulence with distance so obtained corresponds to the rate of decay with time. The results of the studies on decay are therefore, generally presented in terms of distance from the grid.

For the decay pattern behind grids, Taylor (60)argued that for any given type of grid, the micro scale λ could be expressed as

$$\lambda/M = A \sqrt{\frac{\nu}{M\sqrt{\overline{u_1^2}}}}$$

where M is the mesh width and A an absolute constant for all grids of a definite type . On this basis he gave the decay law as

$$\frac{\overline{u_1}}{\sqrt{\overline{u_1^2}}} = \frac{5x_1}{A^2 M} + \text{constant}$$

where x_1 represents the distance downstream from
the grid. This equation however, was thought of as applying
only for large values of $M \sqrt{\overline{u_1'^2}} / \nu$. From experimental
data Taylor found a value of A varying between 1.95 and 2.2.

The data collected in the present investigation has
been plotted with $\overline{u}_1 / \sqrt{\overline{u_1'^2}}$ and x_1/M as the parameters
in Fig.5.5. Shown there is also the line $\overline{u}_1 / \sqrt{\overline{u_1'^2}} = 8.9$
$+ 1.035 \, x_1/M$ as given by Taylor(60), for square mesh grids.
The present data do not show agreement with Taylor's line. The
value of A for these data was worked out and in general it wa s
found to be very high i.e. varying between 4.0 and 15.0. The
reason for the departure could be the low values of $M \sqrt{\overline{u_1'^2}} / \nu$
in the present case, which render the equation for variation
of micro scale and hence the decay law inapplicable. Similar
results were obtained by Taylor (60) using Dryden's data for
which the $M \sqrt{\overline{u_1'^2}} / \nu$ values were low.

A decay law for turbulence behind single grid can
be obtained on the basis of Kolmogoroff's theory also. In this
case one gets, for the initial stages of decay, a linear law of
the type $\overline{u'^2} \propto t^{-1}$ which, interpreted in terms of distance,
would mean that $\overline{u_1'^2}$ varies in proportion to the distance
from the grid. Batchelor and Townsend (7,8) carried out a series
of experiments on the decay behind grids of various shapes
and sizes. They gave the following equation for decay of turbu-
lence behind square mesh grids during the initial period of
decay.

$$\frac{\overline{u}_1{}^2}{\overline{u_1'^2}} = 135 \left(\frac{x_1}{M} - 10 \right)$$
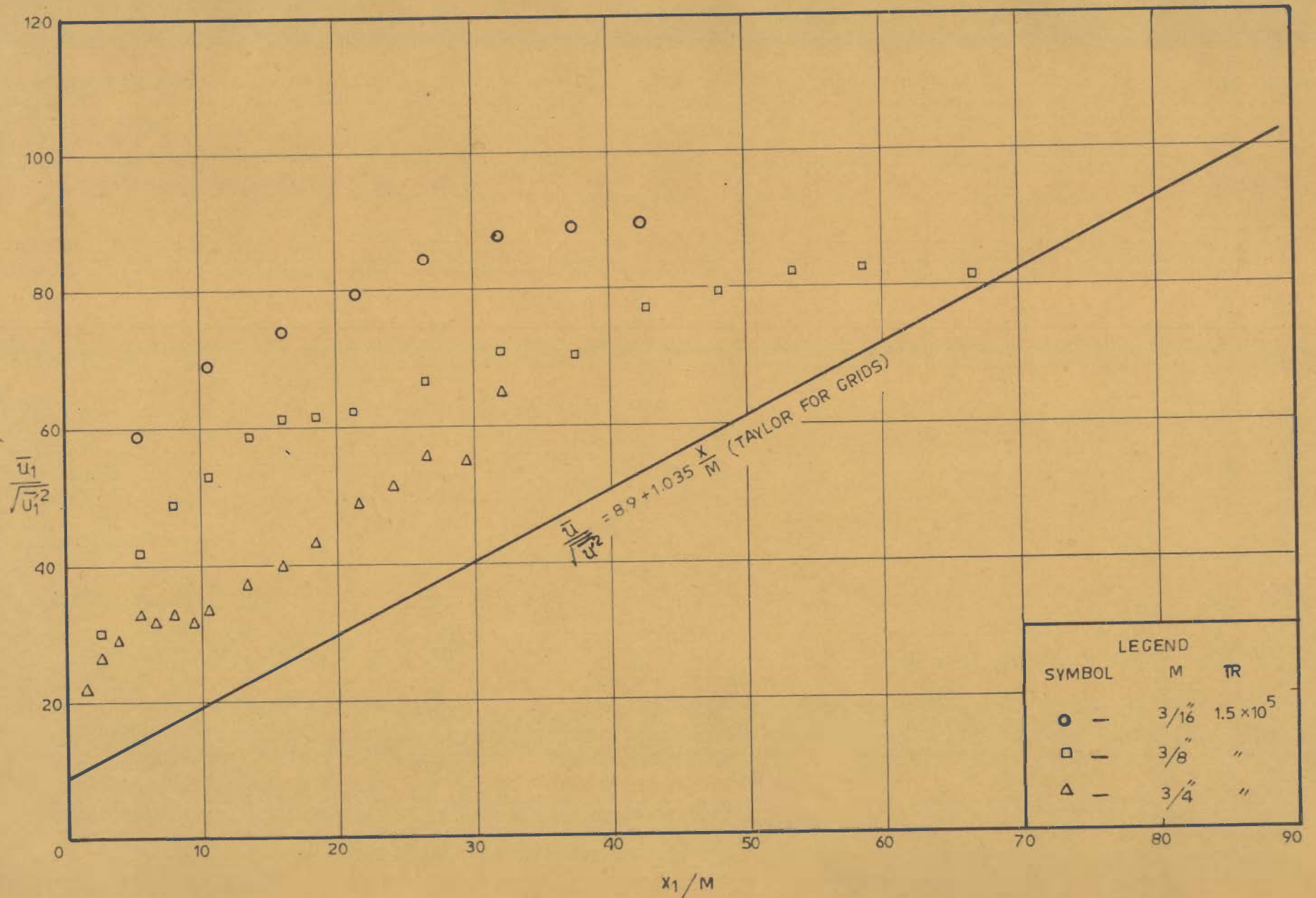
FIG. 5.5 _ VARIATION OF $\overline{u}_1 / \sqrt{\overline{u}_1'^2}$ WITH x_1/M

They also found that this decay law was replaced by one representing a faster rate of decay (final period) at values of x_1/M ranging from 120 onwards. The limiting value of x_1/M for the above law depending mainly on the initial Reynold's number.

The decay of relative energy $\overline{u_1^2} / \overline{u_1'^2}$ with x_1/M for the present work is shown in Fig. 5.6. The decay plots have been prepared for grids of mesh width, 3/16'', 3/8'' and 3/4'' (M/d for all is 3). There are two sets of points for each grid corresponding to Reynolds numbers of 1.54×10^5 and 7.7×10^4. Also shown on the plot is the curve given by Batchelor and Townsend for the initial period. The experimental data in the present work departs from the linear decay law. Further the points corresponding to various grids do not follow a single decay law i.e. a single curve cannot be obtained for the various grids tested.

The same data are plotted in Fig. 5.7 alongwith the plot given by Batchelor and Townsend for the decay during and beyond the initial period. The final period starts to set in after the absolute energy $\overline{u_1'^2}$ has fallen to a very low level.

As already mentioned, the linear decay law is based on Kolmogoroff's hypothesis, the requirements of which are satisfied only at very high Reynolds' numbers. An extension of this theory was proposed by Goldstein (22) wherein he generalised it to make it applicable to moderate Reynolds numbers as well. On the basis of this extension, he derived
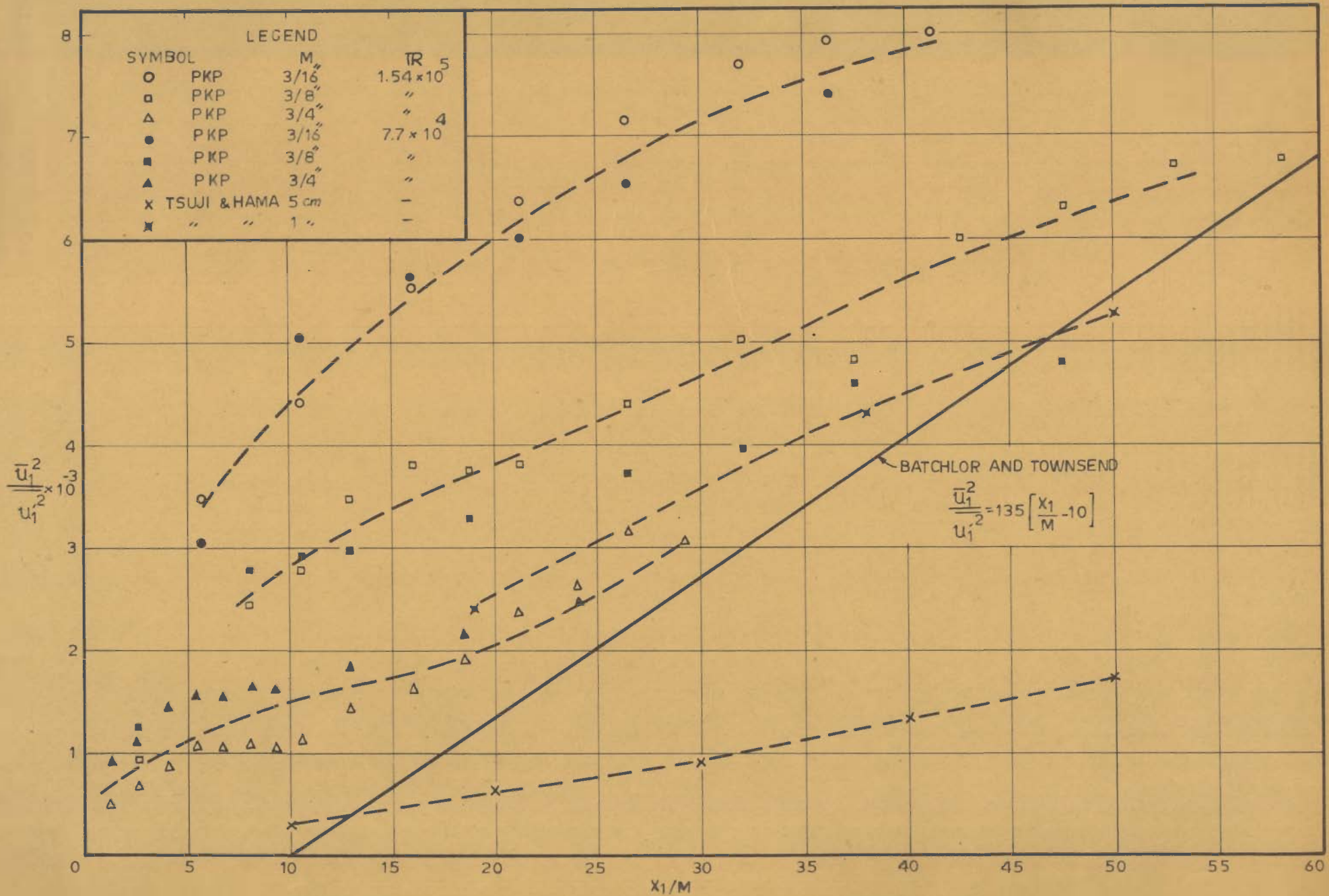
FIG.5.6.-DECAY OF TURBULENCE BEHIND VARIOUS GRIDS

BATCHELOR AND TOWNSEND

$$\frac{\overline{u_1^2}}{\overline{u_1'^2}} = 135\left[\frac{x_1}{M} - 10\right]$$

y-axis: $\dfrac{\overline{u_1^2}}{\overline{u_1'^2}} \times 10^{-4}$

x-axis: $\dfrac{x_1}{M}$

LEGEND			
SYMBOL	M	$\overline{u}_1$	$\overline{R}$
● PKP	3/16″	9.25 ft/s	1.54×10⁵
□ PKP	3/8″	″	″
△ PKP	3/4″	″	″
+ B & T	1.27 cm	1286 cm/s	—
× B & T	0.365 ″	″	—

114
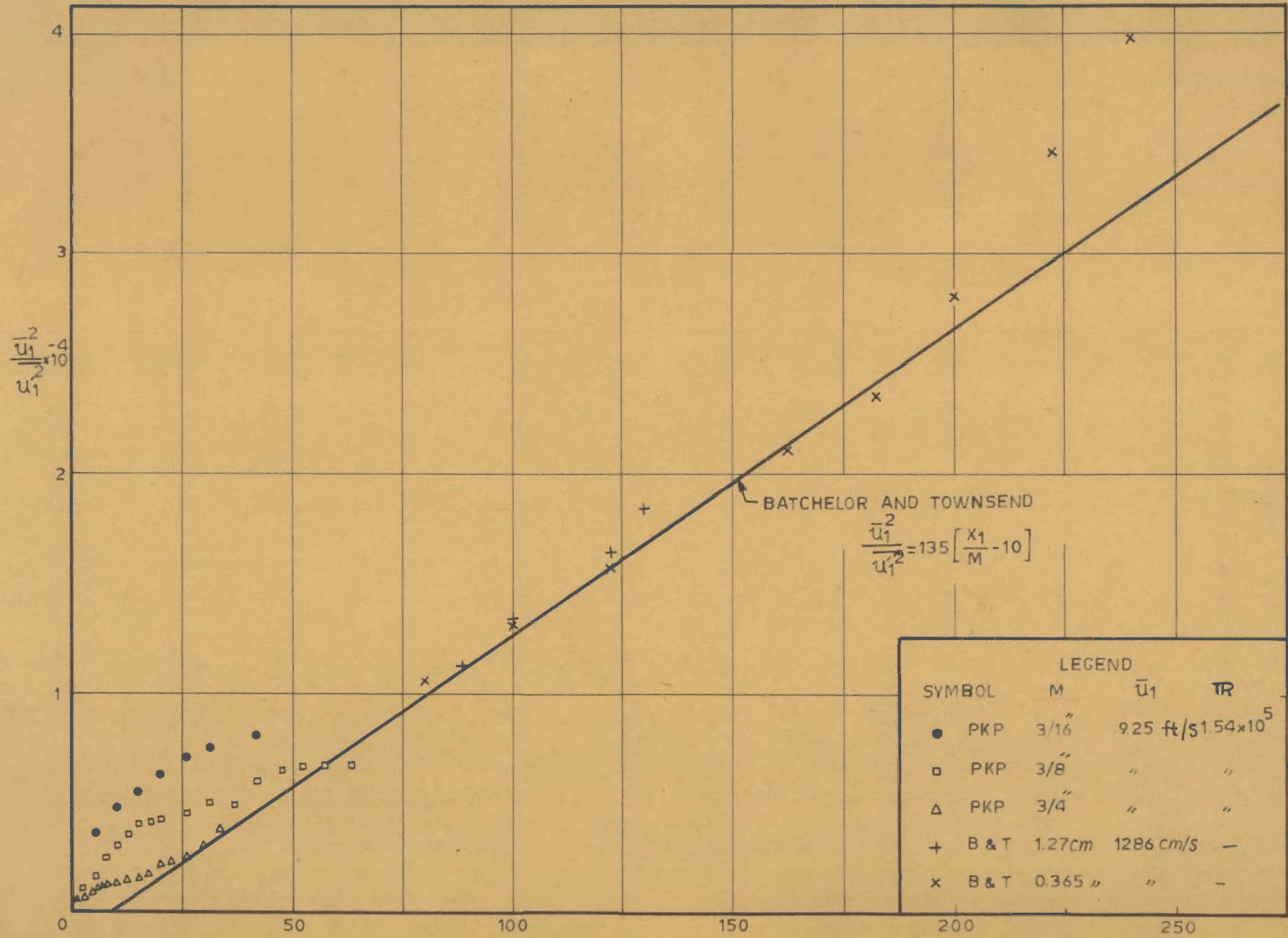
a generalised decay law

$$\overline{u'^2} \ t \ = \ \nu \ R_t \ . \ d \ (t)$$

where R_t was defined as $\dfrac{(\overline{u'^2} \ t)_{t=0}}{\nu}$ and $d(t)$ was a function depending on initial conditions. This function is such that the above relationgives correctly the decay law for the final period, while for very large Reynolds numbers the above law becomes the same as the linear decay law. Goldstein showed that the above law could also be expressed as

$$\overline{u'2} \ t \ = A + Bt + Ct^2 + \ \ldots\ldots$$

and showed that the exact law would depend on the initial conditions i.e. the initial Reynolds number, intensity and scale of turbulence.

The results obtained in the present study can be explained in the light of the above discussion. There are three separate curves obtained for the three grids for any one Reynolds number R. This indicates that the decay law for the three grids in the initial period is not the same. The mesh Reynold's number ($R_m = \overline{u}_1 \ M/\gamma_*$) for the three grids will be different and hence, as pointed out by Goldstein, should reflect in the decay law itself. The range of x_1/M (or t) values for which the data are obtained being not too large, a definite prediction regarding the final period cannot be made, but it can be expected that the curves for different grids should ultimately coincide with the Batchelor and Townsends plot for the final period of decay. It is also seen that for the same grid, the decay law changes with a change in the

Reynolds number IR. This could be because of the change in R_M and the intensity and scale of the approaching turbulence. The study thus shows the dependence of the decay during the initial period on the initial conditions and Reynolds number as envisaged by Goldstein.

Two sets of points obtained by Tsuji and Hama (66) for decay behind grids of mesh widths 5 cm and 1 cm for the same Reynolds number of flow IR are also shown in Fig. 5.6. It is seen that in their case also, the two grids follow different decay laws, showing again the dependence of the decay law on $\bar{u}_1 M/\nu$ for Reynolds' numbers which are not very large so as to satisfy the requirements of Kolmogoroff's theory.

A more definite proof of the dependence of decay law on the initial conditions is provided by the results of decay behind two grids presented in the next section.

5.4 Decay Behind Two Grids :

The decay of turbulence behind two grids is shown in Figs. 5.8, 5.9, 5.10, 5.11. Figure 5.8 gives the decay behind the 3/16'' and 3/4'' mesh grids alone as well as the decay behind the 3/16'' grid with the 3/4'' grid placed upstream of it at distances of 1'', 4''and 7'' respectively. Figure 5.9 gives the same plot for the 3/16''and 3/8'' grids. Both these figures correspond to a Reynolds number of flow (R) of 1.54 x 10^5 . Similar plots for a Reynolds number of flow of 7.7 x 10^4 are prepared in Figs. 5.10 and 5.11 .

Placing of a grid, say the 3/4''mesh, upstream of another (the 3/16'' mesh) means in effect change of the initial
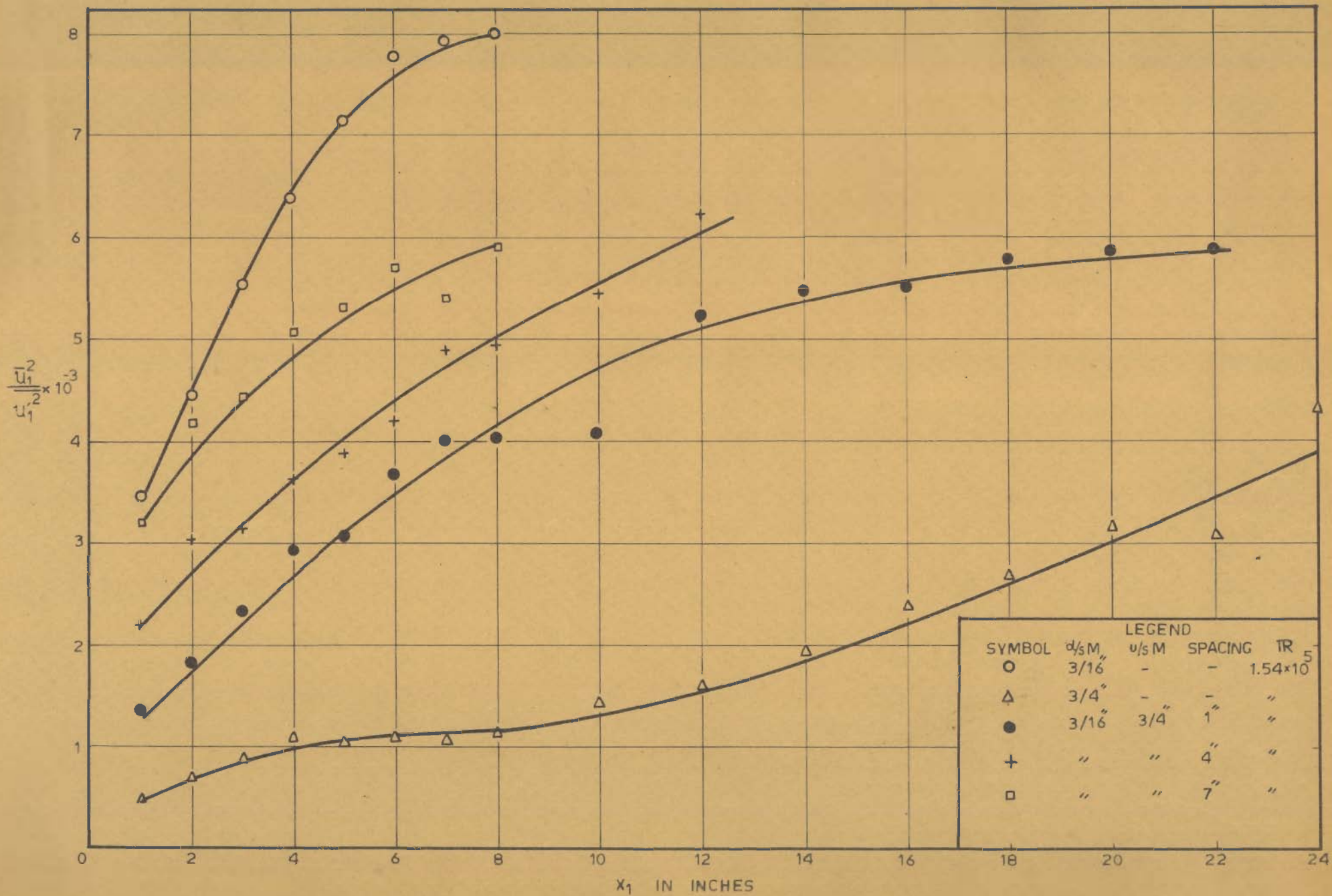
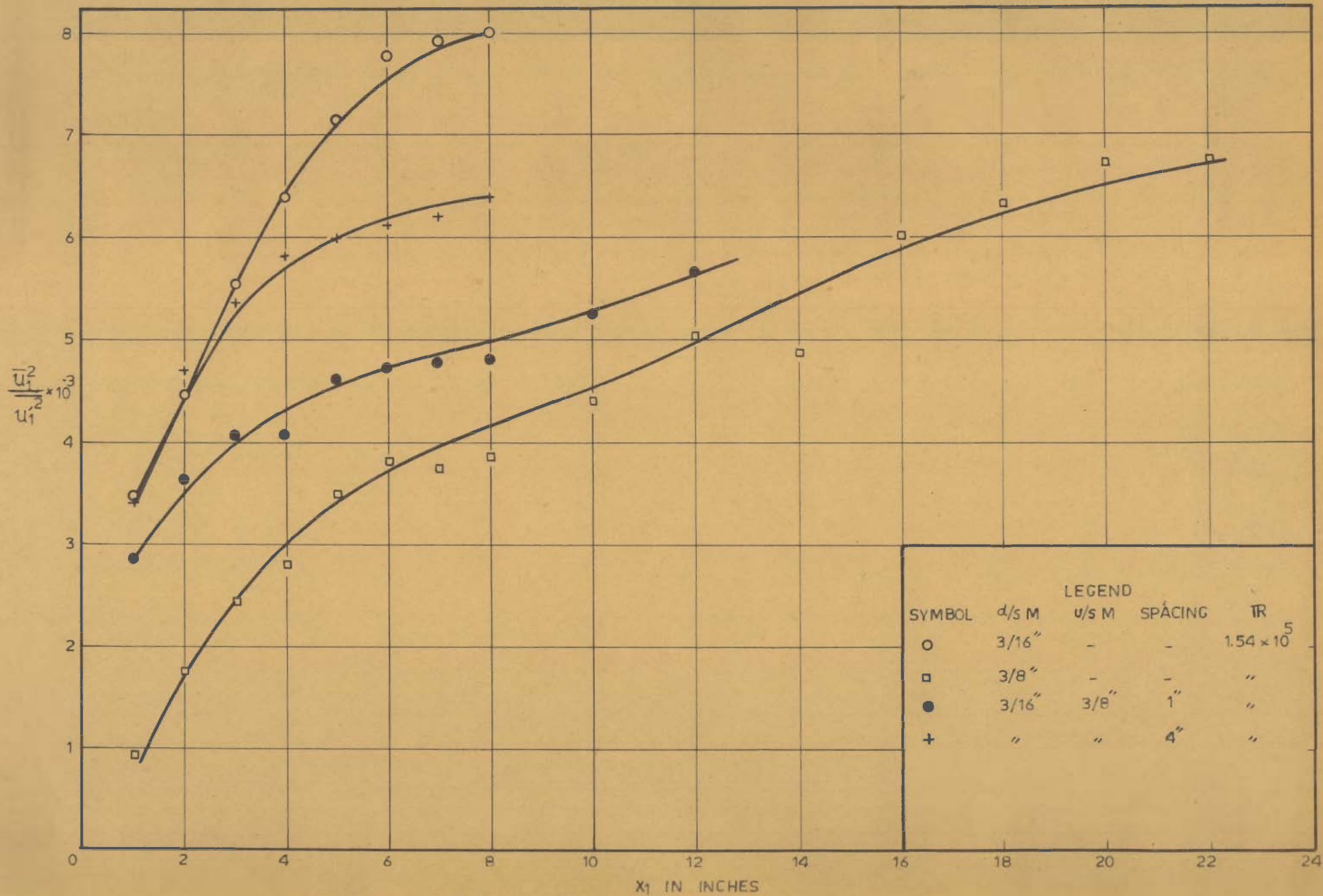FIG. 5.8 _ DECAY OF TURBULENCE BEHIND TWO GRIDS

FIG. 5.9 _ DECAY OF TURBULENCE BEHIND TWO GRIDS.
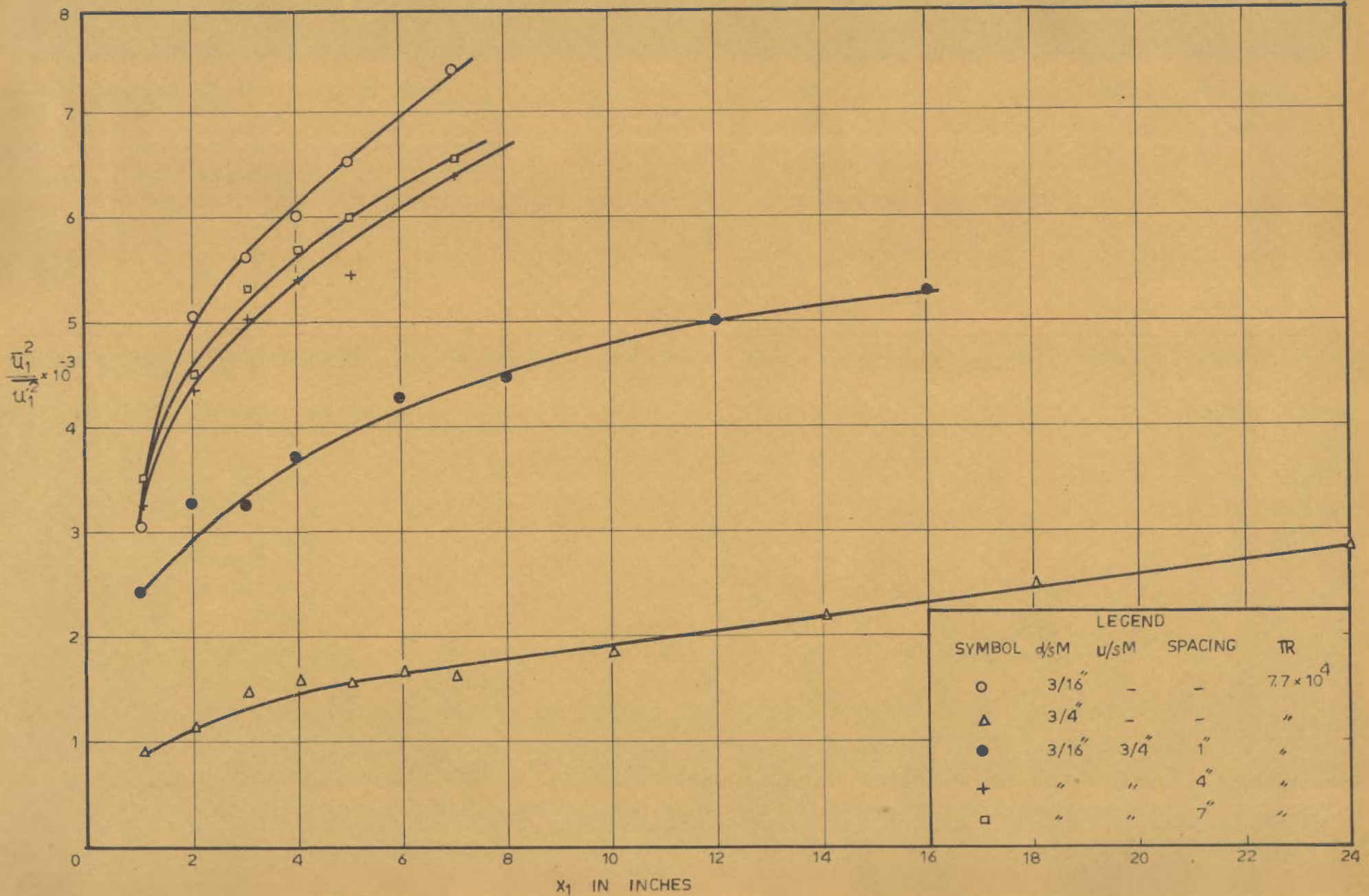
FIG. 5.10_ DECAY OF TURBULENCE BEHIND TWO GRIDS
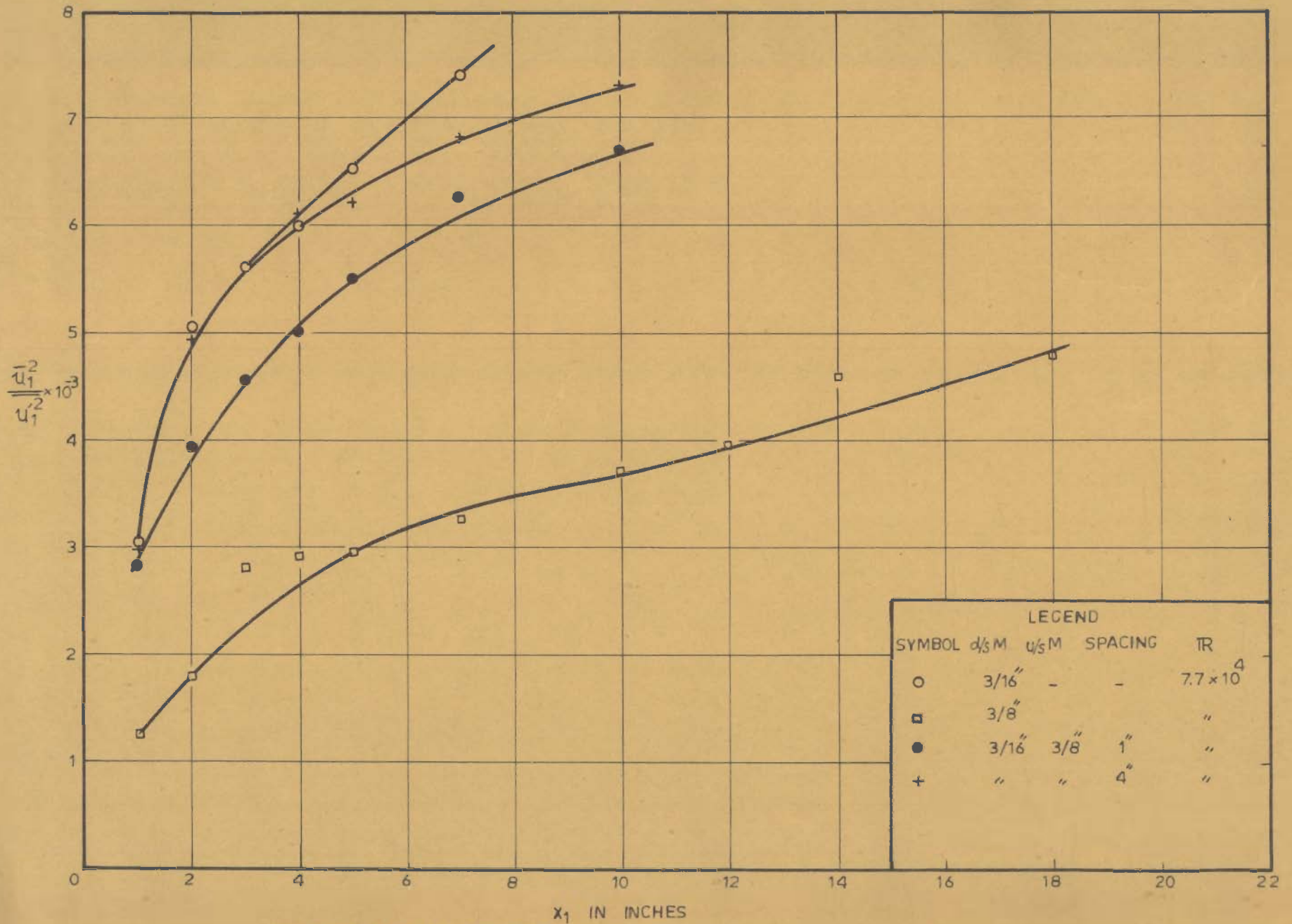
FIG.5.11_DECAY OF TURBULENCE BEHIND TWO GRIDS

conditions. The turbulence produced by the first grid will be
characteristic of its own. In the present case one would
expect the large scale (smaller wave number) components to be
predominant in the turbulence produced by the first grid,
owing to its larger mesh width. Thus when the 3/4'' grid is
placed 1'' upstream of the 3/16'' grid, the initial conditions
for the turbulence produced by the 3/16'' grid will be those
occuring at 1'' downstream from the 3/4'' grid rather than the
free stream turbulence for the pipe. If Goldstein's sugges-
tions regarding the dependence of the decay law on theinitial
conditions are correct, the introduction of the 3/4''' grid
should result in a change of the decay pattern downstream of
the 3/16'' grid. That this is actually the case is clear from
the Fig. 5.8. When the distance between the two grids is 1'',
the decay pattern is widely different from that obtained either
for the 3/16'' grid or for the 3/4'' grid alone. From the
Fig. 5.8 one can also note that as the distance between the
two grids increases, the decay pattern tends to approach that
for the 3/16'' grid alone. Thus, while the points for a spacing
of 1'' are very far off from that for the 3/16'' grid alone,
those for a 4'' spacing are closer to the latter. The
difference between the two sets of points thus decreases
with increase in the spacing. This seems quite natural
since the turbulence produced by the first grid (i.e. the one
placed upstream) will decay with distance downstream from it.
Thus with a larger spacing between the grids, the effect of the
first grid on the initial conditions for the second grid will
not be so marked as that with a smaller spacing. The same

thing can be observed in Figs. 5.9, 5.10 and 5.11.

The generalised decay law given by Goldstein is in the form

$$\overline{u_1'^2}t \quad = \nu \, R_t \, d(t)$$

where R_t is a Reynolds number defined as $\dfrac{(\overline{u_1'^2}t)_{t=o}}{\nu}$ and $d(t)$ is a function of time. According to Goldstein (22) ''For the turbulence produced by a single grid, $d(t)$ is nearly constant for a range of t in the initial period; this needs further explanation and detailed calculation since $d(t)$ is certainly not exactly constant. It is also suggested that '' the course of $d(t)$ and the number of constants needed to specify it, depend on the initial conditions ''. The first of these two statements, that $d(t)$ is not exactly constant during the initial period has been borne out by the data for a single grid, while the data for two grids lends support to the second statement. Results similar to those obtained in this work were reported by Tsuji and Hama (66,67) while carrying out experiments on decay with two grids in a wind tunnel.

The decay law given above can be expressed in the form

$$\frac{\overline{u_1'^2}}{\overline{u_1}^2} \quad = \quad \frac{L}{x_1} \, d \left(\frac{x_1}{\overline{u_1}} \right)$$

where L is some length scale. The function $d(x_1/\overline{u_1})$ will again depend on the initial conditions. Since the initial conditions can be described fairly well by defining the intensity and scale of turbulence as well as the Reynolds number R, a plot between $\overline{u_G'^2} / \overline{u_1'^2}$ and x/λ should give a

single curve for various initial conditions for any one Reynolds number. In the above $\overline{u'^2_g}$ is the value of $\overline{u'^2_1}$ at the downstream grid and $\hat{\lambda}$ is the microscale. The data for decay behind two grids at various spacings is replotted in this manner in Figs. 5.12 and 5.13 . Here $\overline{u'^2_g}$ was taken as the value of $\overline{u'^2_1}$ produced by the upstream grid at the downstream grid and $\hat{\lambda}$ the corresponding microscale. The two figures correspond to Reynolds numbers R of 1.54×10^5 and 7.7×10^4 respectively. As can be seen from the figures, the various points corresponding to different initial conditions tend to follow the same trend for any one Reynolds number. Thus it would appear that $\overline{u'^2_g} / \overline{u'^2_1}$ and x/λ should be the relevant parameters to describe the decay downstream of grids, besides the Reynolds number R.

5.5 Energy Spectra Behind a Single Grid :

The energy spectra behind a single grid are shown in Figs. 5.14 - 5.16. These plots of Taylor's normalised one-dimensional spectrum function F_1 (k) vs the wave number k are prepared for all the three grids used in the study, viz. 3/16'', 3/8" and 3/4'' mesh. The spectra shown are for a Reynolds number of flow R = 1.54×10^5 only, as those obtained for IR = 7.7×10^4 were similar to these. The observed spectra agree with those already obtained by many other authors e.g. by Liepmann, Laufer and Liepmann (42), Tsuji (66, 67) etc. Certain features of these spectra can be noted from these plots. As is well known, F_1(k) tends to a constant value F_1(0) as k tends to zero and decreases rapidly as k
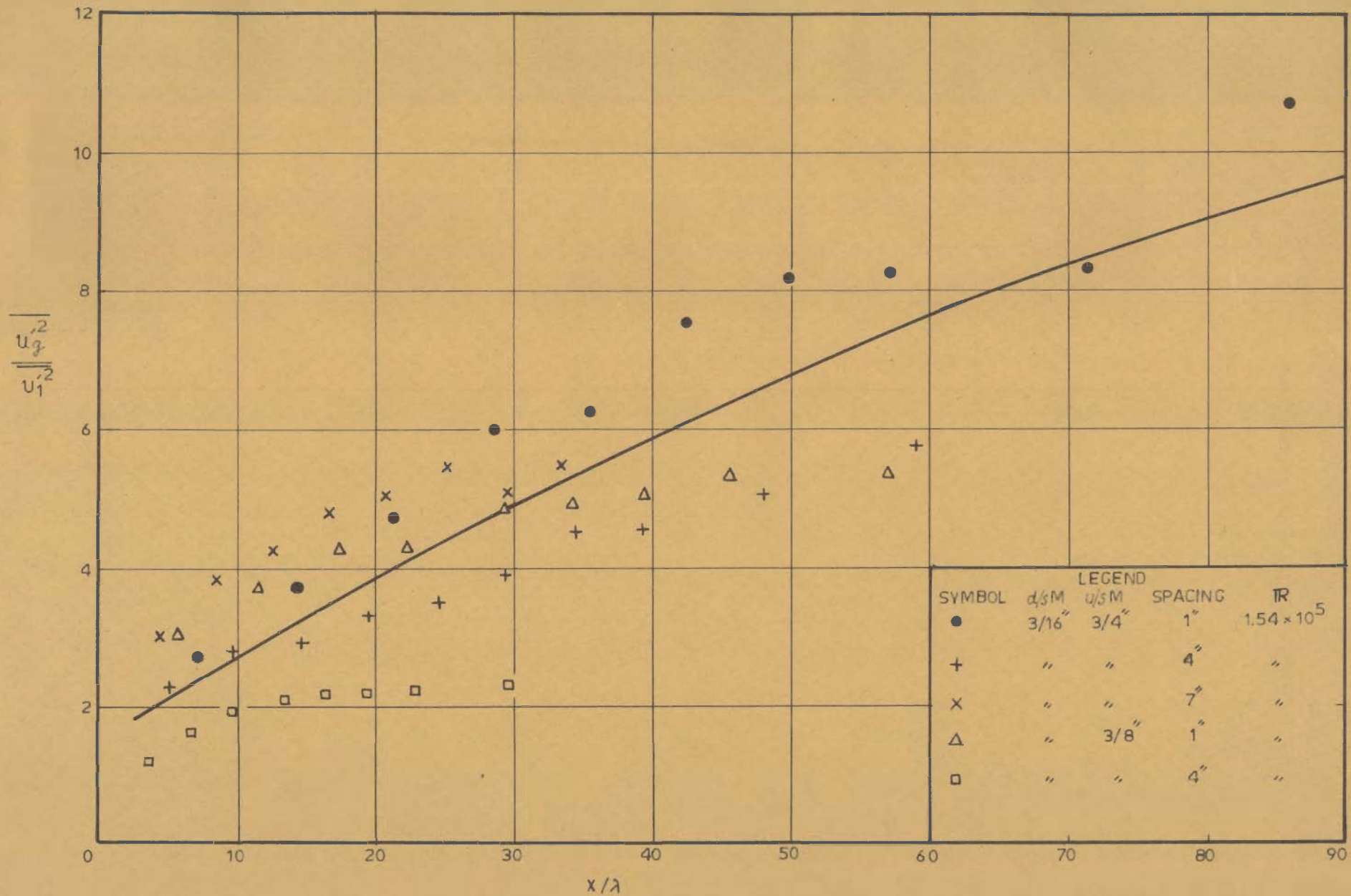
FIG.5.12_DECAY OF TURBULENCE BEHIND TWO GRIDS

124

LEGEND

SYMBOL	d/s M	u/s M	SPACING	ℝ
●	3/16"	3/4"	1"	7.7 × 10⁴
+	,,	,,	4"	,,
×	,,	,,	7"	,,
△	,,	3/8"	1"	,,
□	,,	,,	4"	,,

$\dfrac{\overline{u_g'^2}}{\overline{u_1'^2}}$

x/λ
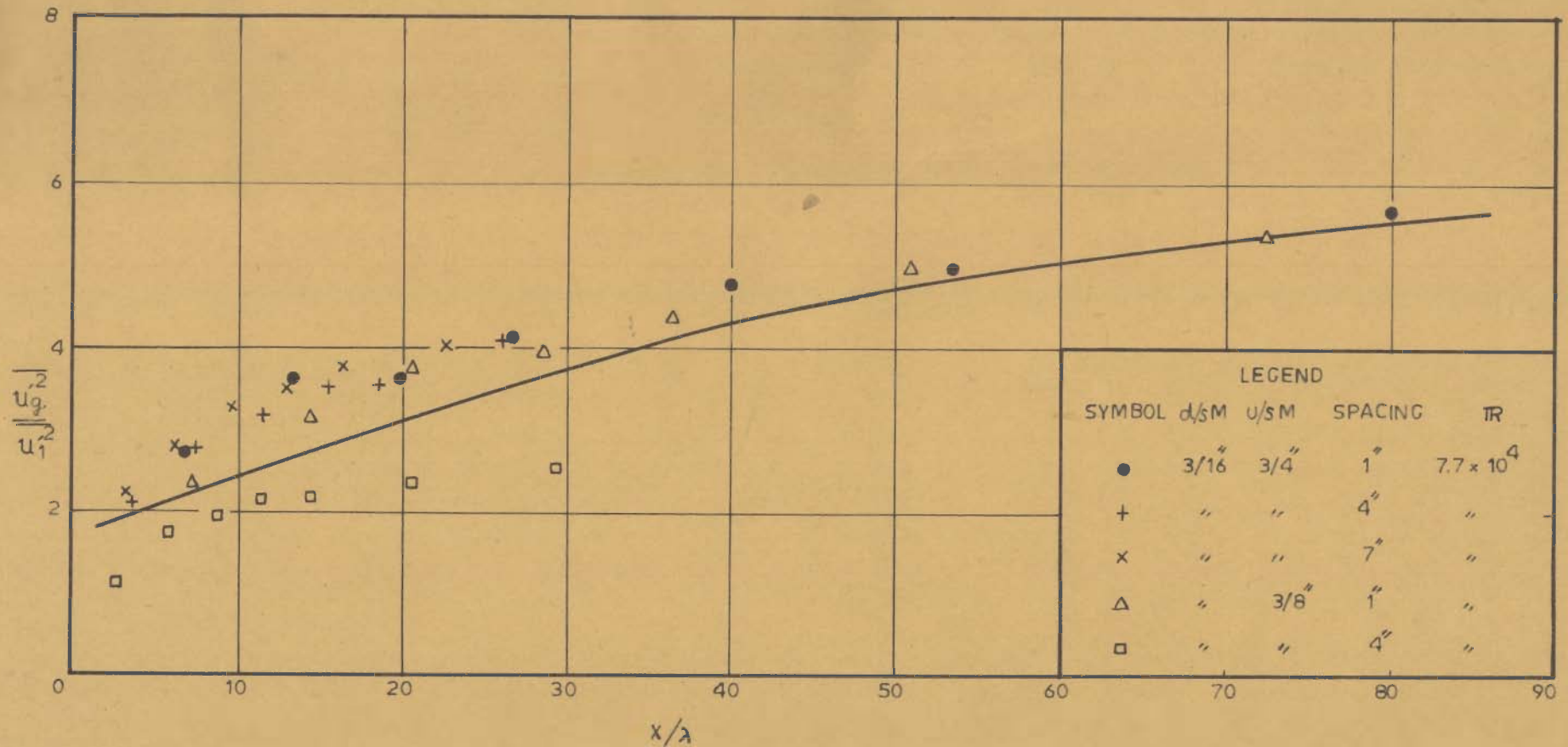
FIG. 5.13 _ DECAY OF TURBULENCE BEHIND TWO GRIDS

increases. The value of $F_1(0)$ increases with increase in distance downstream from the grid (which also means the increase in decay time). Since

$$F_1(k) = \frac{2}{\pi} \int_0^\infty f(x_1) \cos kx_1 \, dx_1$$

and $\Lambda_f = \int_0^\infty f(x_1) dx_1$

therefore, $F_1(0) = \lim_{k \to 0} F_1(k) = \frac{2}{\pi} \int_0^\infty f(x_1) \, dx_1$

or $F_1(0) = \frac{2}{\pi} \Lambda_f$

Thus an increase in $F_1(0)$ corresponds to an increase in the integral scale Λ_f or an increase in the average size of the eddies present. That this is actually the case is evident from the plots, where the value of $F_1(k)$ as k becomes very small, increases for larger values of x_1.

Another feature of the spectra that is evident from these plots is the effect of mesh width on the energy spectrum. As the mesh width of the grid increases there is a larger contribution of energy from the low wave number region. This is indicated by the increase in the value of $F_1(k)$ at low k values for grids of larger mesh width.

A line with $-5/3$ slope representing the Kolmogoroff's spectrum law is also drawn on the plots. The agreement between this line and the observed spectra is however confined to wave numbers between about 50 to 250 ft. Again the agreement, howsoever small, seems to be better for grids of larger mesh widths as compared to those for smaller ones. Similar results were obtained by Liepmann and coworkers (42) who showed that for mesh Reynolds numbers ($IR_M = \bar{u}_1 M/\nu$)

of the order of 10^4 , there was a very narrow wave number range to approximate the measured one-dimensional spectrum by the Kolmogoroff spectrum law. However, for larger mesh Reynolds' numbers (of the order of 3×10^5) they obtained a much better agreement with the Kolmogoroff spectrum in the higher part of the measured wave number range. Stewart and Townsend (57) showed that in order to have a sufficiently large inertial sub-range , such as is required by Kolmogoroff's theory, the mesh Reynolds number should be at least of the order of 10^6.

In the very high wave number range, another line with a - 7 slope is drawn representing the Heisenberg's form of the energy spectrum. This line also does not seem to give very good agreement with the observed spectra. No definite conclusions regarding a power law of spectrum in this region can, however, be drawn since the signal to noise ratio being small, the accuracy of the measurements and hence the conclusions drawn therefrom in the very high wave-number region must remain tentative.

The spectra for the various grids at two locations have also been plotted with $\bar{u}_1 F_1(n) / \Lambda_f$ and $n \Lambda_f / \bar{u}_1$ as the parameters and are shown in Figs. 5.17 and 5.18. Also shown in both figures is a curve represented by the equation $\dfrac{\bar{u}_1 F_1(n)}{\Lambda_f}$

$$= \frac{4}{1 + \dfrac{4\pi^2 n^2 \Lambda_f^2}{\bar{u}_1^2}}$$. This equation corresponds to an exponential form of the $f(\tau_1)$ correlation. From these two figures, it is apparent that the Reynolds number of flow R does not materially affect the spectra for any particular grid. Also, there is a

systematic variation for the various grids and the above equation cannot be said to be followed. Thus it appears that the correlation curves donot remain exponential throughout.

These measurements of the spectra behind grids seem to lend further support to the contention that the similarity spectrum as envisaged in Kolmogoroff's theory is inadequate to describe the turbulence behaviour at low or moderate Reynolds numbers and that its range of validity is accordingly limited by the Reynolds number. The similarity of the energy spectra has, however, been examined later.

5.6 Energy Spectra Behind Two Grids :

The energy spectra behind two grids are presented in Figs. 5.19 - 5.21. The spectra were measured for different spacings of the 3/16'' and 3/8'' and the 3/16'' and 3/4'' grids. For each case, measurements were made at two Reynolds numbers of flow i.e. $IR = 1.5 \times 10^5$ and 7.7×10^4 respectively. However, only a representative set of three spectra has been presented in the above figures, the other ones being similar to these.

The spectra $F_1(k)$ for a spacing of 1'' between the 3/16'' and 3/4'' grids for a Reynolds number of 1.54×10^5 are shown in Fig. 5.19. The shapes of the $F_1(k)$ vs k curves in this case quite resemble those for the 3/4'' grid alone. This is due to the fact that the fine scale turbulence produced by the 3/16'' grid decays out rather rapidly and the large scale turbulence produced by the 3/4'' grid remains comparatively untouched.

The spectra for a 7'' spacing between the two and 3/4'' grids viz. 3/16''/are given in Fig. 5.21. The distance between the two grids being large in this case, the high wave number components of the turbulence produced by the 3/4'' have already decayed out and the low wave number components are superposed on the turbulence produced by the 3/16'' grid. Comparison of these results with Fig. 5.14 shows that the effect of the large scale turbulence produced by the 3/4'' grid predominates and the value of the spectrum function $F_1(k)$ at low wave numbers is much larger than that resulting from the 3/16'' grid alone.

The spectra for a 4'' spacing between the 3/16'' and 3/4'' grids also show a similar trend. The $F_1(k)$ values for low wave numbers here also are definitely larger than those for the 3/16'' grid alone. The same tendency was observed for the other spectra viz. those for the 1'' and 4'' spacings between the 3/16'' and 3/8'' grids and those for a Reynolds number of flow of 7.7×10^4 for all the above cases.

These measurements thus show that a change in the initial conditions, which in this case is brought about by means of the 3/4'' or 3/8'' grids placed upstream of the 3/16'' grid, brings about a change in the spectra downstream of a grid and consequently a change in the decay pattern. A more definite proof of this can be obtained by examining the similarity of spectra as has been done in the next section.

5.7 Similarity of Energy Spectra :

With the values of λ , the micro scale, determined by integrating the $k^2 F_1(k)$ curves, the value of $F_1(k)/\lambda$ was plotted against λk. The results are shown in Figs.5.22 to 5.37. These plots in effect are just the non-dimensionali-sation of the spectra with the help of a characteristic length λ . If complete similarity of spectra were to hold over the entire wave number range i.e. if the spectra preserved their shape, over all wave numbers, during decay, all the points on $F_1(k)/\lambda$ vs λk plot should fall on a single curve, irrespective of the distance of the point of observation from the grid. That this is not actually the case is apparent from Figs. 5.22 - 5.24 and Figs. 5.30 - 5.32. The various points, which correspond to observations at different distances behind a single grid, do not fall on the same curve for all wave numbers. An examination of these plots also reveals that while the points tend to fall on a single curve at larger values of λk, the deviations increase for smaller λk values . This is in agreement with the results of measure-ments made by many other workers such as Stewart and Townsend (57) for the turbulence produced by grids in wind tunnel. The scatter of the data at very large λk values is probab-ly more due to the small signal to noise ratio in this region, which makes the sensitivity of the equipment rather low, than due to departures from similarity itself.

The $F_1(k)/\lambda$ vs λk plot for the 3/16'' grid when the 3/4'' grid is placed 1'' upstream of it is shown in Fig. 5.25. This plot is prepared for a Reynolds number of

flow of 1.54×10^5. If the similarity of spectra and consequently the decay law, were independent of the initial conditions, this plot should have been similar to Fig. 5.22. Comparison of the Figs. 5.22 and 5.25 however, show that there is a large difference between the data points obtained in the two cases upto λk values of the order of 4. After this, the two plots seem to be quite similar to each other. As the spacing of the two grids increases, the range of λk values in which the two sets of points are wide apart decreases as is seen from Figs. 5.25 and 5.26. This indicates that the change of initial conditions destroys the similarity of spectra and hence results in a change of the decay law. It has already been shown earlier (Figs. 5.8 - 5.11) that the decay law does change with change in initial conditions. The above plots merely confirm the premise that this change in decay law is because of the change in initial conditions, which in turn decrease the range of validity of the similarity spectrum. The same trend is observable from the other plots viz. those for 3/16" and 3/4" grids at various spacings for a Reynolds number of 7.7×10^4 and for 3/16'' and 3/8'' grids at various spacings for Reynolds numbers of 1.54×10^5 and 7.7×10^4.

5.8 Similarity of the Spectra of Vorticity :

The plot of $k^2 F_1(k)$ vs k is known as the dissipation spectra and describes the distribution in wave number of the rate of decay of turbulent energy to heat. The quantity $k^2 F_1(k)$ is also proportional to the spectrum of vorticity $(\partial u_1'/\partial x_1)^2$. This can be measured directly

from a frequency analysis of the derivative du_1'/dt by
using a differentiator circuit along with the harmonic ana-
lyser. In the present work, however, it was computed from
the measured energy spectrum $F_1(k)$.

The similarity of the spectrum of vorticity has
been examined by plotting $k^2F_1(k)$ vs k. The plots are
shown in Figs. 5.38 - 5.43 . As can be seen, there is a con-
siderable scatter in the data. This may be due to the fact
that the value of λ has been determined from the measured
$F_1(k)$ values and hence the integration of $k^2F_1(k)$ for
determining λ is not carried out from $k = 0$ to ∞ but
upto a finite value of k. However, the data conform well
to the trend obtained for the dissipation spectra by other
workers. One of the feature that is noticeable in the above
figures is that the spectra $k^2F_1(k)$ behind the 3/16" grid,
when the 3/4" grid is placed 4" or 7" upstream of it are
quite similar to those for the 3/16" grid alone, even at
low wave numbers. Only when the 3/4" grid is placed upstream
at 1", is there a marked departure in the shape of the spec-
tra compared to the one for the 3/16" grid alone. This too
is confined to the lower wave-numbers only. Similar results
are obtained for the other grids also. This indicates that
the departure from similarity for the dissipation spectra is
smaller than that for the spectrum of energy, while the
initial conditions are changed. The effect of this devia-
tion, therefore, will be less in computation of the rate of
dissipation than in the computation of energy on the basis of
similarity spectra. This is also confirmed by observations
made by Stewart and Townsend (57) behind a single grid in a

wind tunnel. They measured the $\frac{\partial u_1'}{\partial x_1}$, $\frac{\partial^2 u_1'}{\partial x_1^2}$ and $\frac{\partial^3 u_1'}{\partial x^3}$

spectra for single grids at various mesh Reynolds number

(R_M) , effectively giving measurements of the functions

$k^2 F_1(k)$, $k^4 F_1(k)$ and $k^6 F_1(k)$, and found that the

departure from similarity for different Reynolds numbers

decreased as the order of the function increased, being a

minimum for $k^6 F_1(k)$. In the present case, one

can see that the departures from similarity are less

for $k^2 F_1(k)$ compared to those for $F_1(k)$ alone and it

may be expected that these departures will decrease

further for higher moments i.e. $k^4 F_1(k)$ etc.

Thus one can see that the spectra of vorti-
city conform to the similarity hypothesis better than
the spectra of energy, even when the initial conditions
are changing. It may be expected that the departures
will further decrease with higher moments as envisaged
in the generalised theory of similarity spectra and decay
law proposed by Goldstein.

5.9 Energy Spectra with Wall to Wall Probes :

The spectra of energy for the 3/16'' grid alone
measured with the wall to wall probe at a Reynolds number
of flow of 1.54×10^5 are shown in Fig.5.44. Comparison
of these with Fig.5.14 shows that while for low wave numbers
these spectra are similar to those obtained with the traverse
probe, the difference between the two is considerable for high
wave numbers. The spectrum function $F_1(k)$ has a smaller value

for high wave numbers. when measured with the wall to wall probes. This may be because of the interaction of smaller eddies (high wave numbers) within the probe gap, thereby cancelling the effect of each other. The size of the probe gap therefore seems to have an important bearing on the frequency response. While a small gap will reduce the strength of the signal and thereby decrease the signal to noise ratio, a large gap will cut off larger wave number components. This was observed to be the case for the spectra with other grids also. Thus a compromise has to be made between the conflicting requirements of high signal to noise ratio and wider frequency response vis a vis the probe gap.

-:o:-

CHAPTER - VI

CONCLUSIONS AND SUGGESTIONS FOR FURTHER STUDY

6.1 Conclusions :

From the experimental study and subsequent discussion of results, the following conclusions can be drawn :

1) The method of electromagnetic induction can be said to be quite suitable for turbulence measurements in water. The agreement of the results obtained with those obtained by Laufer for pipe flows and the reproducibility of data observed during the experimentation further underline the suitability of the method.

2) The decay of turbulence behind a single grid is found to depart from the decay law given by Taylor or from the linear decay law derived on the basis of Kolmogoroff's theory. On the other hand, the results substantiate the ideas put forth by Goldstein in his generalised theory of equilibrium and similarity spectra and the resulting decay law wherein the decay law is said to be governed by the Reynolds' number and initial conditions.

3) The decay pattern behind a grid depends on the initial conditions. With a change in initial conditions the decay law also changes. Thus if two grids are placed some distance apart with the grid of larger mesh width upstream, the decay law is not the same as for

the downstream grid alone. This change in decay
law depends upon the spacing apart of the two grids.

4) If $\overline{u'^2_g}$ and λ are used to non dimensionalise $\overline{u'^2_1}$
and x_1 where $\overline{u'^2_g}$ is the intensity and λ the
microscale of turbulence produced by the upstream
grid at the position of the downstream grid, then
the plot ($\overline{u'^2_g}$ / $\overline{u'^2_1}$) vs (x_1/λ) tends to
give a single curve for a given value of the Reynolds'
number IR. This seems to indicate that $\overline{u'^2_g}$ and λ
which represent the initial conditions are the
important parameters governing the decay law in
addition to R. This again is in keeping with
Goldsteins' contention about the dependence of decay
law on initial conditions and Reynolds' number.

5) There exists no complete similarity of the energy
spectra during decay. The similarity however increa-
ses with increase in wave numbers.

6) A change in initial conditions bring about a strong
departure from similarity of the energy spectra,
consequently bringing about a change in the decay
law.

7) The spectra of vorticity show a smaller departure
from similarity during decay even when the initial
conditions are changed. Accordingly the departure
in practice from any decay law derived on the assum-
ption of similarity of spectra of vorticity will be
smaller than that from a law assuming similarity of
energy spectra (Linear decay law). This, in other

words, means that the effect of deviation from similarity will be large in computation of energy and will be smaller for computation of rate of energy dissipation. It may be expected that this deviation will further decrease for higher moments and therefore a generalised decay law as proposed by Goldstein should hold for all ranges of Reynolds numbers and all initial conditions.

8) Wall to wall probe does not give results comparable to the traverse probe. While the low frequency components are relatively unaffected, the high frequency components are cut off while using the wall to wall probe. The size of the probe gap thus has a significant bearing on the frequency response of the system

6.2 Suggestions for Further Work :

The following aspects are suggested for continuing work in the field pertaining to the present work :-

1) A detailed investigation of the induced currents in the flowing water resulting from electromagnetic induction in order to express the induced-voltage-velocity-fluctuation relationship more exactly.

2) Building up of three and four wire probes to measure u_2' and u_3' fluctuations and their spectra.

3) Setting up of a differentiator circuit alongwith the present set up in order to enable microscale (λ) measurements to be made directly. This will

also enable the spectra of vorticity to be measured directly by using another wave form analyser or by recording the signal on the F.M. tape recorder and playing it back to the analyser used for measurement of energy spectra.

4) Setting up of a series of differentiator circuit to record the spectra of higher moments of $E_1(k)$. These measurements under a wider variety of initial conditions will give more insight into the nature of similarity of spectra.

5) Self contained probes may be developed where the magnet is not a separate one but is a permanent magnet attached to the probe itself. This will add to the flexibility of the instrumentation and enable a wider range of Reynolds numbers to be used for the investigations. A relationship between the function d(t) formulated by Goldstein in his decay law and the Reynolds numbers for various initial conditions could then be investigated.

-:o:-

REFERENCES

1. Baines, W.D. and E.G.Peterson 'An Investigation of Flow Through Screens' Trans. ASME, 73, 467, 1951.

2. Batchelor G.K. - 'Energy Decay and Self-Preserving Correlation Functions in Isotropic Turbulence' Quart. Appl.Math.6, 97, 1948.

3. Batchelor G.K.-'The Role of Big Eddies in Homogeneous Turbulence' Proc.Roy.Soc.(Lond.),A 195, 513, 1949.

4. Batchelor G.K.-'The Theory of Homogeneous Turbulence' Camb. Univ.Press, 1960.

5. Batchelor G.K. and I. Proudman.- 'The Large Scale Structure of Homogeneous Turbulence'.Phil. Trans.Roy.Soc.(Lond).248,No.949,369,1956.

6. Batchelor G.K. and A.A.Townsend.-'Decay of Vorticity in Isotropic Turbulence' Proc.Roy Soc.(Lond.) A 190, 534, 1947.

7. Batchelor G.K. A.A.Townsend.-'Decay of Isotropic Turbulence in The Initial Period' Proc.Roy. Soc.(Lond.) A 193,539, 1948.

8. Batchelor G.K. A.A.Townsend.-'Decay of Isotropic Turbulence in the Final Period' Proc.Roy.Soc. (Lond.) A 194, 527, 1948.

9. Binder G.J. and J.E.Cermak.-'Stream Potential Fluctuations Produced by Turbulence', The Physics of Fluids, Vol.6, No.8, 1963.

10. Cermak J.E. and L.V.Baldwin.-'Measurements of Turbulence in Water by Electrokinetic Transducers'

Paper No.2, Fluid Mech.Papers,Colo.State Univ.

11. Chuang, H. and J.E. Cermak.-'Turbulence Measured by
     Electrokinetic Transducers' Proc.A.S.C.E.
     91,HY 6, 4526, 1965.

12. Chandrasekhar S.-'On Heisenberg's Elementary Theory of
     Turbulence' Proc.Roy.Soc.(Lond) A 200,
     20, 1949.

13. Corrsin, S.-'Turbulent Flow' American Scientist,49,
     300, 1961.

14. Day H.J.- 'Energy Changes in Liquid Turbulent Flow'
     Ph.D. Thesis, Univ. of Wisconsin,1963.

15. Dryden H.L.- 'A Review of the Statistical Theory of
     Turbulence' Quart.App.Math.1,7, 1943.

16. Dryden H.L .-'Turbulence Investigations at the National
     Bureau of Standards' 5th Intl.Cong. for
     Appl.Mech. Camb.Mass. 1930.

17. Dryden H.L. and G.B.Schubauer.-' The use of Damping
     Screens for the Reduction of Turbulence'
     Jour.Aero.Sci.Vol.14,No.4, 221, 1947.

18. Dryden H.L., G.B.Schubauer, W.C.Mock and H.K.Skramstadt-
     'Measurement of Intensity and Scale of Wind
     Tunnel Turbulence and Their Relation to
     Critical Reynolds Number of Spheres'
     NACA, TR 581, 1937.

19. Eagleson P.S. and F.E. Perkins .-'A Total Head Tube
     for the Broad Band Measurement of Turbulent
     Velocity Fluctuations in Water' I.A.H.R.9th
     Convention, Yugoslavia, 1961.

20. Frankiel, F.N.- 'Comparison Between Theoretical and
Experimental Results on the Decay of Turbu-
lence' Proc.7th Intl.Cong.Appl.Mech.2,112,
1948.

21. Frankiel, F.N.-'The Decay of Isotropic Turbulence'
Trans.A.S.M.E.,Vol.70, 311, 1948.

22. Goldstein, S., 'On the Law of Decay of Homogeneous
Isotropic Turbulence and the Theories of
the Equilibrium and Similarity Spectra' Proc.
Camb.Phil.Soc. Vol.47, 554, 1951.

23. Goldstein, S., 'Modern Developments in Fluid Dynamics!
Oxford University Press.

24. Grant, H.L. and I.C.T.Nisbet.-'The Inhomogeneity of
Grid Turbulence', Jour.Fl.Mech.Vol.2,
263, 1957.

25. Gratz R.L.- 'Turbulence Spectra for Disturbed Turbu-
lent Flow' M.S. Thesis, Univ. of Wisc., 1965.

26. Grossman, L.M., H.Li and H.A. Einstein.-'Investigations
in Liquid Shear Flow by Electromagnetic
Induction' Proc. A.S.C.E., 83, HY 5, 1394,
1957.

27. Hall, A.A., -'Measurements of the Intensity and Scale
of Turbulence' Rep.Memor. Aero.Res.Comm.
(Lond.) No. 1842.

28. Hinze, J.O.,-' Turbulence' McGraw Hill, 1959.

29. Hubbard, P.G.,-' Recent Developments in Electronic
Instrumentation', Proc. of 6th Hyd.Conf.,
State Univ.of Iowa, Bulletin 36, 1955.

30. Ippen, A.T. and F.Raichlen.-'Turbulence in Civil Engineering' Measurements in Free Surface Streams' Proc. A.S.C.E. Jour.Hyd.Div.,HY 5 1957.

31. Kampe de Feriet, J.,-' The Spectrum of Turbulence' Jour.Aero.Sci., 7, 518, 1940.

32. Kampe de Feriet, J. -'Le Tenseur Spectral de la Turbulence Homogene Non Isotrope dans un Fluide Incompressible' Proc. 7th Intl.Cong.Appl. Mech., introd. Vol. 1948.

33. Karaichnan, R.H.-' The Structure of Isotropic Turbulence at Very High Reynolds Numbers' Jour. of Fl. Mech. Vol.5, 497, 1959.

34. King, L.V. -' On the Convection of Heat from Small Cylinders in a Stream of Fluid: Determination of the Convection Constants of Small Platinum Wires with Applications to Hot-Wire Anemometry' Phil.Trans.Roy.Soc.(Lond.) A 214, 373, 1914.

35. Kolin,A.- 'Electromagnetic Velometry: Method for the Determination of Fluid Velocity Distribution in Space and Time' Jour.Appl.Phy. 15, 150, 1944.

36. Kolmogoroff, A.N.,-'The Local Structure of Turbulence in Incompressible Viscous Fluids for very large Reynolds Numbers'-Comptes Rendus (Doklady) de l'Academic des Sciences, l'URSS 30, 301, 1941.

37. Kolmogoroff, A.N.-'On Degeneration of Isotropic Turbulence in an Incompressible Viscous Liquid' Comptes Rendus (Doklady) de l'Academie des Sciences de l'URSS.,31, 538, 1941.

38. Kolmogoroff, A.N.-'Dissipation of Energy in Locally Isotropic Turbulence' Comptes Rendus (Doklady) de l'Academie des Sciences de l'URSS, 32 16, 1941.

39. Laufer, J.,-' The Structure of Fully Developed Pipe Flow' NACA TR 1174, 1954.

40. Lettau H.,-' A Generalised Mathematical Model of the Mean-Velocity Distribution in Fully Turbulent Flow' Tech.Rpt.No.3, Deptt.of Meteor. Univ. of Wis. 1961.

41. Lettau , H.,-'A New Vorticity -Transfer Hypothesis of Turbulence Theory' Jour. of Atmos-Sciences, Vol.21, No.4, 453, 1964.

42. Liepmann, H.W., J.Laufer and K.Liepmann,-'On the Spectrum of Isotropic Turbulence' NACA TN 2473, 1951.

43. Lin C.C.,-' Remarks on the Spectrum of Turbulence' Proc. 1st Symp. in Appl.Math.Amer.Math.Soc. 81, 1947.

44. Lin C.C.,-'Statistical Theories of Turbulence' Princeton Aeronautical Paperbakes, Princeton University Press, 1961.

45. Lin C.C. and S.F.Tchen.-'Studies of Von-Karman's Similarity Theory and Its Extension to Compressible Flows. A Critical Examination of Similarity

Theory for Incompressible Flows' NACA,TN 254
1951.

46.   Ling S.C.,-'Measurement of Flow Characteristics by the
            Hot Film Technique' Ph.D.Dissertation,State
            Univ. of Iowa, 1955.

47.   MacPhail,D.C.,-' An Experimental Verification of the
            Isotropy of Turbulence Produced by a Grid'
            Jour.Aero.Sci.8,73, 1940.

48.   Pai,S.I., -'Viscous Flow Theory-Vol.II' Van Nostrand,
            1957.

49.   Proudman, I.- 'A Comparison of Heisenberg's Spectrum
            of Turbulence with Experiment' Proc.Camb.
            Phil.Soc. 47, 158, 1951.

50.   Rao, M.V. -' A Study of the Structure of Shear Turbu-
            lence in Free Surface Flows' Ph.D.Thesis ,
            Utah State University, 1965.

51.   Robertson, H.P.,-'The Invariant Theory of Isotropic
            Turbulence' Proc.Camb.Phil.Soc.,36,209,1940.

52.   Rouse, H., and S.Ince,-' History of Hydraulics' Dover
            Paperback.

53.   Sato, H.- 'Decay of Spectral Components in Isotropic
            Turbulence' Jour.Appl.Phy.22, 525, 1951.

54.   Simmons L.F.G., and C.Salter.- 'Experimental Investi-
            gation and Analysis of the Velocity Vari-
            ations in Turbulent Flow' Proc.Roy Soc.
            (Lond) A 145, 212, 1934.

55.   Simmons, L.F.G., and C.Salter,-' An Experimental Deter-
            mination of the Spectrum of Turbulence' Proc.
            Roy.Soc.(Lond).165,920,73, 1938.

56. Stewart R.W.- 'Triple Velocity Correlations in Isotropic Turbulence' Proc.Camb.Phil.Soc.47,146, 1951.

57. Stewart, R.W. and A.A.Townsend.-'Similarity and Self-Preservation in Isotropic Turbulence' Phil. Trans. Roy Soc.(Lond) A 243, 359, 1951.

58. Tan, H.S. and S.C.Ling.-'Final Stage of Decay of Grid Produced Turbulence' The Physics of Fluids, 6, No.12, 1693-1699, 1963.

59. Taylor, G.I., -'The Transport of Vorticity and Heat Through Fluids in Turbulent Motion' Proc.Roy Soc.(Lond.) A 135, 635, 1932.

60. Taylor, G.I., 'Statistical Theory of Turbulence, Parts I-IV', Proc.Roy.Soc.(Lond.) A 151, 421-478, 1935.

61. Taylor, G.I., 'The Spectrum of Turbulence' Proc.Roy. Soc.(Lond.) A 164, 47-490, 1938.

62. Taylor, G.I.-'Diffusion by Continuous Movements' Proc. Lond. Math. Soc., 2,20, 196-211, 1921.

63. Taylor G.I.- 'Production and Dissipationof Vorticity in Turbulent Fluid' Proc.Roy.Soc.(Lond) Vol. 164, 916, 15, 1938.

64. Taylor,G.I. and A.E.Green,- 'Mechanism of the Production of Small Eddies from Large Ones' Proc Roy Soc. (Lond) Vol.158, 895, 499, 1937.

65. Townsend, A.A., -'The Measurement of Double and Triple Correlation Derivatives in Isotropic Turbulence' Proc.Camb.Phil.Soc. 43, 560, 1947.

66. Tsuji, H. and F.R.Hama.-'Experiment on the Decay of turbulence Behind Two Grids' Jour.of the Aero. Sci.Vol.20,848, 1953.

67. Tsuji H., - 'Experimental Studies on the Spectrum of Isotropic Turbulence Behind Two Grids' Jour. Phy.Soc.,Japan, 2, 1096,-1104, 1956.

68. Von Karman, T.- 'Some Aspects of the Turbulence Problem' Proc. 4th Intl.Cong.Appl.Mech., 54, 1934.

69. Von Karman, T. -'The Fundamentals of the Statistical Theory of Turbulence' Jour.of the Aero.Sci. 4, 131-138, 1937.

70. Von Karman, T. -'Progress in the Statistical Theory of Turbulence' Jour.of Marine Res., 7,252-264, 1948.

71. Von Karman,T.- 'On the Statistical Theory of Isotropic Turbulence' Proc.Roy Soc.(Lond)., A 164, 192-215, 1938.

72. Von Karman, T. ' and C.C. Lin.-' On the Concept of Similarity in the Theory of Istoropic Turbulence' Reviews of Modern Physics, 21, 516-519, 1949.

73. Von Karman, T. and J.C.Lin.-'On the Statistical Theory of Isotropic Turbulence', Advances in Appl. Mech. Vol. II, 1-19, 1951.

-:o:-